

REMOTELY SENSED DATA FUSION AS A BASIS FOR ENVIRONMENTAL
STUDIES: CONCEPTS, TECHNIQUES AND APPLICATIONS

Dissertation
zur Erlangung des Doktorgrades
der Mathematisch-Naturwissenschaftlichen Fakultäten
der Georg-August-Universität zu Göttingen

vorgelegt von

Ali Darvishi Bolorani

Göttingen, 2008

D7

Referent: Professor Dr. Martin Kappas

Korreferent: Professor Dr. Gerhard Gerlod

Remotely Sensed Data Fusion as a Basis for Environmental Studies: Concepts,
Techniques and Applications

Ali Darvishi Bolorani

To my parents I forever was devoted to
To my loving wife, Kolsoum Ghazanfari
To my special friend, Ali Mousivand.

ABSTRACT

Following the dramatic qualitative and quantitative developments of remote sensing systems and digital imaging technologies, numerous kinds of images have been captured, processed and analyzed in several aspects of earth applications. Almost all of image sensors are designed for specific purposes therefore the utilization of remotely sensed data is very diverse. While these datasets are highly useful for some applications, for some others are incomplete, imprecise, and redundant. For example the information contained in hyperspectral and multispectral datasets provide a valuable basis for environmental studies while the low spatial resolution characteristics of these datasets reduce their performances in many applications. For several remote sensing applications, data fusion is the process of alleviating the shortages of data sources. Data fusion is a formal framework that provides means and tools for the alliance of data originating from different sources. It aims at obtaining information of greater quality; the exact definition of greater quality will depend upon the application. Data fusion is usually carried out in three levels of processing: pixel, feature and decision. In an ideal data fusion framework the level of process will be adapted based on data characteristics and the user requirements.

This PhD. work explores the concepts and techniques of multi-source remotely sensed data fusion for the purpose of visual spatial resolution enhancement and improvement the accuracy of land cover classification. The investigation datasets were selected from the Earth Observation-One satellite imager which has Hyperion, hyperspectral, ALI, multispectral, and ALI, panchromatic sensors.

For the first part of work, 10 of the most common pixel level DF techniques and two innovated ones, named Radon and fanbeam, were investigated and obtained results were compared. Results showed that these two innovated techniques have good abilities in spectral preservation but their ability in spatial quality of fused images was weak. More than the spectral quality of fused images a new technique in spatial quality assessment called coefficient of variance of image autocorrelation was developed. The qualities of fused images were evaluated using this new methodology and its ability was efficient and informative in fused imagery quality assessment. For

hyperspectral feature (i.e. spectral band) reduction an innovative methodology called Maximum Spectral and Spatial Information Indicator (MSSI) was introduced and its ability evaluated in comparison to two common feature reduction techniques i.e. Transformed Divergence (TD) and Bhattacharyya Distances (BD). Outcome results showed that MSSI has almost the same ability as for TD and BD. Another evaluated aspect was the comparison of hyperspectral and multispectral datasets fused with panchromatic image. Using the investigated datasets, the measured qualities of fused images showed that in pixel level data fusion MS has higher ability than HS datasets. For the second part of this work, decision level data fusion, two procedures for decision level fusion were innovated. These methodologies called hyperspectral Wavelength Based Decision Fusion (WBDF) and Class Based Decision Fusion (CBDF). The ability of these two new procedures was evaluated for hyperspectral data fusion in land cover mapping accuracy improvement. Final produced maps showed an about 4 % overall accuracy improvement. Also another methodology for decision level data fusion called Multi Classifier Decision Fusion (MCDF) was evaluated which could improve the accuracy of results to about 8%.

More than these experimental and technical investigations and innovations the literature of DF and its usability for several applications like environmental, agriculture, mining, urban, medicine studies, etc was studied. Finally, some experimental recommendations for future works in data fusion are drawn.

ACKNOWLEDGMENTS

First of all I would like to take this opportunity to thank God the Almighty for granting me the wisdom. If it were not His grace, I would not be what I am at present.

I would also like to thank Professor Dr. Martin Kappas for supervising me through this research. Thank you very much for your support, guidance and understanding.

I would also like to thank Dr. Stefan Erasmi, for his supports, guidance and helps throughout the doing and writing of this thesis, also all other friends that helped me during this period of PhD. Performance.

During this for years of research I collaborated with different researchers and colleagues that I would like to express my sincerest thanks to all of them for sharing their knowledge with me.

I would like to acknowledge the Ministry of Science Research and Technology of Iran (MSRTI), who was my sponsor for these four years.

Finally, from the bottom of my heart I would deeply like to take this opportunity to thank Kolsoum Ghazanfari, my loving wife, for her patiently supports and helps.

CONTENTS

ABSTRACT	V
ACKNOWLEDGMENTS	VII
CONTENTS	VIII
LIST OF FIGURES	XII
LIST OF TABLES	XIV
LIST OF ACRONYMS	XV
INTRODUCTION	1
<i>The nature of remote sensing images</i>	2
<i>Image resolution and data fusion</i>	3
<i>Research background</i>	5
<i>Research motivations</i>	5
<i>Thesis outline</i>	7
CHAPTER ONE	11
1 Literature review and data fusion applications	11
<i>1.1 Data fusion definitions</i>	13
<i>1.2 Data fusion categorizations</i>	14
1.2.1 Schowengerdt categorization [Schowengerdt, 1997]	15
1.2.2 Categorization based on classification accuracy improvement [Richards and Jia, 1999]	15
1.2.3 Military based categorization of Joint Directors of Laboratories (JDL)	16
1.2.4 Categorization based on processing level	17
1.2.4.1 Pixel (measurement) Level Data Fusion (PLDF)	18
1.2.4.2 Feature Level Data Fusion (FLDF)	18
1.2.4.3 Decision Level Data Fusion (DLDF)	19
<i>1.3 Why more and new data fusion algorithms?</i>	20
<i>1.4 Data fusion applications</i>	21
1.4.1 Non-military Applications	24
1.4.1.1 Remote Sensing	25
1.4.1.2 Spatial information extraction	27
1.4.1.3 Environmental studies	29
1.4.1.4 Agricultural studies	30
1.4.1.5 Natural disasters studies	31
1.4.1.6 Mineral exploration	32
1.4.1.7 Urban studies	33
1.4.1.8 Medical Applications	35
1.4.2 Military applications	36
CHAPTER TWO	39

2 Pixel Level Data Fusion (PLDF)	39
2.1 <i>PLDF categorization</i>	40
2.1.1 PLDF using all panchromatic band frequencies	40
2.1.1.1 Principal Component Transformation (PCT)	41
2.1.1.2 Intensity, Hue, Saturation (IHS)	44
2.1.1.3 Gram-Schmidt Transformation (GST)	46
2.1.1.4 Brovey Transformation (BT)	49
2.1.1.5 Color Normalized (CN)	49
2.1.1.6 Fanbeam (FB)	50
2.1.1.7 Radon Transform (RT)	52
2.1.2 PLDF using selected panchromatic band frequencies	54
2.1.2.1 Wavelet Transformation (WT)	54
2.1.2.1.1 Discrete Wavelet Transformation (DWT)	54
2.1.2.2 High Pass Filter (HPF)	58
2.1.2.3 ARSIS concept data fusion	59
2.1.2.3.1 A Troust Wavelet Transform (ATWT)	60
2.1.3 PLDF using panchromatic band indirectly	61
2.2 <i>Pixel level data fusion quality assessment</i>	61
2.2.1 Objective PLDF quality assessment indices	62
2.2.1.1 Wald's property indicators	63
2.2.1.2 Wald's requirements	64
2.2.1.3 Reference image creation	65
2.2.2 Spectral indices	66
2.2.3 Spatial indices	70
2.2.3.1 Normalized Difference of Entropies (NDE)	71
2.2.3.2 Normalized Difference of Autocorrelations (NDA)	72
2.2.4 Subjective image distortion indicators	74
2.3 <i>Feature Reduction (FR)</i>	75
2.3.1 Feature reduction levels	77
2.3.1.1 Block Based Feature Reduction (BBFR)	77
2.3.2 Feature selection techniques	78
2.3.2.1 Bhattacharyya Distance (BD)	78
2.3.2.2 Transformed Divergence (TD)	79
2.3.2.3 Maximum Spectral and Spatial Information Indicator (MSSI)	80
2.3.3 Feature reduction	84
CHAPTER THREE	87
3 Decision Level Data Fusion (DLDF)	87
3.1 <i>Data fusion for classification</i>	89
3.1.1 DLDF for image classification	90
3.2 <i>DLDF techniques</i>	94
3.2.1 Dempster-Shafer Theory (DST)	95
3.3 <i>Image classifiers</i>	96
3.3.1 Fuzzy classification	96
3.3.2 Bayesian Theorem (BT) classification	98
3.3.3 Spectral Angle Mapper (SAM) classifier	99
3.4 <i>DLDF accuracy assessment</i>	100
CHAPTER FOUR	104
	IX

4 Data sources and test areas	104
4.1 <i>Satellite imagery</i>	105
4.1.1 Hyperion	106
4.1.1.1 Pre-processing	106
4.1.1.1.1 De-striping	108
4.1.1.1.2 Radiometric transformation	110
4.1.2 Advanced Land Imager (ALI)	111
4.1.3 Explored EO-1/ALI and Hyperion datasets	112
4.2 <i>Test areas</i>	113
4.2.1 Palolo valley, Indonesia	113
4.2.2 Ahmadabad, south Tehran, Iran	114
CHAPTER FIVE	116
5 Results	116
5.1 <i>PLDF results (EO-1 Hyperion and ALI datasets, Indonesia, 2005)</i>	116
5.1.1 Objective evaluation	117
5.1.1.1 Spectral distortion evaluation	117
5.1.1.2 Spatial distortion evaluation	119
5.1.2 Subjective evaluation	121
5.1.3 Histogram comparison	126
5.2 <i>DLDF results (EO-1- Hyperion, Iran dataset, 2005)</i>	128
5.3 <i>MSSI feature reduction evaluation</i>	131
5.4 <i>Block based feature selection evaluation</i>	132
CHAPTER SIX	135
6 Conclusions, recommendations and future works	135
6.1 <i>Comparing the evaluated techniques</i>	135
6.1.1 Pixel level data fusion	135
6.1.2 Decision level data fusion	138
6.1.3 Feature selection	139
6.2 <i>Strengths and limitations of data fusion</i>	139
6.2.1 Data fusion strengths	139
6.2.1.1 Pixel level	140
6.2.1.2 Decision level	140
6.2.2 Data fusion limitations	141
6.2.2.1 Pixel level	142
6.2.2.2 Decision level	143
6.3 <i>Recommendations and future works</i>	144
REFERENCES	147
Appendix I	1
<i>Data fusion organizations, journals and useful websites</i>	1
Appendix II	3
<i>Author's publication in data fusion</i>	3

LIST OF FIGURES

<i>Figure 1-1. The human brain and perception system: a biological fusion process. After Wald [2002].</i>	11
<i>Figure 1-2. Block diagram of pixel level data fusion procedure.</i>	18
<i>Figure 1-3. Block diagram of data fusion at feature level.</i>	19
<i>Figure 1-4. Block diagram of data fusion at decision level of processing.</i>	20
<i>Figure 1-5. Spatial data fusion flow diagram. After Hall and Llinas [2001].</i>	28
<i>Figure 2-1. Single fanbeam projection at rotation angle theta. (a) the geometry of fanbeam function when FSG is set to arc; (b) fanbeam function when FSG is set to line. From Matlab help, [2008].</i>	51
<i>Figure 2-2. (a) Single Radon projection at a specified rotation angle with parallel-beam projection at rotation angle theta; (b) The Radon transform for one beam across an image. After Toft [1996].</i>	53
<i>Figure 2-3. Block diagram of the DWT image fusion scheme.</i>	57
<i>Figure 2-4. 5*5 window from an image: (a) original image and (b-f) different probable results from a pixel level data fusion process.</i>	70
<i>Figure 2-5. Statistic image for EO-1/Hyperion, with 133 spectral bands, Indonesia, 2004.</i>	78
<i>Figure 2-6. Spatial autocorrelation. (a) a monochrome image; (b) spatial domain of a pixel; and (c) adjacency rules.</i>	81
<i>Figure 2-7. Spectral autocorrelation. (a) 3D cube of a hyperspectral dataset with N bands; (b) the spectral respond (reflectance) of a pixel as a function of the wavelength; and (c) spectral dimension of a pixel in a selected subset with n bands.</i>	82
<i>Figure 3-1. Spectral response characteristics of green vegetation, as resultant of absorption, reflection and transmittance of light. After Hoffer [1978].</i>	91
<i>Figure 3-2. Block diagram of Wavelength Based Decision Fusion (WBDF) Where EM is the Electromagnetic spectrum.</i>	93
<i>Figure 3-3. Block diagram of Class Based Decision Fusion (CBDF).</i>	93
<i>Figure 3-4. Block diagram of Multi Classifier Decision Fusion (MCDF).</i>	94
<i>Figure 4-1. EO-1 land sensing mode. After Shaw and Burke [2003].</i>	105
<i>Figure 4-2. Visual inspection of bands where (a) band 56 and (c) band 77 were eliminated; (b) band 57 and (d) band 78 were selected.</i>	108
<i>Figure 4-3. (a) Stripped band 94 continuous with constant zero DN value; (b) Stripped column 92; and (c) De-stripped band.</i>	110
<i>Figure 4-4. Study area 1: (a) Indonesia; (b) Solawesi province; and (c) RGB 210, 60 and 20 bands for the study area, Palolo valley.</i>	114

- Figure 4-5. Study area 2: (a) Iran; (b) Tehran province; and (c) the RGB 110, 43 and 11 bands, Ahmadabad village.* 114
- Figure 5-1. EO-1/Hyperion (HS), ALI-Multispectral (MS) and ALI-Pan images of Palolo valley, Indonesia. First row: ALI-Pan image; second row: left column HS and right column MS images. The rest are fused images which named based on fusion techniques (see acronym list).* 126
- Figure 5-2. Histograms comparison. (a) Hyperion bands 14, 21, 30; (b) ALI bands 2, 3, 4; (c) Hyperion fused by DWT-Haar; (d) ALI fused by DWT-Haar; (e) Hyperion fused by Brovey; (f) ALI fused by Brovey.* 128
- Figure 5-3. Final maps of DLDF procedures and SAM classification. (a) WBDF; (b) CBDF; (c) MCDF and (d) SAM.* 130

LIST OF TABLES

<i>Table 1-1. Summary: techniques in data fusion literature. Modified based on Zeng [2006].</i>	12
<i>Table 1-2. General categorization of multisensor data fusion. After Hall and Llinas, [2001].</i>	23
<i>Table 1-3. Civil applications of data fusion.</i>	25
<i>Table 1-4. Mostly first publications in DF.</i>	34
<i>Table 2-1. Scores for a fused image subjective quality assessment</i>	74
<i>Table 4-1. EO-1 sensor characteristics. After Richards [2006]</i>	105
<i>Table 4-2. Spectral overlap bands between VNIR (50-57) and SWIR (71-78).</i>	107
<i>Table 4-3. Statistic: Signal-to-noise ratios for four overlap bands.</i>	107
<i>Table 4-4. Bands with defected columns.</i>	109
<i>Table 4-5. Spectral and spatial resolutions of ALI. After USGS, EO-1 user's guide [2007].</i>	112
<i>Table 4-6. Selected bands from three Hyperion datasets after pre-processing.</i>	113
<i>Table 5-1. Spectral quality metrics. Wald's properties 1 and 2 for MS dataset.</i>	117
<i>Table 5-2. Spectral quality metrics. Wald's properties 1 and 2 for HS dataset)</i>	118
<i>Table 5-3. Spatial quality metrics.*</i>	119
<i>Table 5-4. Selected bands based on two explored feature selection procedures.</i>	129
<i>Table 5-5. Accuracy of DLDF techniques in compare to SAM classifier*.</i>	129
<i>Table 5-6. Selected bands using three different feature selection methodologies (Iran dataset).</i>	131
<i>Table 5-7. The spatial and spectral accuracies of selected subsets*.</i>	131
<i>Table 5-8. Block based feature reduction. Selected bands and their statistical properties. Hyperion dataset, Palolo valley, Indonesia, 2004.</i>	133
<i>Table 6-1. PLDF techniques ranked based on the ability of techniques to preserve the spatial and spectral properties of fused images.</i>	136

LIST OF ACRONYMS

Acronym	Definition
$d_{Earth-Sun}$	<i>Earth-Sun distance in astronomical units</i>
$ESUN_{\lambda}$	<i>mean solar exoatmospheric irradiances</i>
θ_s	<i>the solar zenith angle in degrees</i>
1DWT	<i>One-Dimensional Wavelet Transform</i>
2DWT	<i>Two-Dimensional Wavelet Transform</i>
ALI	<i>Advance Land Imager</i>
ARSIS	<i>French: amélioration de la résolution spatiale par injection de structures. English: improvement of spatial resolution by structure injection</i>
ATWT	<i>A Trous Wavelet Transform</i>
AVIRIS	<i>Airborne Visible Infrared Imaging Spectrometer</i>
AVIRIS	<i>Airborne Visible Infrared Imaging Spectrometer</i>
BBFR	<i>Block Based Feature Reduction</i>
BD	<i>Bhattacharyya Distance</i>
Bel	<i>Belief</i>
BT	<i>Brovey Transformation</i>
BT	<i>Bayesian Theorem</i>
C.V.	<i>Coefficient of Variances</i>
CBDF	<i>Class-Based Decision Fusion</i>
CN	<i>Color Normalized</i>
CTF	<i>Classification-Then-Fusion</i>
D	<i>Downsampled (from 10 to 30 m)</i>
DBFR	<i>Data Based Feature Reduction</i>
DEM	<i>Digital Elevation Model</i>
DF	<i>Data Fusion</i>
DLDF	<i>Decision Level Data Fusion</i>
DST	<i>Dempster-Shafer Theory</i>
DWT	<i>Discrete Wavelet Transformation</i>
DWT	<i>Discrete Wavelet Transform</i>
EARSeL	<i>European Association of Remote Sensing Laboratories</i>

ELINT	<i>Electronic Intelligence</i>
EM	<i>Electromagnetic spectrum</i>
EO-1	<i>Earth Observation one</i>
EO-1	<i>Earth Observation one</i>
ERGAS	<i>French: erreur relative globale adimensionnelle de synthèse. English: relative dimensionless global error in synthesis.</i>
ESM	<i>Electronic Support Measures</i>
EST	<i>Energy Subdivision Transform</i>
EST	<i>Energy Subdivision Transform</i>
F	<i>Fused image</i>
FE	<i>Feature Extraction</i>
FFT	<i>Fast Fourier Transform</i>
FLDF	<i>Feature Level Data Fusion</i>
FR	<i>Feature Reduction</i>
FS	<i>Feature Selection</i>
FSG	<i>Fan Sensor Geometry</i>
FST	<i>Fuzzy Set Theory</i>
FTC	<i>Fusion-Then-Classification</i>
GIS	<i>Geographical Information System</i>
GST	<i>Gram-Schmidt Transformation</i>
H	<i>High spatial resolution</i>
HFI	<i>High Frequency Information</i>
HFM	<i>High Frequency Modulation</i>
HPF	<i>High-Pass Filtering</i>
HS	<i>Hyperspectral</i>
HVS	<i>Human Vision System</i>
IEEE	<i>Institute of Electric and Electronic Engineers</i>
IFF	<i>Infrared Identification Friend Foe</i>
IFOV	<i>Instantaneous Field Of View</i>
HIS	<i>Intensity, Hue, Saturation</i>
IS	<i>Image Spectrum</i>
ISPRS	<i>International Society for Photogrammetry and Remote Sensing</i>
JDL	<i>Joint Directors of Laboratories</i>

Kb	<i>Kilo Bite</i>
KC or κ	<i>Kappa Coefficient</i>
L	<i>Low spatial resolution</i>
LAC	<i>LEISA Atmospheric Corrector</i>
LEISA	<i>Linear Etalon Imaging Spectral Array</i>
LOGP	<i>Logarithmic Opinion Pool</i>
LS	<i>Library Spectrum</i>
LUT	<i>Look Up-Table</i>
M	<i>meter</i>
MCDF	<i>Multi-Classifier Decision Fusion</i>
MIR	<i>Middle Infra Red</i>
MIT	<i>Massachusetts Institute of Technology</i>
MLC	<i>Maximum Likelihood Classifiers</i>
MNFT	<i>Minimum Noise Fraction Transformation</i>
MODTRAN	<i>Moderate resolution atmospheric Transmission</i>
MOS	<i>Mean Opinion Score</i>
MS	<i>Multispectral</i>
MSM	<i>Multiscale Model</i>
MSSI	<i>Maximum Spectral and Spatial Information Indicator</i>
MTI	<i>Multi-Temporal Image</i>
NASA	<i>National Aeronautics and Space Administration</i>
NDA	<i>Normalized Difference of Autocorrelations</i>
NDE	<i>Normalized Difference of Entropy</i>
NIR	<i>Near Infra Red</i>
NMP	<i>NASA's New Millennium Program</i>
NNC	<i>Neural Network Classifier</i>
OA	<i>Overall Accurassy</i>
PA	<i>Producer Accurassy</i>
Pan	<i>Panchromatic</i>
PCT or PCA	<i>Principal Component Transformation or Analysis</i>
PLDF	<i>Pixel Level Data Fusion</i>
Pls	<i>Plausibility</i>
PSNR	<i>Peak Signal to Noise Ratio</i>
RDM	<i>Relative Difference of Means</i>
RDV	<i>Relative Difference of Variances</i>

RGB	<i>Red, Blue, Green</i>
RS	<i>Remote Sensing</i>
RSDF	<i>Remote Sensing Data Fusion</i>
RT	<i>Radon Transform</i>
RTM	<i>Radiative Transfer Model</i>
RWM	<i>Ranchin, Wald, Mangolini</i>
SAM	<i>Spectral Angle Mapper</i>
SAR	<i>Synthetic Aperture Radar</i>
SEE	<i>Society for Electricity and Electronics</i>
SF	<i>Sharpening Factor</i>
SFIM	<i>Smoothing Filter based Intensity Modulation</i>
SNR	<i>Signal to Noise Ratio</i>
SO	<i>Spectral Overlap</i>
SRTM-2	<i>Shuttle Radar Topography Mission-Two</i>
SSIM	<i>Structural Similarity</i>
St.D.	<i>Standard Deviation</i>
STORMA	<i>The Stability of Rainforest Margins in Indonesia</i>
SVA	<i>Stacked Vector Approach</i>
SVM	<i>Support Vector Machine</i>
SWIR	<i>Short Wave Infra Red</i>
TD	<i>Transformed Divergence</i>
TDWT	<i>Two-Dimensional Wavelet Transform</i>
TIMS	<i>Thermal Infrared Multispectral Scanner</i>
TRW	<i>Thompson Ramo Woolridge</i>
U	<i>Upsampled (e.g. from 30 to 10 m)</i>
UA	<i>User Accuracy</i>
UIQI	<i>Universal Image Quality Index</i>
Vis.	<i>Visible</i>
VISSR	<i>Visible Infrared Spin Scan Radiometer</i>
VL	<i>Very Low Resolution</i>
VNIR	<i>Visible and Near Infra Red</i>
WBDF	<i>Wavelength-Based Decision Fusion</i>
WT	<i>Wavelet Transformation</i>
Mm	<i>Micro meter</i>

INTRODUCTION

Remote Sensing (RS) is the acquisition of information of an object or phenomenon, by the use of some device(s) that are not in physical or intimate contact with the object or phenomenon [Campbell, 2002]. In the last four decades a high number of earth remote sensing systems have been used, assessed and contemplated for detection and evaluation of land surface materials and objects. The applications of remotely sensed imagery are very diverse and also most of the image sensors are designed for specific purposes; therefore, for some applications they are incomplete while for some others are redundant or complementary. For example the information contained in hyperspectral and multispectral datasets provide a valuable basis for environmental studies while the low spatial resolution characteristics of these datasets reduce their performances in many applications. Data Fusion (DF) is a formal framework in which the means and tools for the alliance of data originating from different sources are summarized. It aims at obtaining information of enhanced quality where the exact definition of the term “quality” will depend upon the application of fused datasets [Wald, 1999]. The RS instruments provide a huge number of diverse datasets that can not be studied in such a work thus we limited the objectives of this research on the evaluation of datasets obtained by optical passive remote sensing satellite imager (i.e. EO-1/Hyperion and ALI). The developed methodologies are multi-sensor frameworks of data fusion using three modalities of datasets: Panchromatic (Pan), Multispectral (MS) and Hyperspectral (HS). Due to the nature of RS imagery it could be denoted that diverse physical properties of materials are measured by different sensors from different points of view. For instance panchromatic images produce data at higher spatial resolution while they suffer from the lack of high spectral quality and on the contrary MS and HS sensors are providing images with lower spatial resolution but they have the advantages of higher spectral resolution. In such circumstances, multi-sensor data fusion to make beneficiary from all available datasets is supposed to be an effective paradigm for increasing the usability of remotely sensed imagery.

In the literature, the most common forms of fusion is putting various sensors together in order to detect and parametrically evaluate a sensed object, therefore as synergetic fused dataset is more useful than the original individual datasets for a specific application. As stated by several authors (see chapter one, literature review and data fusion applications), data fusion is useful for several purposes such as land surface objects and phenomena detection, recognition, identification, tracking, classification, etc. These objectives may be encountered in many fields of study like remote sensing, defense systems, robotics, medicine, space, environmental, urban, agricultural studies, etc. Based on Dasarthy [1994]; Pohl and Van Genderen [1998] and Hall *et al.* [2004] data fusion processes are formally categorized into three levels of processing: pixel, feature and decision. Notwithstanding the fact that this triple categorization does not perfectly cover all possible fusions, we have adapted 2 levels (i.e. pixel and decision) of fusion as the subject of this thesis. Of course in the literature several hybrid fusion methodologies are introduced and strict borders of this categorization are not always obeyed.

The nature of remote sensing images

During the last four decades, remote sensing image acquisition systems have offered a huge amount of information to the community of geo-scientists, environmentalists, geographers, etc to identify and characterize the properties of entities, objects and phenomena of the Earth. For example agricultural resources monitoring, natural resources management, man-made and natural disasters monitoring and predicting, etc are very common examples of the applications of these images.

From the technical point of view remotely sensed energy which emitted or reflected from the Earth's surface is measured using a sensor mounted on an airborne or space-borne platform. The measured energies are used to produce an image from the landscape beneath the platform [Richards, 2006]. Remote sensing images can be categorized by their spatial, spectral, radiometric, and temporal resolutions and also coverage characteristics. Spatial resolution is described by the pixel size [Richards,

2006] or the size of smallest detectable (or sensible) object from the under investigation area. Spectral resolution or the number of bands in a dataset is expressed as sensor's bandwidth over which a sensor collects information from the understudy scene. Radiometric resolution is expressed in terms of the number of binary digits or bits which are necessary to represent the range of available brightness values. For example data with 8 bit radiometric resolution has 256 levels of brightness. The temporal resolution refers to the time elapsed between consecutive images of the same ground location taken by a sensor. Finally coverage characteristic of a sensor (i.e. swath width) refers to the extent of the Earth's surface from which data are collected that expressed as the length and width of one scan line of a remote sensing imager. E.g. the swath width of EO-1/Hyperion is 7.7 km, whereas for EO-1/ALI it is 37 km. Because of these magnificent possible kinds of satellite image resolutions, they are in the interest of the community of scientists and users of these datasets. Consequently the optimized application and exploitation of such data sources is due to the development of appropriate data fusion techniques.

Image resolution and data fusion

From the technical and economical viewpoints, any incensement in any kinds of resolutions will result in an increase of the volume and costs of the collected datasets. As a general rule, in any remote sensing system data properties must be a trade off between next parameters: transmission rate, the capacity of instrument, archiving and storage largeness, and the data handler and image processing capabilities. Consequently, an increase in one type of resolution usually has to be counterbalanced by a decrease in other ones.

Two important resolutions that are concerned in this work are the spatial and spectral. The relationship between these two properties of datasets mostly is a function of the sensor specific Signal to Noise Ratio (SNR). To achieve a specific level of SNR, the emitted or reflected energy from object must has enough power to stimulate the sensor's detectors. Due to the size of the Instantaneous Field Of View (IFOV) of a

sensor the power of reflected energy will decrease over a wider IFOV [Richards, 2006] therefore the spectral coverage of a band (bandwidth) must be increased to compensate the shortage of energy and vice versa. Therefore, with a fixed SNR for a sensor, spatial and spectral resolutions are in balance. In this regard, from one hand the simultaneous improvement of sensor's spatial and spectral resolutions is bounded by the mentioned limitations (e.g. data volume and signal to noise ratio) and in other hand users of these data want both, high spatial and spectral resolutions. In order to alleviate this problem, remote sensing systems which simultaneously carry two or more sensors (e.g. Landsat/ETM+ with multispectral and panchromatic sensors and EO-1 with hyperspectral, multispectral and panchromatic sensors) are very rapidly developing. However, the appropriate data fusion techniques which are robust for the exploitation of such multi-modality datasets still needed to be investigated.

Based on the definition of Wald [1999] the main goal of data fusion is to obtain greater quality. Consequently and expectedly the fused datasets will have a higher information content compared to any individual imagery. As the number of data fusion applications concerning the combination of multi-sensor images is dramatically high, therefore a high number of data fusion techniques and methodologies can be found in the literature, for example, Van Genderen *et al.* [1994]; Pohl *et al.* [1998] and Wald [1999 and 2002].

Based on the intended applications, the fusion process can be carried out at three levels of processing: pixel, feature and decision. Pixel Level Data Fusion (PLDF) techniques which combine the spatial information from a lower spectral but higher spatial resolution image (e.g. ALI-Pan) with the higher spectral but lower spatial resolution image (e.g. ALI-MS) in order to produce a high spatial and spectral resolution image [Sunar and Musaoglu, 1998 and Chavez, 1996]. Feature Level Data Fusion (FLDF) is the process of fusing the extracted features from pre-processed input datasets and merging them based on some mechanisms in which the final results will have the highest possible accuracy. In this level of process features correspond to obtained properties which are highly related to their circumstances in the data source like texture, extent, shape and neighborhood [Mangolini, 1994].

Decision Level Data Fusion (DLDF) methods work based on post classification or post analysis fusion of classified data or information (i.e. decisions or class labels which can be hard or soft labels) by a proper fusion algorithm.

Research background

Prior to this PhD work an almost in-depth literature study on methodologies, applications, limitations and abilities of data fusion, especially in PLDF, was performed. Some experimental researches were carried out and the obtained results were discussed and published (Appendix II). From the studied literature and the obtained experiences from “primary testing phase” some limitations became visible which underlined the goals of this work:

1. The need for a comprehensive comparison of PLDF techniques.
2. The limited evaluation techniques where most of the common quality measurements were based on image spectral quality.
3. The lack of comparison between hyperspectral and multispectral in fusion with panchromatic datasets.
4. The ability of EO-1 datasets in the framework of DF.
5. The problematic phenomenon of high dimensional hyperspectral images for fusion process.

In order to fulfill these necessities and shortages, the main topic of this work was defined as “Remotely sensed data fusion as a basis for environmental studies: concepts, techniques and applications”.

Research motivations

The three mentioned levels of data fusion constitute the fundamentals of remotely sensed DF. Within this thesis two of the three levels were investigated, namely PLDF and DLDF. These two levels of data fusion are related to two main groups of

remote sensing data analysis and applications: Visual interpretation by means of PLDF and image classification by means of DLDF.

Following the performed investigations in DF, some experimental works were carried out which motivated the objectives of this work. For instance, from preceding experimental works in Darvishi Boloorani *et al.* [2006¹] the synergetic fusion of spectral information from multispectral dataset and spatial information from panchromatic imagery in urban land cover and land use mapping using Ikonos imagery were investigated; in Darvishi Boloorani *et al.* [2006²] the ability of combined multi-temporal ENVISAT/ASAR satellite Synthetic Aperture Radar (SAR) images for monitoring and temporal discrimination of fields under different rice cropping systems (Palolo valley, Central Sulawesi, Indonesia) were investigated; in Darvishi Boloorani *et al.* [2005¹] the quality of fused images using Principal Component Transform (PCT) and Gram-Schmidt Transformation (GST) fusion techniques in the spectral domain were investigated. Accordingly, three datasets were evaluated as EO1- Hyperion, Quickbird-MS and SPOT-panchromatic; and in Darvishi Boloorani *et al.* [2005²] the usability of fused Landsat ETM+ multispectral and panchromatic images was evaluated for urban road network extraction (Tehran, Iran). In this work three different kinds of PLDF techniques were verified and evaluated (see appendix II).

Therefore in order to fulfill the above-mentioned limitations and based on these experiments the main objectives of this study were:

1. Making comprehensive investigations into the concepts, techniques, limitations, strengths and applications of data fusion.
2. Investigate the quality of pixel level fused images from spectral and spatial points of view.
3. Introducing new methodologies for hyperspectral dimension reduction for the purpose of data fusion.
4. Comparing hyperspectral with multispectral datasets in fusion with panchromatic imagery.

5. Investigating the potentials of EO-1 datasets at pixel and decision levels of fusion.

Since the Earth Observation-One (EO-1) sensors offer three modalities of spectral resolutions and two different spatial resolutions (Hyperion-hyperspectral with 242 spectral bands and 30 m spatial resolution; ALI-multispectral, with 9 spectral bands and 30 m spatial resolution and ALI-panchromatic with 10 m spatial resolution) therefore, it was found to be an ideal remote sensing dataset for the purposes of this work.

Two different study areas in different parts of the world were selected for the evaluation intentions. The first study area is located in Palolo valley, central Sulawesi, Indonesia which covers a variety of land surface classes. Therefore this very heterogynous area is ideal for the evaluation of PLDF techniques. The second area is in Ahmadabad, south Tehran, Iran which is an almost homogenous agricultural area. This area is an almost ideal study area for post classification DLDF techniques evaluation.

Thesis outline

This thesis demonstrates how data fusion techniques were used for remotely sensed datasets. The thesis is organized in six chapters; beginning with introduction and background discussions followed by exploitation and investigations and development of data fusion techniques. Finally the accuracy of methodologies is assessed and some conclusions and recommendations are addressed.

Chapter 1 presents the general background and applications of data fusion. In this chapter various data fusion methodologies found in literature are described. The definitions and categorizations of DFs are introduced. The referenced scientific documents provide invaluable sources for scientists interested in data fusion and more specifically remotely sensed image fusion. Non-military applications of DF in

several aspects of remotely sensed image analysis are explained. Also military and none remotely sensed data fusion techniques like medicine imagery are mentioned.

Chapter 2 describes the details of pixel level data fusion as a tool for increasing the spatial resolution of datasets (i.e. hyperspectral and multispectral image which have higher spectral resolution) by combining with a higher spatial resolution (i.e. panchromatic image). A pixel level data fusion categorization has been adapted. The most common techniques have been explained. Two novel fusion procedures as fanbeam and Radon fusions are introduced. Feature reduction is explained. An innovative feature selection methodology named Maximum Spectral and Spatial Information Indicator (MSSI) is offered. As the numbers of Pan-sharpening (or PLDF) techniques is dramatically high therefore, we just tried to explore the most common ones. The metrics used for quantitative assessment of the Pan-sharpened images are described in details.

Chapter 3 gives details of decision level data fusion. As this kind of fusion relies on the information or decisions provided by classifiers, therefore, some of the most powerful soft classifiers i.e. Fuzzy, Bayes and Dempster-Shafer were explored. Two new developed decision level data fusion techniques named Wavelength Based Decision Fusion (WBDF) and Class Based Decision Fusion (CBDF) are explained.

Chapter 4 describes the data sources and test areas. The Earth Observation One (EO-1) Hyperion hyperspectral, ALI multispectral and ALI panchromatic datasets are explained. The needed pre-processing procedures are outlined. Finally, the test areas that are located in Iran and Indonesia are introduced.

Chapter 5 examines the results obtained from the mentioned different fusion techniques. Also the accuracy of feature reduction procedures is evaluated.

In chapter 6 conclusions are drawn. Based on the accuracy of the obtained results and the purposes of the work some conclusions are drawn. The benefits and limitations of present data fusion techniques are illustrated. Finally some suggestions for future works are mentioned.

In appendix I some useful data fusion organizations are addressed and some useful web-based addresses are mentioned; in appendix II the author's publications in data fusion during the four years of study in data fusion are listed.

CHAPTER ONE

1 Literature review and data fusion applications

Data Fusion, as a general term, has different definitions, categorizations and applications. Before going into the contexts of Remote Sensing Data Fusion (RSDF), having a closer look to the exploitation of data fusion in biological systems can make better clarification on the topic. Human sensors acquire information on sight, smell, touch, hearing and taste. In the brain all collected information will be processed in combination with other sources of information that is called a priori knowledge e.g. memory and earlier experiences. Based on reasoning abilities of the mind, fusion of all input data and information will produce a representation of the sensed object in the mind and a proper order of action will be issued [Wald, 2002] (Figure 1-1). These sensing, fusion and action procedure is a perfect biological model that can be simulated for data collection, fusion and decision making to solve specific problems in earth phenological applications using remotely sensed images.

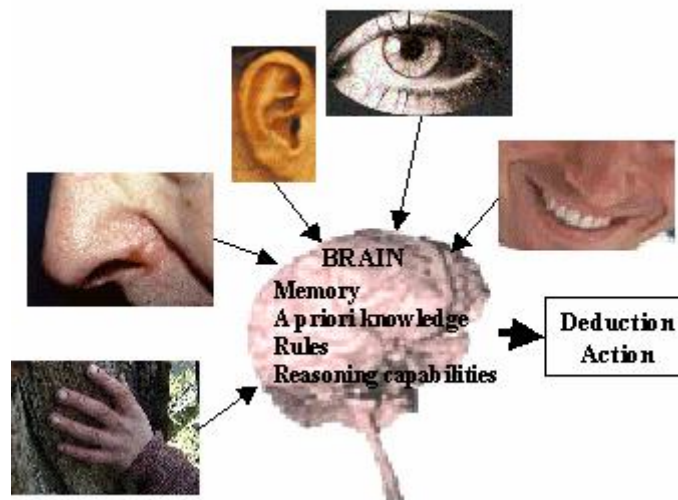


Figure 1-1. The human brain and perception system: a biological fusion process.
After Wald [2002].

Fusing remote sensing datasets is like a framework in which in one hand the higher spectral satellite like hyperspectral sensors supply enough spectral bands which are good for spectrally object discrimination and identification and in another hand high spatial resolution panchromatic satellite sensors provide finer spatial resolution for spatially object separation. From the application point of view the combination of these data sources can provide more information than that could be achieved by the use of a single sensor alone [Wang *et al.* 2005]. Some of the most important techniques have been summarized in table (1-1). As will be discussed in next sections of this chapter there are almost three main levels of data fusion algorithms: pixel, feature, and decision. Here pixel and decision levels are chosen for the purpose of spatial resolution enhancement and classification accuracy improvement.

The following section explains data fusion definitions from the viewpoint of most famous authors in this field of study. Second section introduces the main categorization of DF in the literature. Categorization based on processing level will be discussed in more details. Finally the most applications of DF are drawn.

Table 1-1. Summary: techniques in data fusion literature. Modified based on Zeng [2006].

Pixel level	Feature level	Decision level
Intensity, Hue, Saturation	Logical templates	Logical templates
Principal component transformation	Expert systems	Expert systems
Brovey transformation	Dempster-Shafer theory	Dempster-Shafer theory
Wavelet transformation	Neural network	Neural network
Gram-Schmidt transformation	Bayesian inference	Bayesian inference
High frequency modulation	Cluster analysis	Contextual fusion

High Pass Filter

Color normalization

ARSIS concept

Fuzzy logic

Voting strategies

Syntactic fusion

Classical inference

1.1 Data fusion definitions

The exact meaning of data fusion varied from one scientist to another and from one application to another. Indeed, DF is inter – and multidisciplinary by essence and is at the crossing of several sciences. Consequently making an exact definition is not so easy [Wald, 2002]. Here a short review to the literature of data fusion definitions is introduced and, finally, Wald’s definition [1999] as the accepted and most popular one will be discussed in more details.

- Data fusion as a group of methods and approaches using multi-sources data of different nature to increase the quality of information contained in the data [Mangolini, 1994]
- Labeling pixels by drawing inferences from several available sources of data is referred to as data fusion [Richards and Jia, 1999].
- Data fusion techniques combine data from multiple sensors and related information from associated databases, to achieve improved accuracy and more specific inferences that could be achieved by the use of a single sensor alone [Hall *et al.* 1997].
- Image fusion is the combination of two or more different images to form a new image by using a certain algorithm [Genderen *et al.* 1994].
- Data fusion is a process dealing with data and information from multiple sources to achieve refined/improved information for decision making [Hall, 1992].

Wald [1996] criticized most of these definitions that they are focusing too much on methods while paying little attention to quality. He also added that there is no reference to concept in them, while the need for a conceptual framework is clearly expressed by scientists and practitioners. Finally in [1996] after several meeting and discussions a European working group for data fusion in association with the French Society for Electricity and Electronics (SEE, French affiliate of the Institute of Electric and Electronic Engineers (IEEE)), the European Association of Remote Sensing Laboratories (EARSeL) and the European affiliate of the International Society for Photogrammetry and Remote Sensing (ISPRS) has been committed. Following to this symposium and based upon the works of Buchroithner [1998] and Wald [1997], the next definition was adapted “Data fusion is a formal framework in which are expressed the means and tools for the alliance of data originating from different sources. It aims at obtaining information of greater quality; the exact definition of greater quality will depend upon the application”. In this delineation in compare to earlier ones there is strong emphasis on framework and fundamentals underlying data fusion instead of on tools and means. The word “data” is used as a general word and can be replaced by information. In this delineation “quality” does not have very specific meaning and its satisfactory depends to “customer”. “Different sources” implies that spectral channels of a same sensor (e.g. Visible, VNIR, SWIR in hyperspectral imagers) are to be considered as different sources and also images taken by the same sensor at different times. This definition was adapted in this work and has been followed across the whole document. Also some other definitions based on principals, methods and tools of DF can be found in Van Genderen *et al.* [1994]; Pohl *et al.* [1998]; Wald [1999 and 2002].

1.2 Data fusion categorizations

In data fusion writings and literature and from the remote sensing community viewpoint, there are several assortments that four important ones are presented in this work. There are no hard lines to separate these categorizations because they are

categorized from some common aspects of remote sensing data fusions. These categorizations always have similarities and overlap with each other, for example based on Richards and Jia, [1999] consensus theory is one of the statistical approaches while it is categorized in decision fusion category by Pohl and Van Genderen [1998]. In this work the Schowengerdt assortment [1997], military categorization of Joint Directors of Laboratories (JDL), and categorization based on classification accuracy improvement are briefly mentioned. The levels-based categorization that is basis in this work is discussed in more details.

1.2.1 Schowengerdt categorization [Schowengerdt, 1997]

1. *Spatial domain fusion* in which mostly higher resolution image transfer into lower resolution image. E.g. High Frequency Modulation (HFM) was used by Munechika *et al.* [1993] over Landsat-TM and SPOT-panchromatic images for classification accuracy improvement.
2. *Spectral domain fusion* that is based on the original data spectral coordinates transformation into another spectral coordinate. E.g. Gram-Schmidt data fusion [Lanben and Brower, 2000] and Principal Component Analysis (PCA) [Chavez, 1991].
3. *Scale space techniques* which work based on the spatial information extraction in different range of scales. The techniques generally behave as filters but are applied repeatedly on scaled versions of the image (resolution pyramids). One of the most famous and popular method is wavelet transformation [Yocky, 1995 and Gauguet-Duport *et al.* 1996].

1.2.2 Categorization based on classification accuracy improvement [Richards and Jia, 1999]

1. *The Stacked Vector Approach (SVA)* in which different datasets will be overlaid (stacked) as one vector that will be treated in next steps of data processing like classification.

2. *Statistical approaches* that work mostly based on some statistical decision makers like posterior probability derived from Bayes theorem. For instance Shi *et al.* [2007] used the Bayes theorem to update prior estimates of changes in land cover maps. Consensus theory is another procedure in this category which implemented by Benediktsson *et al.* [1992] over four different datasets: Landsat-MSS, DEM, Slop and Aspect for land cover classification in mountainous area of Colorado, USA.
3. *The theory of evidence* in which data sources will separately be treated and combined based on their contribution. More details of implementations and sophisticated knowledge behind can be found in Richards and Jia [1999].
4. *Knowledge-based approaches* which deal with different datasets as separate sources of knowledge and try to combine this knowledge in a proper way based on some sophisticated rules. For example Richards and Jia [1999] used a knowledge based data fusion procedure over Landsat-MSS and L band SIR-B SAR images for urban area in Sydney, Australia.

1.2.3 Military based categorization of Joint Directors of Laboratories (JDL)

Level 1: object refinement is an iterative process of fusing data to determine the identity and other attributes of entities and also to build tracks to represent their behavior. The term entity refers here to a distinct object. A track is usually directly based on detections of an entity, but can also be indirectly based on detecting its actions.

Level 2: situation refinement is an iterative process of fusing spatial and temporal relationships between entities in order to bring them together and form an abstracted interpretation of the patterns in a battle data. The product from this level is called situation assessment.

Level 3: threat refinement is an iterative process of fusing the combined activity and capability of enemy forces to infer their intentions and assess the threat that they pose. The product from this level is called threat assessment.

Level 4: process refinement is an ongoing monitoring and assessment of the fusion process to refine the process itself and to regulate the acquisition of data to achieve optimal results (Klein, 1993).

The above mentioned categorizations have their properties and limitations that more insight and discussions can be found in Richards and Jia [1999]; Schowengerdt [1997]; Gross and Schott [1998]; Benediktsson [1992 and 1997]; Hall [1992]; and Klein [1993].

1.2.4 Categorization based on processing level

1. Pixel (Measurement) level data fusion.
2. Feature level data fusion.
3. Decision (information) level data fusion.

This categorization is the basis to outline in this thesis. Wald [1999] highlighted two drawbacks for level-based data fusion categorization. He mentioned that pixel is only a support of information and it does not carry any semantic significance. Therefore, pixel can not carry the true means of data fusion. In this level also this categorization may wrongly imply that DF can not be lunched simultaneously within all levels. For the first problem Wald [2002] proposed measurement, signal, or observation as appropriate words than pixel. In addition, for the second drawback he mentioned that several papers and works are found which use a combination of three levels as the possible crossing between levels can be easily done. Despite the mentioned drawbacks this categorization is still one of the most popular categorization of data fusion. Thus it has been adapted in this work and the rest of this document will follows this framework.

1.2.4.1 Pixel (measurement) Level Data Fusion (PLDF)

Image fusion at pixel level means fusion at the lowest processing level, referring to merging of measured physical parameters (e.g. pixels) [Pohl *et al.* 1994]. From the literature of PLDF there are a large number of techniques used over an indefinite number of datasets each of which is for a specific application. As here this whole cannot punctually be reviewed consequently we looked over mostly common PLDF techniques: Intensity–Hue–Saturation (IHS), Brovey transform, principal component transformation, wavelength and Gram-Schmidt techniques, which are used and evaluated by our team group in the Stability of Rainforest Margins in Indonesia (STORMA) project. In addition to these techniques two innovative fusion procedures named fanbeam and Radon are introduced and evaluated. For getting an overhead view to a detailed literature, see reviews by Pohl and Van Genderen [1998] and Wald [1999 and 2002]. Figure (1-2) shows general flow diagram of PLDF which is followed by mentioned techniques in this level of fusion.

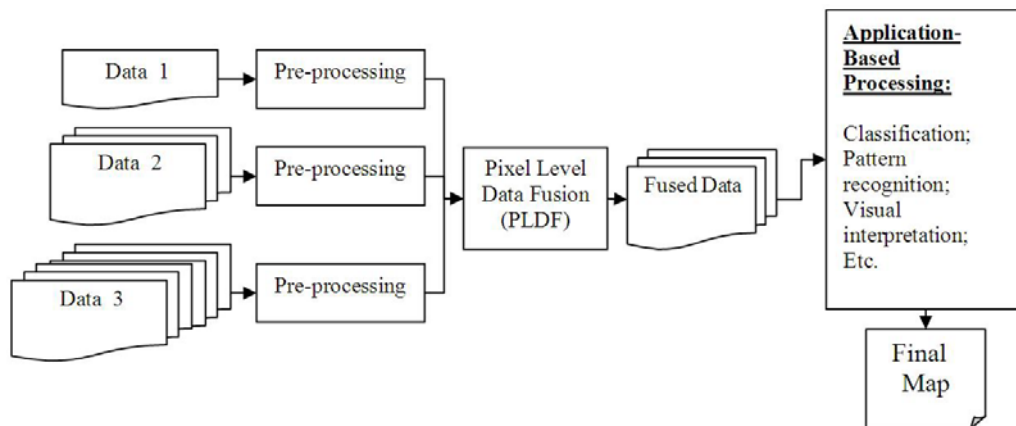


Figure 1-2. Block diagram of pixel level data fusion procedure.

1.2.4.2 Feature Level Data Fusion (FLDF)

In order to fuse at feature level first features from different data sources are extracted, than they will be fused in a common framework. In this level of process features correspond to obtained properties are highly related to their circumstances in the data sources like extent, shape and feature neighborhood properties [Mangolini, 1994].

Therefore, similar objects (e.g. regions) [Pohl and Van Genderen, 1998] from multiple sources will be fused using a framework that can be parametric like Bayesian theorem or non-parametric like artificial neural networks. Figure (1-3) illustrates the general routine of FLDF process.

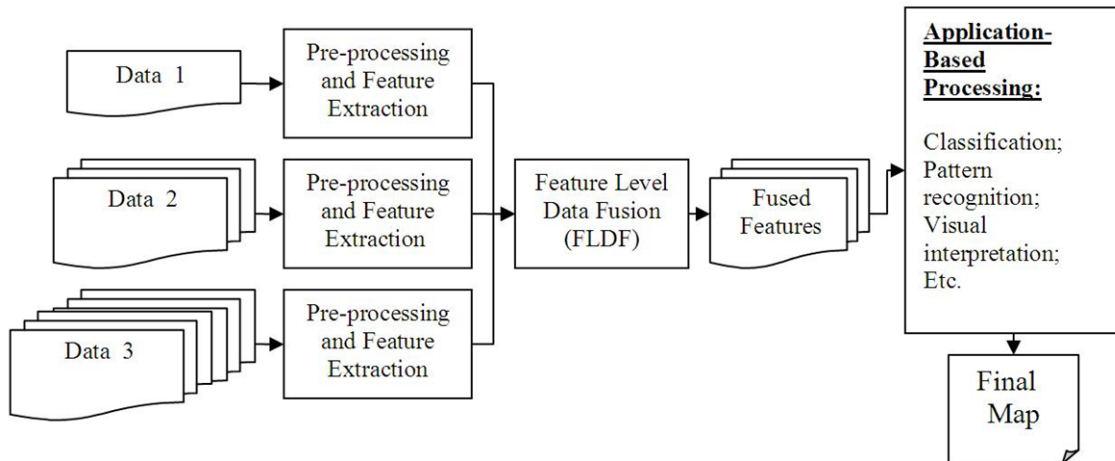


Figure 1-3. Block diagram of data fusion at feature level.

1.2.4.3 Decision Level Data Fusion (DLDF)

DLDF like other levels of data fusion has some different definitions in the literature. For example Pohl and Van Genderen [1998] defined decision fusion (adapted from Shen [1990]): “Decision or interpretation level fusion represents a method that uses value-added data where the input images are processed individually for information extraction”. The obtained information is then combined applying decision rules to reinforce common interpretation and resolve differences and furnish a better understanding of the observed objects. Benediktsson and Kanellopoulos [1999] made an explanation that “Decision-level data fusion is the process of fusing information from several individual data sources after each data source has undergone a preliminary classification” (Figure 1- 4). In the DLDF writings several methods are discussed and evaluated. If the techniques based on their abundance of application be listed probably Bayesian theorem is the first that followed by Dempster-Shafer Theory (DST), Fuzzy Set Theory (FST), Neural Network (NN), etc. in this work DST

has been carried out and evaluated for comparison the two new procedures in this level of fusion (i.e. WBDF and CBDF). For more explanation see chapter 4.

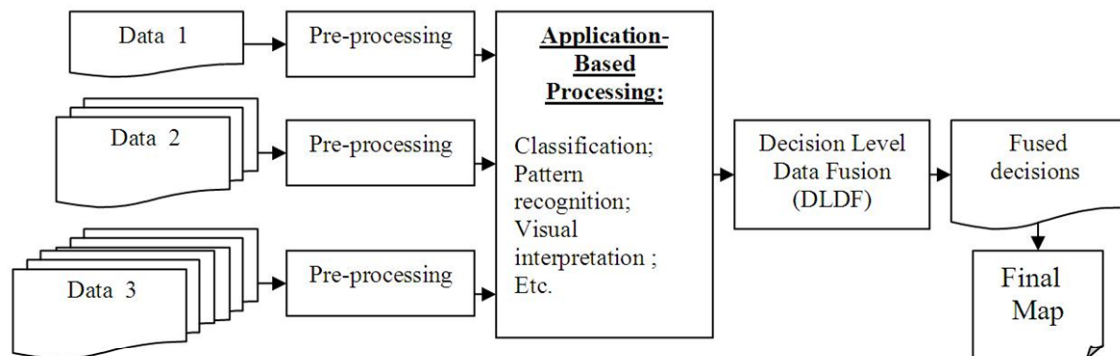


Figure 1-4. Block diagram of data fusion at decision level of processing.

1.3 Why more and new data fusion algorithms?

From the launch of the first Landsat (23/07/1972) a huge number of data fusion algorithms and techniques have been developed, adapted, evaluated and documented. But this field of study is still fresh and there is more room for work, research and improvement. The reason is return to dynamic nature of remote sensing and data fusion as well. As a general rule next parameters are the most important reasons to make new algorithms and developments.

1. Increasing demands of the users for data with higher and higher spectral, spatial, radiometric and temporal resolutions.
2. Availability of new and divers satellite images with better and better resolutions
3. Diversity of the fused data applications is getting higher and higher.
4. Development the new software and hardware facilities for remotely sensed data analysis is facilitating the usage of data more and more.
5. More than the usage of DF in satellite imagery combination, the applicability of these techniques in other data sources for environmental applications e.g. GIS, urban planning and utility, traffic, etc are fast growing up.

6. None-remotely sensed applications like medicine and military activities are other very fast growing domains of DF.

1.4 Data fusion applications

Data fusion has been the objective of very many researches from the beginning of remote sensing. In this regard, many works have recognized the benefits of fusion high spectral and spatial resolution images. For instance, DF has been used in many aspects of RS image analysis: multi sensor fusion [Pohl and Van Genderen, 1998]; image processing and analysis [Mascle *et al.* 1998]; classification [Chen *et al.* 2005]; image sharpen [Chavez *et al.* 1991]; improve geometric corrections [Strobl *et al.* 1990]; provide stereo-viewing capabilities for stereophotogrammetry [Bloom *et al.* 1988]; land mapping applications [Wald *et al.* 1997]; enhance certain features not visible in either of the single data alone [Leckie, 1990]; complement datasets for improving classification accuracy [Schistad-Solberg *et al.* 1994]; etc. Single data sources usually offer limited information due to their limited maneuver abilities in the data collection.

The ideal of data fusion is getting the highest potential of the fused images; the highest potential can be defined as any properties of dataset. Nevertheless, in reality despite developing new techniques and algorithms, fused data eventually losses some useful information. The literature of data fusion covers high variety of data, techniques, and applications. Therefore no rule of thumb exists for making borders of data fusion's applications and objectives. For example some methods are useful for visual interpretation [Gross and Schott, 1997] and some others are needed for classification and spectral information analysis. For instance Liu [2000] used Smoothing Filter-based Intensity Modulation (SFIM) over TM and SPOT-Pan images of south-east Spain for improving spatial details for soil and lithology studies; Yocky [1995] discussed the theoretical framework of IHS and also mentioned that this transform technique distorts colors (especially red color), as he compared DWT with IHS for fusion of panchromatic and MS images. He mentioned

that the wavelet merger performing better and preserving spectral–spatial information for the test images. Chavez *et al.* [1991] compared three different methods including PCT, IHS and High-Pass Filter (HPF) over Landsat-MS and SPOT-Pan images, they made insight these techniques based on spectral characteristics using statistical, visual and geographical properties of fused images and finally mentioned that HPF gives better results than other techniques, PCT and IHS. Zhou *et al.* [1998] performed a quantitative comparison between wavelet transformations of WV4 and WV8, IHS, PCT and Brovey for the sake of merging Landsat-TM and SPOT-Pan images; they concluded, in compare to other techniques, WV4 achieves the best spectral quality in all bands except in band 4, whereas WV8 achieves the best spatial quality in all bands. PCT works in a similar way as the IHS method, but with the main superiority that an infinite number of bands can be used [Zhou *et al.* 1998]. In another example Bradley [2003] stated that in comparison with other techniques the spectral fidelity of the Pan-sharpened images obtained with the discrete wavelet transform is excellent. The DWT is not “shift invariant” [Bradley, 2003] which means small spatial displacements in the input array can cause major variations in the wavelet coefficients; at their various scales. This technique has no effect on perfect reconstruction and simply lossless inverts transformation can be carried out. However a small misalignment can occur when the multispectral bands are "injected" into the panchromatic image pyramid. This sometimes leads to spatial artifacts (blurring, shadowing, and staircase effect) in the sharpened image [Yocky, 1996]. Another matter of fact is about IHS, in compare to color related techniques like CN and Brovey, that it has the ability to vary IHS component independently, without affecting other components [Lillesand *et al.* 2004]. This property causes very good results than the CN and Brovey.

Thanks to the high numbers of sensors and availability of multi-sensor images in many domains of applications like remote sensing, computer vision, military applications and medical imaging data fusion has become an attractive and effective field of research in recent years. For managing and surveying the environmental phenomena caused by the unprecedented pressure on all over the glob, more than any

other application the use of data fusion in environmental studies is crucially needed. Due to the complexity of the Earth phenomena mostly the obtained information by single sources of data are insufficient, incomplete and incompatible. In this regard a multi-sensor data source is expected to alleviate the shortages and problems. Hall and Llinas, [2001] mainly categorized DF applications into military and non-military which are summarized in table (1-2).

Table 1-2. General categorization of multisensor data fusion. After Hall and Llinas, [2001].

Application	Inferences Sought	Primary Observable Data	Surveillance Volume	Sensor Platform
Ocean surveillance	Detection, tracking and identification of targets and events.	Acoustics; Electromagnetic radiation and Evidence of nuclear radiation.	Hundreds of nautical miles; Air, surface and subsurface.	Ships; Aircraft; Submarines; Ground-based and Ocean-based.
Strategic warning and defense	Detection of indications of impending strategic actions and Detection and tracking of ballistic missiles and warheads.	Electromagnetic radiation. Nuclear particles.	Global surveillance.	Satellites; Aircraft.
Law enforcement	Transportation and location of drug shipments	Electromagnetic radiation; Acoustics.	Country and state borders.	Tethered balloons; Aircraft and Ground-based.

Remote sensing	Identification, location of mineral deposits, crop and forest conditions.	Electromagnetic radiation; Human reports and observations.	Hundreds of miles.	Aircraft; Satellites and Ground-based.
Automated monitoring of equipment	Status and health of equipment; Identification of impending fault conditions.	Electromagnetic radiation; Acoustic emissions; Vibrations; Temperature and pressure and Human observations.	Volume of the monitored machine or factory.	Organic sensors associated with the machine or factory.
Medical diagnosis	Diagnosis of disease, tumors and physical condition.	Electromagnetic radiation; Nuclear magnetic resonance; Chemical reactions; Biological data and Human observations.	Volume of the human body or observed component.	Sensors placed in and around the body.
Robotics	Identification and location of obstacles	Electromagnetic radiation	Near-location about the robot	Robot platform

1.4.1 Non-military Applications

The applications of data fusion for civil purposes have a long history as the availability of the remotely sensed data. The reality of remotely sensed imagery is the robustness for some applications and shortage in some others. For example hyperspectral imagers like EO-1/Hyperion have good spectral presentation but suffering from low spatial resolution and on the contrary the Quickbird/panchromatic satellite imager suffering from the lack of high spectral resolution. For this reason, In any case of application if the different characteristics of images like high spectral and high spatial resolutions are simultaneously needed, data fusion is a suggested and

recommended procedure. As a general rule there is not a fixed recipe for using data fusion and it depends to very many parameters like data sources, applications, user needs, techniques, etc. Based on this background here is tried to give some tips in table (1-3) to make a short insight into the concept.

Table 1-3. Civil applications of data fusion.

Application	Data*
Agricultural purposes	MTI, MS, HypI, HSpatRI, VLSpatRI
Natural resource management	MS, Pan
Forestry	MS, Pan
Water management	MS, HSpatRI,
Land use and land cover mapping	MS, HSRI, HypI,
Weather and climatology	LSpatRI, MS, VLSpatRI
Environmental monitoring	MTI, MS, Pan
Urban planning	HSpatRI, HypI
Transportation	HSpatRI, MTI
Traffic controlling	VHMTI, VHSpatRI
Change detection	MTI, MS, HSpatRI, HypI
Geology and exploration	HypI, RSI,
Marin and Coastal	RSI, MS
Cartography	HSpatRI, LSpatRI

*Multi-Temporal Images (MTI), High Spatial Resolution Images (HSpatRI), Panchromatic (Pan), Hyperspectral Image (HypI), Very Low Spatial Resoluion Image (VLSpatRI), Low Spatial Resolution Image (LSpatRI), Very High Spatial Resolution Image (VHSpatRI), Very High Multi Temporal Image (VHMTI), Radar and Sar Image (RSI). The mentioned categorization is very general thus some data in some conditions may perform better than others.

1.4.1.1 Remote Sensing

In resent years, the resolution of earth observation satellite images in all aspects: spatial, spectral, radiometric and temporal have been increased. For example the spatial resolution is available from a few centimeters to few kilometers, spectral

resolutions from 3 bands to some hundred bands, etc. These overwhelming data sources, in one hand makes new horizons in the applications of remotely sensed data and in the other hand the new and state-of-art hardware and software felicities are much needed then any time before. In this regard the most fruitful scenario will be synergetic fusion of the available datasets in the most efficient way.

As an example, in a city several objects like buildings, streets and vehicles can be easily characterized using the panchromatic in combination with multi-spectral datasets. Another aspect is return to the environmental applications of data fusion e.g. vegetation monitoring, studies on marine or air pollution, thematic mapping, precision farming, etc which are easily achievable using fused dataset. The visual improvement of data using color composition is another applicability of RSDF.

If we defined the optimal situation of remote sensing data exploration as the obtaining a better result than the one obtained by a separate data source, therefore the exploitation of satellite images and more generally of observations of the earth and our environment are presently the most productive in data fusion. Observation of the Earth is perforated by means of satellites, planes, ships and ground-based instruments. It results to a great variety of measurements, partly redundant, partly complementary. These measurements can be simultaneous or time-integrated, bi-dimensional or three-dimensional for instance oceanic and atmospheric profiler, sounder at ground level, or satellite-borne, or ship-borne measurements. Data fusion is a subject becoming increasingly relevant because it efficiently helps scientists to extract increasingly precise and relevant knowledge from the available information. The operation of data fusion by itself is not new in environment. For example, meteorologists predict weather for several tens of years. In remote sensing (i.e. Earth observation from spacecraft or aircraft) classification procedures are performed since long times and are obviously related to data fusion. Data fusion allows formalizing the combination of these measurements, as well as to monitoring the quality of information in the course of the fusion process [Hall and Llinas, 2001]. As the DF related motivations are high and can not be described here just some examples are mentioned: classification improvements [Haak and Bechdol, 1999], spatial resolution

enhancement [Ehlers, 1991], visual interpretation enhancement, and defected image reconstruction are the main ones that can be found in several DF related publications. Sometimes remotely sensed images are influenced by a number of malfunctioning that causes the final products can not provide the needed qualities and completeness. This imagery shortage is return to gaped (e.g. missed area in an image) and damaged (e.g. noisy dataset) areas in an image. Here all of these data drawbacks called image defection. As image defections could have dynamic and diverse characteristics thus there are a variety of techniques that could be applied for the reconstruction process. Reconstruction of gapped areas from satellite imagery is of high interest for visual image interpretation and digital image classification purposes. Image gaps can have several reasons e.g. cloud coverage for optical imagery, shadowed area for SAR datasets, or instrumentation problems e.g. SLC-off problem for Landsat-7/ETM+ [Scramuzza, 2004] and line striping in a dataset [Richards and Jia, 1999]. Gap areas can have different sizes, dimensions and locations. For instance the striping problem may affect just one column and/or row of pixels while the cloudy area in an image could be more than 50% of a satellite imagery scene [Kittler and Pairman, 1985]. From the literature there are several techniques that have been evaluated to solve these problems. For example [Haefner *et al.* 1993] used Optimal Resolution Approach using ERS-1 SAR data for snow cover determination and Darvishi Bolorani *et al.* [2008^{1,2}] used PCT for filling gapped parts of Landsat image using earlier obtained images.

1.4.1.2 Spatial information extraction

As explained above we just evaluated the satellite imagery fusion. But data fusion as a general frame can be extended outside the limitations of RS imagery. For example geographic information system spatial datasets including digital terrain data, demographic data, land-based spatial data etc can be fused in proper ways. Non-imagery data fusion (e.g. DLDF) could be one of the most sophisticated applications of data fusion. In this regard the most active area of research and development are

related to the development of geographic information systems by combining earth imagery, maps, demographic and infrastructure or facilities mapping (geospatial) data into a common spatially-referenced database [Hall and Llinas, 2001]. As seen in figure (1-5) data fusion can be extended to several domains of geo-based datasets which will open new horizons in spatial data and information analysis and several applications can be defined in this framework. More can be found in Star [1991] and Mesev [2007].

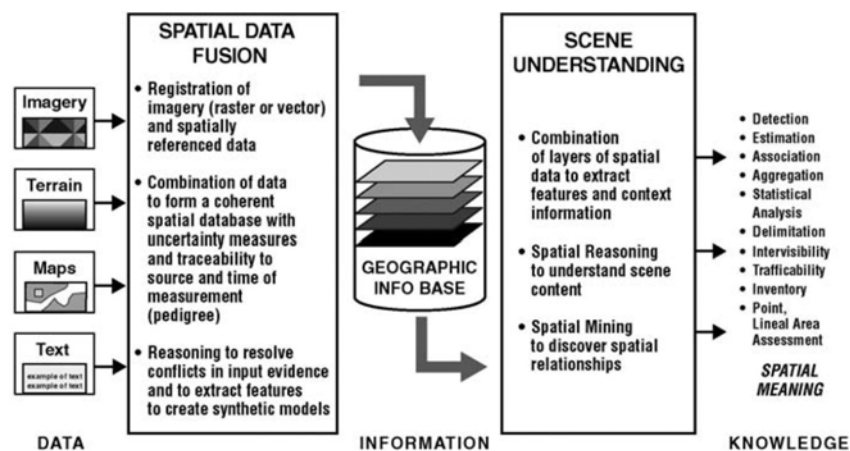


Figure 1-5. Spatial data fusion flow diagram. After Hall and Llinas [2001].

Stereoscopic information extraction is another useful aspect of data fusion. Diversity of remote sensing systems provides opportunities for collecting images of the earth's surface in different stereoscopic views. This technological advancement has facilitated the generation of Digital Elevation Models (DEMs). For example SPOT as one of the earliest optical land imagers has provided stereo abilities for several years. And also several other sensors nowadays are providing such facilities to extract 3D stereo data. Sensors like LIDAR and SAR in combination with optical datasets are also offering opportunities for generating 3D data sources for visualization of environmental and land surface monitoring. DEM extraction using data fusion has been explored in several publications e.g. Cheng [1999] and Toutin [2001].

1.4.1.3 Environmental studies

The increasing human-based pressures that are the main causes to the environmental changes during two last centuries have introduced a couple of new needs for knowing and understanding of environmental phenomena [Parr *et al.* 2003]. The principal aspects of environmental investigations like biodiversity loss, atmospheric pollution, desertification, fire burning, land use changes, sustainable development and climate changes have been studied for several reasons and using several facilities of combined remotely sensed datasets [Oldfield and Dearing, 2003]. As stated by Shengli Huang [2005] approximately 320 remotely sensors are available for studying the Earth including land, ocean, atmosphere, etc. This high numbers of sensors will provide a tremendous volume of data; the combination of them in a proper way will cause a lot of advantages. Of course they will include some few disadvantages as well. The high dimensionality of multi-sensor datasets will introduce more complete view of the environmental phenomena. For example Haak and Bechdol [1999] offered a good insight in the multi-sensor data fusion. Also some very useful recipes in the environmental applications of DF can be found in Simone *et al.* [2002] and Kalluri *et al.* [2003].

The environmental pollution is a multi-face phenomenon which contains water, soil and air contaminations. As these polluters could have divers sources with different characteristics accordingly a variety of data sources is needed to handle such circumstances. As a very common example Pujadas *et al.* [1997] offered a DF technique to study air pollution in cities. They investigated Madrid plume in winter, as one of the most important cases of urban pollution taking place in southern Europe. Another example is the study of Schäfer *et al.* [2004] using the fusion procedure that the data from the ground-based monitoring network and from satellite retrievals are fused in the ICAROS NET (Integrated Computational Assessment of Air Quality Via Remote Observation System) platform to the Munich region, Germany.

Desertification as the process of land degradation in arid, semi-arid and dry environments could be caused by climatic variations and human activities. With

reference to this fact that desertification is one of the most pressing environmental issues affecting human life, therefore studying this phenomenon on local, regional and global scales is one of the most important aspects for environmental studies [Collado *et al.* 2002]. The fusion of remotely sensed data providing a framework that we can extend the obtained results of field investigations to higher levels of regional and probably global scales. The fused data has enough spatial information needed for local scale analysis of the relationships between climate change, land degradation and desertification processes. Too many fusion procedures for combining the remotely sensed and the field collected data have been developed that mostly are in multi-temporal data combination. This multi-temporality characteristic of RS data is more useful than other aspects like multi-resolution, multi-frequency, etc for the monitoring desertification procedures. [Verbyla, 1995; Tucker *et al.* 1994]. Another aspect of data fusion is return to the vegetation monitoring in the dry environments that is very crucial. Sellers [1989] and Bannari *et al.* [1995] studied these phenomena using the combination red and infrared reflectance of vegetation land covers.

1.4.1.4 Agricultural studies

The application of DF in agricultural is a very broad field of study that can be roughly categorized into two dynamic or real-time multi-sensor DF and static or delay-time multi-sensor DF. The first one is mostly categorized in the field of precision farming in which the data from several sources like GPS, machine-based fertilization sensors, office-based previously provided maps, etc will be fused instantaneously with the movement of tractor or other vehicles in the field. The fused data will guide the vehicle to act based on the wishes of farmers. As an example Guo and Zhang [2005] adapted a wireless data fusion system to automatically collect and process operational data from agricultural machinery in order to provide real-time support for precision farming. The second aspect of DF in agricultural is return to the static face of field monitoring or surveying in which the collected data including remotely sensed data and ground-based information will be fused a time later and the

results will be explored for the next steps of farming. This kind of DF can have a temporal range from one day to one year or more. For example combination of multi-temporal satellite images helps to predict the amount of serials production for one year, or time to time information for the health situation of plants. Ostermeier [2007] developed a DF methodology that high resolution SPOT-XS is used to provide spatial information at the parcels level and very low spatial resolution NOAA-AVHRR which outputs images of large areas every day. Both datasets were fused to make the possibility to daily estimate reflectance of main cultivations at the parcels level.

1.4.1.5 Natural disasters studies

Due to the high number of sensors most of the natural disastrous phenomena like flood can be monitored and probably predict. Like other aspects of DF applications this field also contains a lot of instances. Here we just shortly introduce two cases and readers are referred to the mentioned references. Singh [2007] introduced a multi sensor remote sensing data fusion procedure after the Sumatra tsunami and earthquake of 26 December 2004. In this work multi-sensors datasets were analyzed to study the changes in ocean, land, meteorological and atmospheric parameters. Based on the prior and after phenomenon comparison using a DF framework it has been cleared that changes in ocean, atmospheric and meteorological parameters, as useful signs for disaster monitoring, are detectable. Another example is about the Geometric modeling of buildings in urban areas, which helps to detecting and interpreting their changes to obtain fast damage information after earthquakes. This information is valuable inputs for a disaster management system. For instance in Vögtle and Steinle [2005] airborne laserscanning data fusion was carried out for earthquake studies.

Flood forecasting and monitoring is of very important in evaluation all aspects of damages from the human and non-human viewpoints. Almost due to the large size, remoteness and dynamic nature of the flood phenomenon, this procedure can mostly be carried out using remote sensing. As an example Temimi *et al.* [2005] introduced

an approach that a combination of microwave data and discharge observations presents a high potential in flood and discharge prediction. Toyra *et al.* [2002] evaluated the usefulness of radar and visible/infrared satellite imagery for mapping the extent of flooded wetland areas. In their work the extent of standing water in the Peace–Athabasca Delta, Canada, during May 1996 and May 1998 was mapped using RADARSAT and SPOT imagery. The RADARSAT scenes and the SPOT scenes separately and in a combination mode of the two were classified. Using the fused datasets the results of classification has increased about 15%. Therefore they showed that the information from radar and visible/infrared satellite imagery are complementary and that flood mapping can be achieved with higher accuracy if the two image types are used in combination.

1.4.1.6 Mineral exploration

From the literature the remotely sensed images for the purpose of mineral exploration are mostly categorized into two domains of applications [Sabins, 1999]: geology mapping and the faults and fractures that localize and recognize hydro thermally altered rocks by their spectral signatures. Due to the fact that different materials have different behaviors in different parts of electromagnetic spectrum therefore a diversity of sensors needed to reach the mineral exploration goals. For example, as mentioned by Sabins [1999] the digitally processed TM ratio images can identify two assemblages of hydrothermal alteration minerals; iron and clays. Hyperspectral imaging systems can identify individual types of iron and clay minerals, which can provide details of hydrothermal zoning. In this regard a proper fusion framework will provide a valuable source of data in mineral exploration. The usage of RS data can be ranged from a very simple band rationing to a complicated hyperspectral and ground data fusions tasks. For example clay minerals have a diagnostic absorption around ~2200 nm (ASTER SWIR band 3) while the reflectance maximum for clays is at around 1600 - 1700 nm (ASTER SWIR band 1). Therefore a simple band ration

of these two bands will provide good information about the abundant of clay minerals.

1.4.1.7 Urban studies

Data fusion application in urban areas is one of the most practical and common cases of DF. The fusion of spatial and spectral complementary datasets can facilitate human-based visual and machine-based automatic image interpretation. Numerous studies have demonstrated the usefulness of fused data for the study of urban areas e. g. Couloigner *et al.* [1998]. As the urban objects are always heterogeneous thus the high-quality of the fused spectral content of the MS images, when increasing the spatial resolution, allows further processing such as classification and image interpretation. Aiazzi *et al.* [2001] used the generalized Laplacian pyramid for PLDF. They also offered a fruitful discussion on simulated SPOT 5 data of an urban area obtained from the MIVIS airborne imaging spectrometer.

Traffic-based multi-source data fusion supplies a basis in which the network efficiency is high, the road safety is improved and also the transportation is more adapted to the environmental conditions.

Implementing systems like the Intelligent Transport Systems (ITS) and Regional Traffic Control Centers (RTCC) in order to implement the traffic information systems and traffic management systems are new aspects of data fusion. In order to make proper decisions, precise information is needed. Having this kind of information is relying on usage of several sources of data. But in other hand having stationary sensors is very expensive. Therefore using few but synergistically combined data sources is one of the best applicable strategies for traffic managing. El Faouzi [2004] evaluated the most recent applications of data fusion in road traffic engineering: traffic monitoring, automatic incident detection, traffic forecasting and intelligent transportation systems. Sroka [2004] compared five different data fusion methods in process of vehicle classification. The models of vehicle classes have been defined by using fuzzy measures with triangular and Gaussian shapes.

Irrespective to the levels of fusion the earliest publications in different aspects of data fusion are summarized in table (1-5).

Table 1-4. Mostly first publications in DF.

Data	Application	Author
GEOSAT and SPOT	Petroleum and mineral exploration	Baker and Henderson, 1988
Airborne-SAR and Landsat-MSS	Geological hazard mapping	Koopmansa and Forero, 1993
Landsat-TM and digitized NHAP	Land surface mapping	Chavez, 1987
MSS and VISSR	Change detection	Chavez and Mackinnond, 1994
TM, TIMS and airborne SAR	Classification of sedimentary rocks	Evans, 1988
Landsat and SEASAT	Land Use Classification	Clark, 1981
SEASTA and SPOT	Geologic structures extraction	Yesou H. Merging, 1993
Landsat MSS and SIR-A Images	Lithology and Surface Deposit	Chavez <i>et al.</i> 1983
Landsat and RADAR	Crop Classification	Li, 1980
Airborne Radar and Landsat	Crop Classification	Ulaby, 1982
Landsat and HCMM	Thermal Mapping	Schowengerdt, 1992
SPOT and Landsat TM	Mapping	Tanaka, 1989
SIR-B and Landsat	Cartography	Welth and Ehlers, 1988
SPOT and SAR	Urban studies	Houzelle and Glraudon, 1991
Multi temporal Landsat ETM+	Imagery Gap fill	Darvishi Bolorani <i>et al.</i> 2008
SIR-A, SEASAT and Landsat		Rebillard and Nguyen, 1982
RADAR and geophysical data		Harris and Murray, 1989

Acronym note: Thermal Infrared Multispectral Scanner (TIMS) and airborne Synthetic Aperture Radar (SAR). Landsat Multispectral Scanner (MSS). Visible-Infrared Spin-Scan Radiometer (VISSR).

1.4.1.8 Medical Applications

Medical imaging is the most important sources of anatomical and functional information, which is indispensable for today's clinical research, diagnosis and treatment which is an integral part of modern health care [Patias, 2002]. Multimodal imaging plays an increasingly important role in clinical use of medical imaging systems. Therefore to make these images more useful and applicable medical image fusion being a fast-expanding field and appears more and more as a key element for the optimal use of images in medical treatments. Medical image fusion is mostly concerns in improving the interpretation of 3D brain images, providing extra elements for the diagnosis and patient follow up [Colin and Boire, 1999].

Barillot *et al.* [1993] applied image fusion to make a 3D display for epilepsy surgery where multimodal images like CT, MRI and DSA were used to understand the anatomical environment upon which physicians map physiology by priori knowledge, atlas and functional data (EEG, SEEG, MEG).

Barra and Boire [2001] used the fuzziness to manage the uncertainty and imprecision inherent to the images followed by the fusion process in two clinical cases: study of Alzheimer's disease by MR/SPECT fusion and study of epilepsy by MR/SPECT/PET fusion. Other applications like 3D face simulation for beauties operation and denary images fusion and also medical image fusion for educational psychology. Characteristics, advantages, and shortcomings of medical image fusion have been discussed by several authors like Colin and Boire, [1995]; Barra and Boire, [2001]; Patias, [2002]; Malandain *et al.* [2005] and Zhu and Cochoff, [2006].

1.4.2 Military applications

As the accessibility to military literature was limited, this section is mostly based on Hall and Llinas [2001] and Koch [2005]. One of the earliest and more common usages of DF is in military and defense operation systems. On the contrary to civil DF, the military DF mainly focuses on specific object detection that can only be obtained with a certain image resolution [Wald, 1999]. The main stresses on military applications, from the imagery viewpoint, are developing the techniques that can give out some information about the characterization and identification of dynamic entities such as emitters, platforms, weapons, high-level inferences for enemy situation and military units. For the mentioned cases the data fusion has an important role for combination different sensors like radar, sonar, electronic intelligence, observation of communications traffic, infrared, passive electronic support measures, infrared identification friend foe sensors, electro-optic image sensors and visual (human) sightings and Synthetic Aperture Radar (SAR) observations. One of the main properties for this kind of DF is the dynamic nature of targets and fast changes and also the need for rapid decision making and potentially large combinations of target-sensor pairings.

Battlefield intelligence, surveillance and target acquisition systems attempt to detect and identify potential ground targets. Examples include the location of land mines and automatic target recognition. Sensors include airborne surveillance via SAR, passive electronic support measures, photo reconnaissance, ground-based acoustic sensors, remotely piloted vehicles, electro-optic sensors and infrared sensors. The mentioned high numbers of data resources and the complexity of defense systems make high needs for using very sophisticated DF techniques. The military DF is mostly at PLDF but other levels also have their applications.

Multi-sensor measurement which independently senses the physical properties of an object can be fused in a data fusion framework. In such circumstances the weaknesses of one sensor are alleviated by strengths of others. Consequently, a good performance of the complementary sensors is available for a wide variety of landmine detections. As an example, there are several landmine detector sensors

which measure different physical properties of an object. These sensors all have their own strengths and weaknesses that the data fusion is a mechanism to weakness alleviation and strength enhancement. For instance, Sanjeev *et al.* [1999] introduced a framework for multi-sensor data fusion for the detection and identification of anti-personnel mines. They have developed hybrid architecture in order to integrate non-homogeneous and dissimilar datasets from various sensors.

CHAPTER TWO

2 Pixel Level Data Fusion (PLDF)

A panchromatic image covers broadest possible wavelength of the electromagnetic spectrum (e.g. EO-1/ALI-Pan, 480-690 nm). The spectral bandwidth decreases from panchromatic to multispectral (e.g. EO-1/ALI band-3, 450-515 nm) and narrowest bandwidth is for hyperspectral sensors (e.g. EO-1/Hyperion band-50, \approx 849-859 nm). Consequently in order to collect and record the same amount of electromagnetic radiation, the size of a panchromatic detector (i.e. pixel size) can be smaller than that of MS and HS. From the application point of view, synergetic combination of all mentioned datasets in a proper basis (i.e. data fusion) is the ideal scenario to put data into application. In this regard, the fusion of low resolution hyper/multispectral and high resolution panchromatic remotely sensed images is a very challenging subject for the remote sensing community.

As having high spatial and spectral information in one captured image is almost unobtainable therefore the new generation of earth surface imagers, such as EO-1, Landsat/ETM+, SPOT-HRG, IRS-P6, OrbView-3, QuickBird-2, IKONOS, ALOS, etc are capturing panchromatic and multispectral images simultaneously but with different spatial and spectral resolutions. As a consequence, techniques that can productively fuse these images are demanded. From the published works and developed techniques numerous methodologies and software tools have been developed. For instance Cliche et al. [1985], Price [1987], Welch and Ehlers [1987], Albertz et al. [1988], Chavez et al. [1991], Ehlers [1991], Shettigara [1992], Yesou et al. [1993], Munechika et al. [1993], Garguet-Duport et al. [1996], Yocky [1996], Wald et al. [1997], Zhou et al. [1998], Pohl and Van Genderen [1998], Zhang and Albertz [1998], Zhang [1999], Ranchin and Wald [2000], Li et al. [2002], Cakir and Khorram [2003], Chen et al. [2005] and Zhang and Hong [2005], reviews are given

by Pohl and Van Genderen [1998] and Wald [1999 and 2002] are a very rich literature in PLDF.

Image fusion at pixel level means fusion at the lowest processing level referring to the merging of measured physical parameters (i.e. pixel) [Pohl et al. 1994]. The literature of PLDF shows that there are a large number of techniques used over an indefinite number of datasets, each of which for specific applications. Among the numerous methodologies the more effective fusion techniques that have demonstrated the best results in the literature are presented. Here the pixel level data fusion techniques, main concepts, essential qualities, their problems and advantages are reviewed and all methodologies have been evaluated using EO-1 hyperspectral, multispectral and panchromatic datasets.

Hyperspectral (HS) and multispectral (MS) datasets, hereafter both refer to as MS.

2.1 PLDF categorization

In order to make more clarity in borders of the investigated techniques, Hill *et al.* [1999] categorization of PLDF is adapted. In this categorization three groups of procedures are specified which work based on how panchromatic information is used in fusion procedure.

1. Fusion procedures using all panchromatic band frequencies.
2. Fusion procedures using selected panchromatic band frequencies.
3. Fusion procedures using panchromatic band indirectly.

2.1.1 PLDF using all panchromatic band frequencies

This group of techniques referred to the mostly common and known component substitution techniques. For instance PCA and IHS; the arithmetic techniques like band addition and multiplication and the Brovey or color normalizing algorithms are categorized in this category.

2.1.1.1 Principal Component Transformation (PCT)

Principal component transformation, originally known as the Karhunen-Loeve transformation, is a linear transformation and rotation which transfers a correlated multivariate dataset to a new de-correlated multivariate dataset (i.e. components) [Loeve, 1955 and Richards, 1986]. In this procedure MS dataset is transformed into the same number of uncorrelated principal components. In this new dataset the first Principal Components (PC-1) contains the common information from all input bands and other uncommon spectral information of the input are transferred to other components [Richards and Jia, 2006]. Therefore first principal component can be replaced by Pan image which is the spectral average of all MS bands. Finally the inverse PCT will produce a high resolution multispectral dataset. In order to illustration, a very brief mathematical explanation of procedure is outlined and more can be found in the literature. The transformation matrix which contains the eigenvectors which is an orthogonal matrix can be calculated based on either from the covariance or the correlation matrixes of MS dataset. [Schowengerdt, 1997 and Richards and Jia, 1999]. When PCT is carried out using the covariance matrix, it referred to as non-standardized, while transformation using the correlation matrix referred to as standardized transformation [Wang *et al.* 2005].

By way of illustration, let n be the number of bands in a multispectral image as the vector X

$$X = [x_1, x_2, x_3, \dots, x_n]^T \quad (2-1)$$

And the covariance of two different bands is expressed as

$$\delta_{ij}^2 = E(x_i - m_i)(x_j - m_j), \quad i, j = 1, 2, 3, \dots, n \quad (2-2)$$

In which m_i and m_j are the mean values of the bands i and j . For a multi-spectral dataset the symmetric covariance matrix is Σ

$$\Sigma = \begin{bmatrix} \delta_{1,1} & \delta_{1,2} & \delta_{1,3} & \dots & \delta_{1,n} \\ \delta_{2,1} & \delta_{2,2} & \dots & \dots & \delta_{2,n} \\ \delta_{3,1} & \dots & \dots & \dots & \delta_{3,n} \\ \dots & \dots & \dots & \dots & \dots \\ \delta_{n,1} & \delta_{n,2} & \delta_{n,3} & \dots & \delta_{n,n} \end{bmatrix} \quad (2-3)$$

In this regard the covariance matrix Σ of a dataset will be diagonalized.

The eigenvectors $\varphi_r = (r = 1, 2, 3, \dots, n)$ are calculated according to the corresponding Eigenvalues from the Σ . The Eigenvalues are given by

$$\varphi_r = [\varphi_1, \varphi_2, \varphi_3, \dots, \varphi_n]^T \quad (2-4)$$

n bands of multispectral images are mapped onto the eigenvector

$$Y = \phi_n * X \quad (2-5)$$

After this short explanation, let PC1 to PCn be the obtained results of MS to PCT domain transformation. Therefore the transformation will be as

$$\begin{bmatrix} \text{PC1} \\ \text{PC2} \\ \dots \\ \text{PCn} \end{bmatrix} = \begin{bmatrix} t_{11} & t_{21} & \dots & t_{n1} \\ t_{12} & t_{22} & \dots & t_{n2} \\ \dots & \dots & \dots & \dots \\ t_{1n} & t_{2n} & \dots & t_{nn} \end{bmatrix} * \begin{bmatrix} \text{DN}_{\text{MS1}}^L \\ \text{DN}_{\text{MS2}}^L \\ \dots \\ \text{DN}_{\text{MSn}}^L \end{bmatrix} \quad (2-6)$$

Where,

$$I = \begin{bmatrix} t_{11} & t_{21} & \dots & t_{n1} \\ t_{12} & t_{22} & \dots & t_{n2} \\ \dots & \dots & \dots & \dots \\ t_{1n} & t_{2n} & \dots & t_{nn} \end{bmatrix} \quad (2-7)$$

Finally and after PC1 to Pan replacing, the inverse transformation is carried out by

$$\begin{bmatrix} DN_{MS1}^H \\ DN_{MS2}^H \\ \dots \\ DN_{MSn}^H \end{bmatrix} = \begin{bmatrix} t11 & t21 & \dots & tn1 \\ t12 & t22 & \dots & tn2 \\ \dots & \dots & \dots & \dots \\ t1n & t2n & \dots & unn \end{bmatrix} * \begin{bmatrix} DN_{Pan}^H \\ PC2 \\ \dots \\ PCn \end{bmatrix} \quad (2-8)$$

Where DN_{Pan}^H is DN_{Pan}^H that statistically adapted to PC1; the generalized form of PCT can be expressed as

$$\begin{bmatrix} DN_{MS1}^H \\ DN_{MS2}^H \\ \dots \\ DN_{MSn}^H \end{bmatrix} = \begin{bmatrix} DN_{MS1}^L \\ DN_{MS2}^L \\ \dots \\ DN_{MSn}^L \end{bmatrix} + (DN_{Pan}^H - DN_{Pan}^L) * \begin{bmatrix} t11 \\ t21 \\ \dots \\ tn1 \end{bmatrix} \quad (2-9)$$

Where I is the transformation matrix; DN_{Pan}^L could be

$$DN_{Pan}^L = (1/n) * [DN_{MS1}^L + DN_{MS2}^L + \dots + DN_{MSn}^L] \quad (2-10)$$

Or

$$DN_{Pan}^L = PC1 \quad (2-11)$$

The first case (Equation 2-10) needs more time for calculations and causes a decrease in color distortion because an average of MS bands are added to Pan image before fusion process. The second scenario (Equation 2-11) is faster because the Pan image is directly injected into the fusion process. L and H superscripts are the signs of Lower and Higher resolution pixel sizes, for example ALI/MS with 30 and ALI/Pan with 10 meter spatial resolutions, respectively. In this technique, in a practical sense, the next steps are almost followed.

$$1. \quad MS_{I, \dots, n}^L \xrightarrow{\text{Resampled to Pan spatial resolution}} MS_{I, \dots, n}^H .$$

2. $MS_{1, \dots, n}^H \xrightarrow{\text{Principal componenet transformation}} PC_{1, \dots, n} .$
3. $Pan \xrightarrow{\text{Statistica lly adapt ion and substitut ion with the PC1}} Pan + PC_{2, \dots, n} .$
4. $Pan + PC_{2, \dots, n} \xrightarrow{\text{Inverse PCT}} MS_F^H .$

Statistically adaptation means Pan is stretched to have the same mean and variance as PC1. Consequently the obtained results MS_F^H will be a high resolution multispectral image that contains high spatial resolution from panchromatic and high spectral properties from MS images. For a fuller discussion on PCT readers are referred to Schowengerdt, [1997]; Richards and Jia, [1999]; Chavez and Kwarteng, [1989] and also good discussions can be found in De Béthune, [1998].

As a general rule in almost all PLDF techniques there is band statistically adaptation procedure that can be done in several ways. In this work the adaptation process is based on Welch and Ehlers [1987]. For example in PCT fusion Pan image must be adapted to PC1 which is carried out using the next equation (2-12). For illustration purpose let A and B be two images where B must be adapted to A thus

$$B' = \frac{(B - \text{MinB})(\text{MaxA} - \text{MinA})}{(\text{MaxB} - \text{MinB}) + \text{MinA}} \quad (2-12)$$

Where B' is the adapted B to A and Min and Max are minimum and maximum values in both datasets, respectively.

2.1.1.2 Intensity, Hue, Saturation (IHS)

The intensity, hue and saturation as a color coordinate transformation is almost a standard technique in image fusion. One of the main limitations is that only three bands are involved [Daily, 1983]. This specific color space transformation is often chosen because the visual cognitive system of human tends to treat these three components as roughly orthogonal perceptual axes [Wang, 2005]. In this color representation system Intensity component (I) presents brightness variation and has

high correlation with spatial variation of data sources, therefore it considered as spatial information and no color properties are associated with [Albertz *et al.* 1988 and Ehlers, 1991]. Due to high correlativity between intensity and panchromatic image, it can be replaced with panchromatic image that contains spatial information. The mathematical rational of IHS is based on the transformation matrix of the IHS which is an orthogonal transformation.

$$\begin{bmatrix} DN_{Pan}^L \\ V1 \\ V2 \end{bmatrix} = \begin{bmatrix} 1/3 & 1/3 & 1/3 \\ -1/\sqrt{6} & -1/\sqrt{6} & 2/\sqrt{6} \\ 1/\sqrt{6} & -1/\sqrt{6} & 0 \end{bmatrix} * \begin{bmatrix} DN_{MS1}^L \\ DN_{MS2}^L \\ DN_{MS3}^L \end{bmatrix} \quad (2-13)$$

Where Hue, $H = \tan^{-1}[V2/V1]$ and Saturation, $S = \sqrt{V1^2 + V2^2}$

$$\begin{bmatrix} DN_{MS1}^H \\ DN_{MS2}^H \\ DN_{MS3}^H \end{bmatrix} = \begin{bmatrix} 1 & -1/\sqrt{6} & 3/\sqrt{6} \\ 1 & -1/\sqrt{6} & -3/\sqrt{6} \\ 1 & 2/\sqrt{6} & 0 \end{bmatrix} * \begin{bmatrix} DN_{Pan}^H \\ V1 \\ V2 \end{bmatrix} \quad (2-14)$$

Since the forward and backward transformations are both linear, replacing V1 and V2 in equation (2-14) by V1 and V2 from equation (2-15) yields the mathematical model of the generalized IHS method.

$$\begin{bmatrix} DN_{MS1}^H \\ DN_{MS2}^H \\ DN_{MS3}^H \end{bmatrix} = \begin{bmatrix} DN_{MS1}^L \\ DN_{MS2}^L \\ DN_{MS3}^L \end{bmatrix} + [DN_{Pan}^H - DN_{Pan}^L] * \begin{bmatrix} 1 \\ 1 \\ 1 \end{bmatrix} \quad (2-15)$$

Where $DN_{Pan}^L = (1/3) * [DN_{MS1}^L + DN_{MS2}^L + DN_{MS3}^L]$ and DN_{Pan}^H is the DN_{Pan}^H that statistically adapted using equation (2-12) to having the same mean and variance as DN_{Pan}^L .

In IHS it assumed that all color characteristics of RGB data are represented in Hue (H) and Saturation (S) components [Zhang, 1999] while Intensity component (I) just contains spatial information. As a general workflow IHS fusion process comprises the next steps.

1. $MS(RGB) \xrightarrow{\text{Color transformation}} IHS .$
2. $Pan \xrightarrow{\text{Statistically adaption and substituted with the Intensity (I)}} Pan + HS .$
3. $Pan + HS \xrightarrow{\text{Inverse color transformation}} MS(RGB)_F^H .$

After MS to IHS transformation, panchromatic high resolution image, Pan_H statistically adapted and substituted with Intensity component (I). Following an inverse transformation from Pan+HS to RGB results a fused MS dataset, MS_F^H that inherited the spectral properties from MS while earned higher spatial resolution from Pan image [Williams, 1995]. As stated in equation (2-15) more than a simple I substitution the average of MS bands can be added to Pan before fusion process. This extra process will increase the spectral preservation ability of the fusion process.

2.1.1.3 Gram-Schmidt Transformation (GST)

Gram-Schmidt orthogonalization, or Gram-Schmidt transformation, is a sophisticated statistical coordinate transformation. Similar to PCT the GST is a procedure to produce a set of uncorrelated or orthogonal variables from a set of correlated and unorthogonal random variables [O'Connell, 1974 and Gong *et al.* 2001]. The mathematical rational behind is explained in several references. Here I just briefly outline the introductory concepts.

Let $\{u_1, u_2, \dots, u_k\}$ be any basis of a k-dimensional subspace W of R^n then by Gram-Schmidt orthogonalisation process, we get an orthonormal set $\{v_1, v_2, \dots, v_k\} \subset R^n$ with $W = L(v_1, v_2, \dots, v_k)$ and for $1 \leq i \leq k$, as $L(v_1, v_2, \dots, v_i) = L(u_1, u_2, \dots, u_i)$.

Suppose we are given a set of n vectors, $\{u_1, u_2, \dots, u_n\}$ of V that are linearly dependent, where exists a smallest k , $2 \leq k \leq n$ such that

$$L(u_1, u_2, \dots, u_k) = L(u_1, u_2, \dots, u_{k-1})$$
 Here it is claimed that in this case, $w_k = 0$.

Since, we have chosen the smallest k satisfying

$$L(u_1, u_2, \dots, u_i) = L(u_1, u_2, \dots, u_{i-1}) \quad (2-16)$$

For $2 \leq i \leq n$ the set $\{u_1, u_2, \dots, u_{k-1}\}$ is linearly independent. So, there exists an orthonormal set $\{v_1, v_2, \dots, v_{k-1}\}$ such that $L(u_1, u_2, \dots, u_{k-1}) = L(v_1, v_2, \dots, v_{k-1})$.

As $u_k \in L(v_1, v_2, \dots, v_{k-1})$, where $u_k = \langle u_k, v_1 \rangle v_1 + \langle u_k, v_2 \rangle v_2 + \dots + \langle u_k, v_{k-1} \rangle v_{k-1}$.

Therefore, in this case, we can continue with Gram-Schmidt process by replacing u_k by u_{k+1} . Let S be a countable infinite set of linearly independent vectors. Then one can apply the Gram-Schmidt process to get a countable infinite orthonormal set. Let $\{v_1, v_2, \dots, v_k\}$ be an orthonormal subset of \mathbb{R}^n . Let $B = (e_1, e_1, \dots, e_n)$ be the standard ordered basis of \mathbb{R}^n . Then there exist real numbers α_{ij} , $1 \leq i \leq k$, $1 \leq j \leq n$ such that $[v_i]B = (\alpha_{i1}, \alpha_{i2}, \dots, \alpha_{in})^t$. Let $A = [V_1, V_2, \dots, V_k]$. Then in the ordered basis B , we have A that is an $n \times k$ matrix

$$A = \begin{bmatrix} \alpha_{11} & \alpha_{12} & \dots & \alpha_{1k} \\ \alpha_{21} & \alpha_{22} & \dots & \alpha_{2k} \\ \dots & \dots & \dots & \dots \\ \alpha_{n1} & \alpha_{n2} & \dots & \alpha_{nk} \end{bmatrix} \quad (2-17)$$

Also, observe that the conditions $\|v_i\| = 1$ and $\langle v_i, v_j \rangle = 0$ for $1 \leq i \neq j \leq n$, implies that

$$1 = \|v_i\|^2 = \langle v_i, v_i \rangle = \sum_{j=1}^n \alpha_{ji}^2 \quad (2-18)$$

$$\begin{cases} 1 = \|v_i\| = \|v_i\|^2 = \langle v_i, v_i \rangle = \sum_{j=1}^n \alpha_{ji}^2 \text{ and} \\ 0 = \langle v_i, v_i \rangle = \sum_{j=1}^n \alpha_{ji} \alpha_{ji} \end{cases} \quad (2-19)$$

Note that,

$$A^t A = \begin{bmatrix} v_1^t \\ v_2^t \\ \dots \\ v_k^t \end{bmatrix} \begin{bmatrix} v_1, & v_2, & \dots & v_k, \end{bmatrix} = \begin{bmatrix} \|v_1\|^2 & \langle v_1, v_2 \rangle & \dots & \langle v_1, v_k \rangle \\ \langle v_2, v_1 \rangle & \|v_2\|^2 & \dots & \langle v_2, v_k \rangle \\ \dots & \dots & \dots & \dots \\ \langle v_k, v_1 \rangle & \langle v_k, v_2 \rangle & \dots & \|v_k\|^2 \end{bmatrix} = \begin{bmatrix} 1 & 0 & \dots & 0 \\ 0 & 1 & \dots & 0 \\ \dots & \dots & \dots & \dots \\ 0 & 0 & \dots & 1 \end{bmatrix} = I_k \quad (2-20)$$

Or in the language of matrices, we get

$$A^t A = \begin{bmatrix} \alpha_{11} & \alpha_{12} & \dots & \alpha_{n1} \\ \alpha_{21} & \alpha_{22} & \dots & \alpha_{n2} \\ \dots & \dots & \dots & \dots \\ \alpha_{n1} & \alpha_{n2} & \dots & \alpha_{nk} \end{bmatrix} \begin{bmatrix} \alpha_{11} & \alpha_{12} & \dots & \alpha_{1k} \\ \alpha_{21} & \alpha_{22} & \dots & \alpha_{2k} \\ \dots & \dots & \dots & \dots \\ \alpha_{n1} & \alpha_{n2} & \dots & \alpha_{nk} \end{bmatrix} = I_k \quad (2-21)$$

Therefore this transformation can be applied for any number of bands in fusion process. Perhaps readers must have noticed that the inverse of A is its transpose. Such matrices are called orthogonal matrices and they have a special role to play [Golub *et al.* 1996]. GST can easily be extended to an arbitrary number of random variables [Gong *et al.* 2001; Craig *et al.* 2000 and Zang, 2004]. As a practical matter, the GST procedure always follows next steps:

1. $\text{Pan}^H \xrightarrow{\text{Simulation process and resampling to } L \text{ resolution}} \text{Simulated Pan}^L (\text{SPan}^L) .$
2. $\text{SPan}^L + \text{MS}_{j=n}^L \xrightarrow{\text{GST}} \text{Transformed Gram-Schmidt Components} (\text{GSC}_{j=n+1}) .$
3. $\text{Pan}^H \xrightarrow{\text{Statistically adaption with GSC1}} \text{Pan}^{H'} .$
4. $\text{Pan}^{H'} \xrightarrow{\text{substituted with GSC1}} \text{GSC}_{j=2, \dots, n} + \text{Pan}^{H'} .$
5. $\text{GSC}_{j=2, \dots, n} + \text{Pan}^{H'} \xrightarrow{\text{Inverse GS}} \text{MS}_F^H .$

2.1.1.4 Brovey Transformation (BT)

This method assumes that the spectral range of high resolution panchromatic image covers the spectral range of low resolution bands summation which can be written as equation (2-22) [Oguro *et al.* 2003 and Chavez, 1991].

$$MS_{Fk}^H = \frac{MS_k^H * Pan^H}{\sum_{k=1}^N MS^H} \quad (2-22)$$

Where MS_{Fk}^H is the k^{th} fused multispectral band at the resolution of Pan image; the superscript H denotes the high resolution and MS^H is resampled low resolution MS image to the resolution of Pan; N is the number of bands; k is the band under consideration.

From the practical point of view the Brovey transformation is as follows.

1. $MS_N^L \xrightarrow{\text{Selection the spectrally overlaid MS bands with Pan image}} MS_{i=1,\dots,n}^L$
2. $MS_n^L \xrightarrow{\text{Resampling to Pan resolution}} MS_{i=1,\dots,n}^H$
3. $MS_n^H \xrightarrow{\text{Brovey transformation and calculation}} MS_F^H$

Where N is a dataset with n subset that covers the spectral range of Pan image.

2.1.1.5 Color Normalized (CN)

CN image fusion or Energy Subdivision Transform (EST) was mainly developed to fuse hyperspectral dataset with high resolution Pan image [Vrabel *et al.* 2002^{1,2}]. This technique while retain the spatial properties from Pan the spectral properties of MS dataset are also protected. As this technique just work based on spectral correspondence between datasets therefore bands from a MS dataset can be sharpened only if they fall within the spectral range of Pan image. For illustration let have an N band dataset in which there is an n band subset that spectrally

corresponding with Pan image. Thus only this subset can be fused using this procedure. In practice the next steps is followed.

1. MS_N^L and Pan $\xrightarrow{\text{Spectral range correspondence checking}}$ Selected MS_n^L .
2. SMS_n^L $\xrightarrow{\text{Resampling to Pan resolution}}$ SMS_n^H .
3. $MS_{Fk}^H = \frac{SMS_k * Pan}{\sum_k^n MS}$.

As this technique is the extended version of Brovey, therefore final form is normalized to the summation of all input bands in the spectral range. Thus datasets must be in the same units of pixel value quantization, for example both datasets must be in the same units of radiance ($\mu W/cm^2\text{-sr- } \mu m$) and if not they must be converted.

2.1.1.6 Fanbeam (FB)

The fanbeam transformation computes projections of an image matrix along specify directions. An obtained projection of an image $f(x, y)$ is a set of line integrals. The fanbeam function computes the line integrals along paths that radiate from a single source, forming a fan shape (Figure 2-1). To represent an image, the FB takes multiple projections of the image from different angles by rotating the source around the center of the image [Matlab help, 2008].

The Fan Sensor Geometry (FSG) is a parameter that specifies how sensors are aligned. Based on the selected FSG, it positions the sensors along an arc or line of sensors which spaced at a specific degree intervals. The distance between sensors is controlled by specifying the angle between each beam. In an image projection the distance between sensors can be in pixels along x axis which is a new axis orthogonal to the central beam (Figure 2-1).

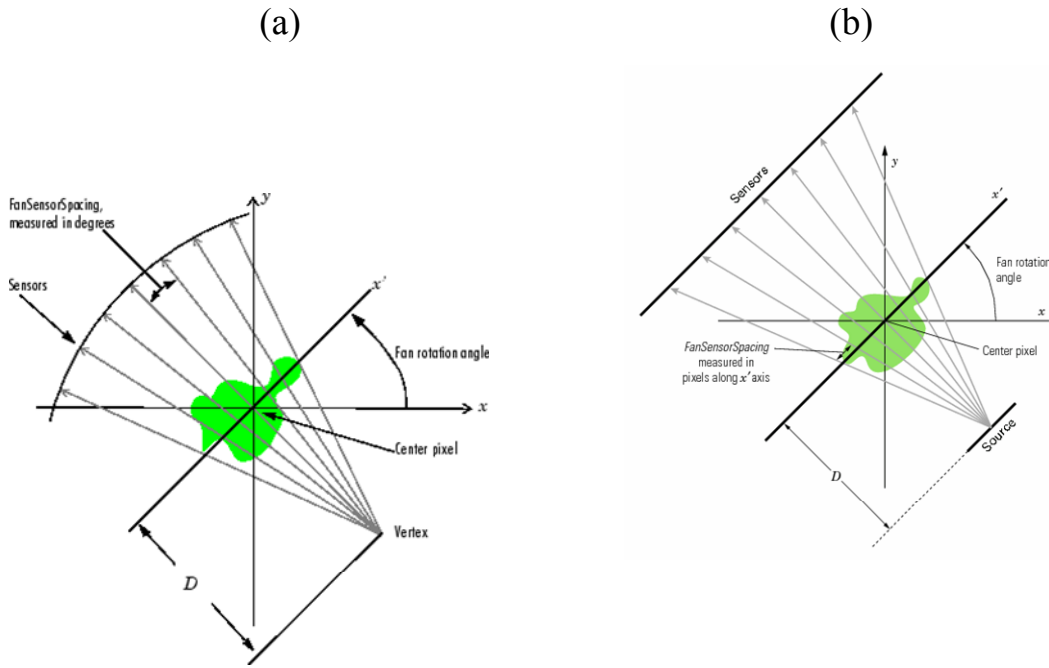


Figure 2-1. Single fanbeam projection at rotation angle theta. (a) the geometry of fanbeam function when FSG is set to arc; (b) fanbeam function when FSG is set to line. From Matlab help, [2008].

The original image can be reconstructed by the help of inverse fanbeam transformation; fanbeam projection data; the distance between the vertex of the fanbeam projections, and the center of rotation. For obtaining the best results, the same values for these parameters that were used when the projection data was created, are needed. In order to carry out FB procedure for data fusion next steps are followed.

1. $MS_{i=1, \dots, n}^L \xrightarrow{\text{Registration and resample to Pan}} MS_{i=1, \dots, n}^H$.
2. $MS_i^H \xrightarrow{\text{Fanbeam transformation}} MS_{Pr_i}^H$.
3. $Pan \xrightarrow{\text{Spectral adaptation to } MS_i^H \text{ and fanbeam transformation}} Pan_{Pr}$.
4. $MS_{Pr_i}^H \text{ and } Pan_{Pr} \xrightarrow{\text{Fusion of projections}} \text{New Pr}$.
5. $\text{New Pr} \xrightarrow{\text{Inverse fanbeam transformation}} MS_F^H$.

Where P_r is the converted projections obtained by FB transformations and the abovementioned steps are routines almost similar to all other image fusion procedures. The fanbeam and inverse fanbeam transformations also follow the explained procedures. The most important one is step four that the fusion of projections happens. This step in the simplest case could be the arithmetic mean of projections $(MS_{Pr}^H \text{ and } Pan_{Pr})/2$ which both inputs will have equal influence to the final fused dataset. Consequently the results of such a fusion will be a fused dataset that spatial information from Pan and spectral information from MS images are equally combined. As this transformation is a loopy therefore some unwanted distortions are unavoidable.

2.1.1.7 Radon Transform (RT)

Comparable to fanbeam, the Radon transformation computes projections of an image matrix along specified directions. In this transformation the projection of an image as a two-dimensional function $f(x, y)$ is a set of line integrals. On the contrary to fanbeam in which the source of beams is single, Radon transformation computes the line integrals from multiple sources along parallel beams, in a certain direction (Figure 2-2(a)). The beams are spaced 1 pixel unit apart. To represent an image, the Radon function takes multiple, parallel-beam projections of the image from different angles by rotating the source around the center of the image.

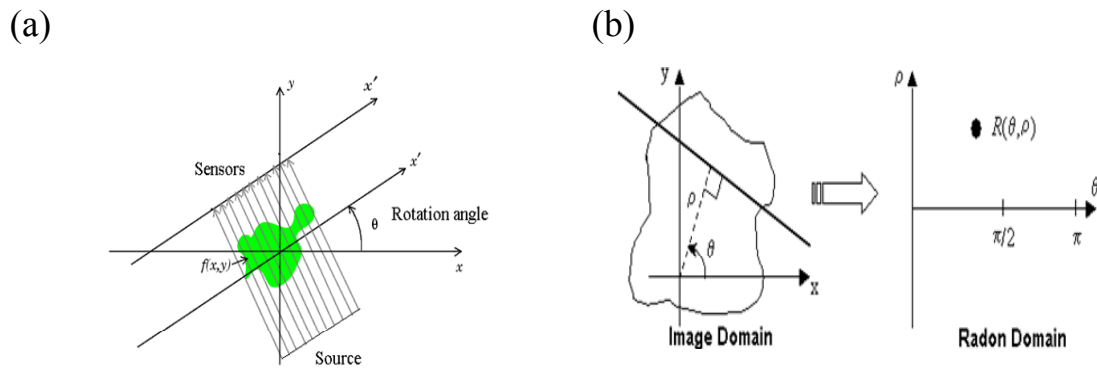


Figure 2-2. (a) Single Radon projection at a specified rotation angle with parallel-beam projection at rotation angle theta; (b) The Radon transform for one beam across an image. After Toft [1996].

The Radon transform has several applications in image analysis: feature detection; liner objects extraction; data compression; etc. For a function $F(x, y)$, the Radon transform describes the integral along a line s through an image (Equation 2-23 and Figure 2-2 (b)).

$$R(\theta, \rho) = \int_{-\infty}^{\infty} F(\rho \cos \theta - s \sin \theta, \rho \sin \theta + s \cos \theta) ds \quad (2-23)$$

Where ρ is the distance of line from the origin and θ is the angle from horizontal axis. In the Radon domain each point $R(\theta, \rho)$ is called a ray-sum, while the resulting projection image called shadowgram. Using an inverse projection (Equation 2-24) a new image $F'(x, y)$ can be reconstructed based on the ray-sums from the $F(x, y)$.

$$F'(x, y) = \int_0^{\pi} R(\theta, x \cos \theta + y \sin \theta) d\theta \quad (2-24)$$

Similar to fanbeam the Radon transform is not a perfect invertible transform, therefore the output, $F'(x, y)$, is an image of $F(x, y)$ which blurred by transformation

[Toft, 1996]. Due to the fact that Radon follows the same transformation routine as the fanbeam therefore the practical implementation is similar.

2.1.2 PLDF using selected panchromatic band frequencies

Following the assumption that Pan images have some spatial information (i.e. high frequencies) that are missing in MS datasets, the second category of PLDF techniques are categorized. The most common techniques in this group are the procedures that additional high resolution spatial information (i.e. high frequencies) of the panchromatic band is injected into the MS datasets. The most famous procedures in this category are those working base on filtering techniques in spatial domain, wavelet transform, and ARSIS concept.

2.1.2.1 Wavelet Transformation (WT)

Wavelets are mathematical functions that cut up data into different frequency components and then study each component with a resolution matched to its scale, therefore the fundamental idea behind wavelets is to analyze according to scale [Graps, 1995]. Wavelet transform as a mathematical tool developed in the field of signal processing [Zhang, 2002]. It widely used for processing and fusion of remotely sensed images. It is an image decomposition algorithm that based on its local frequency contents decomposes image into multiple new layers each of which has a different resolution degree. Since it is isotropic and shift-invariant thus does not create artifacts when used in image fusion procedures [Wang *et al.* 2005 and Zhou *et al.* 1998].

2.1.2.1.1 Discrete Wavelet Transformation (DWT)

Discrete wavelet transform which was introduced by Haar [1910] is defined as any kind of wavelet transformation in which the wavelets are discretely sampled [Zhang, 2002]. The DWT has a high number of applications in mathematics, science,

engineering, image processing, computer science, etc. DWT applications in image and signal processing in general and specifically in image fusion are dramatically increasing. Data fusion using wavelet transformation permits to introducing the concept of details between successive levels of scales or resolutions. For this purpose first we need define a mother function; this function is mainly concentrated near 0 and is characterized by a rapid decrease when $|t|$ increases [Garguet-Dupor, 1996]. In order to provide a good localization in both frequency and space domains [Núñez, 1997] the wavelet transformation of a distribution $f(t)$ can be expressed as dt (Equation 2-25).

$$W(f)(a,b) = \frac{1}{\sqrt{a}} \int f(t) \psi\left(\frac{t-b}{a}\right) dt. \quad (2-25)$$

Where a , b are scaling and translational factors respectively; $\psi\left(\frac{t-b}{a}\right)$ is a base function that is a scaled and translated version of a ψ function and ψ is mother wavelet.

Based on equation (2-25), equation (2-26) can be derived as

$$\int_{-\infty}^{+\infty} \Psi(t) dt = \dots \int_{-\infty}^{+\infty} t^{m-1} \psi(t) dt = 0 \quad (2-26)$$

Thus the loss of information will be 0 and this means it is a lossless transformation that can be applied for a variety of data. In order to decompose image into wavelet planes [Núñez, 1997] the discrete Two-Dimensional Wavelet Transform (2DWT) which is an extension of the One-Dimensional Wavelet Transform (1DWT) [Yocky, 1995] has been used. In this process the decomposition applied over an image which will produce a set of multi-resolution images supplemented with wavelet coefficients for each resolution scale. Obtained wavelet coefficients for each scale contains the spatial differences between two successive resolution scales [Wald *et al.* 1997]. In

general the wavelet-based image fusion is carried out in the following steps (Figure 2-3):

1. $MS_{i=1,\dots,n}^L \xrightarrow{\text{Resampling to Pan resolution}} MS_{i=1,\dots,n}^H$.
2. $MS_i^H \xrightarrow{\text{DWT decompose}} \text{MS wavelet coefficients}_{h,v,d,\alpha}$.
3. $\text{Pan} \xrightarrow{\text{DWT decompose}} \text{Pan wavelet coefficients}_{h,v,d,\alpha}$.
4. Pan high frequency component normalization to that of MS .
5. $\text{Wavelet coefficients} \xrightarrow{\text{Fusion}} \text{Fused wavelet coefficients}_{ms\alpha+Pan\ h,v,d}$.
6. $\text{Fused wavelet coefficients}_{ms\alpha+Pan\ h,v,d} \xrightarrow{\text{Inverse DWT}} \text{Fused MS}^H$.

Where ms is one band from MS. α , h, d, and v are overall, horizontal, diagonal, and vertical wavelet coefficients, respectively.

In order to normalize the high frequency components (i.e. C_{n-3}^z , $z = h, v, d$), they are sampled to estimate radiometric normalization coefficients a^z and b^z for each ms band [Canty, 2007]. $a^z = \hat{\delta}_{ms}^z / \hat{\delta}_{pan}^z$ and $b^z = \hat{m}_{ms}^z / a^z \hat{m}_{pan}^z$ where $\hat{\delta}$ and \hat{m} are the estimated standard deviation and mean of the ms and Pan datasets, respectively. These coefficients are then used to normalize the wavelet coefficients for the panchromatic image to those of each multispectral band at the n-2 and n-1 scales [Canty, 2007 and Ranchin and Wald, 2000] (Equation 2-27).

$$C_k^z(i, j) \rightarrow a^z C_k^z(i, j) + b^z, \quad z = h, v, d, \quad k = n-2, n-1 \quad (2-27)$$

As illustrated in figure (2-3), in this process the replacement and inverse transformation will be carried out in an equal number as the number of MS bands [Garguet-Duport *et al.* 1996 and Zhou *et al.* 1998]. In the used method all the spectral information of the MS image is preserved. Thus, the main advantage of the additive method is that the detailed information from both sensors is used and preserved [Núñez, 1997]; Yocky [1995]; and Ranchin and Wald [2000].

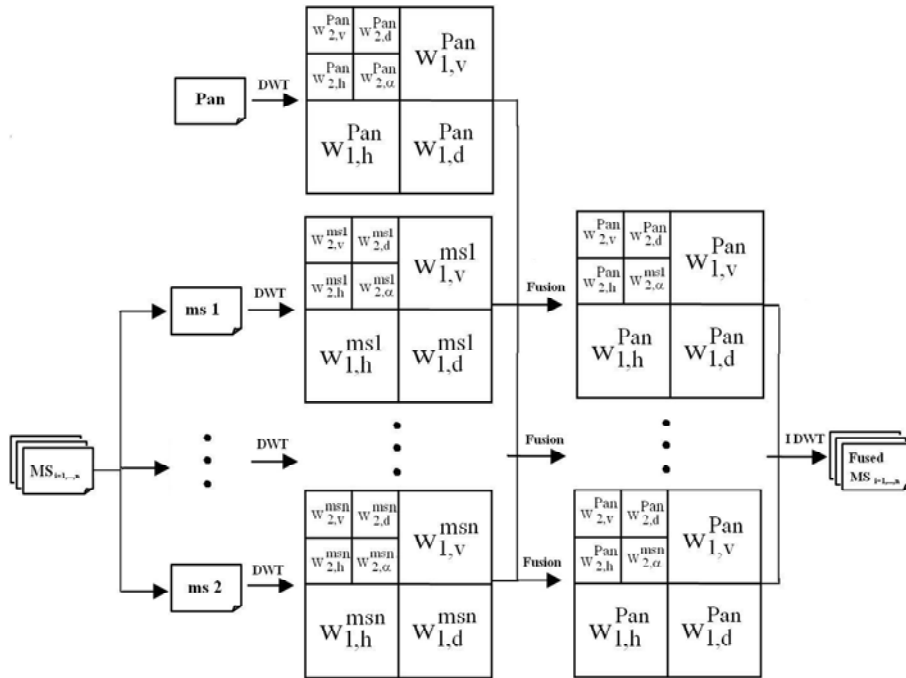


Figure 2-3. Block diagram of the DWT image fusion scheme.

As shown in figure (2-3), the first stage of wavelet fusion is to perform two-dimensional (2D) DWT on Pan and MS datasets separately. By the help of a two-channel filter bank which contains a lowpass and a highpass filters. The 2D DWT is carried out as the extension of a one-dimensional 1D DWT. In this procedure first along the horizontal direction 1D DWT is carried out in which each row being treated as a 1D signal. By sequential execution of lowpass and highpass filters on each row which followed by a 2-to-1 down-sampling operation. In this stage from the first 1D DWT produces the horizontal lowpass output and the horizontal highpass output will be obtained. The same as the first step, the second 1D DWT filters is carried out at vertical direction of the outputs produced by the first 1D DWT. As these operations are sequential and can be carried out till the whole image be decomposed therefore in some levels of decomposition we have to stop the procedure. Two levels of decomposition were carried out over each image separately. With 4 outputs for each one namely: overall wavelet coefficient, α ; horizontal wavelet coefficient, h; diagonal wavelet coefficient, d; and vertical wavelet coefficient, v. As overall wavelet coefficient α from the MS dataset is expected to have the most informative spectral

information, therefore it has been fused with other coefficients from Pan image. Finally an inverse DWT will results a fused MS dataset that has the high resolution properties from Pan, while the spectral information of MS data is highly preserved. As the wavelets mostly are described in terms of wavelet functions and scaling functions, it is also common to refer to them as families: the wavelet function is the mother wavelet, the scaling function is the father wavelet and transformations of the parent wavelets are daughter and son wavelets [Amolins, 2007]. In this work two common families as Haar and Symlet were evaluated.

2.1.2.2 High Pass Filter (HPF)

The high pass filter methodology was used by Chavez and Bowell [1988] and Chavez [1986] to fuse the TM data with digitized national high altitude program and SPOT-Pan dataset. This technique is a kind of weighted addition of higher resolution image with the lower resolution one. The rational behind is that the high spatial frequency information from Pan must be inserted into the MS dataset using the HPF procedure which developed by Schowengerdt [1980]. The practical implementation of methodology follows the next steps.

1. $MS_{i=1,\dots,n}^L \xrightarrow{\text{Resampling to Pan resolution}} MS_{i=1,\dots,n}^H$.
2. $Pan \xrightarrow{\text{High frequency details extraction using } n*n \text{ moving window}} Pan_{HFI}$.
3. $MS_{i=1,\dots,n}^H \xrightarrow{\text{Low frequency details extraction using } n*n \text{ moving window}} MS_{LFI=1,\dots,n}^H$.
4. $MS_{LFI=1,\dots,n}^H \text{ and } Pan_{HFI} \xrightarrow{\text{Spectral adaptation of and adding in a band by band base}} = MS_{i=1,\dots,n}^H$.

The High Frequency Information (HFI) of the Pan is extracted by subtracting a lowpass version of the Pan from itself. The lowpass filtering is obtained by a $n \times n$ sliding window.

2.1.2.3 ARSIS concept data fusion

This concept is called ARSIS, after the acronym of (French) Amelioration de la Resolution Spatiale par Injection de Structures, (English) improvement of spatial resolution by structure injection. Main philosophy behind the ARSIS concept is return to this assumption that the missing spatial information in the lower resolution datasets is linked to the high frequencies information [Wald, 2002]. Therefore the function of ARSIS is to find and model this relationship between high frequency component of two or more datasets e.g. multispectral and panchromatic images. Any method which works based on the ARSIS concept typically follows the next steps [Ranchin *et al.* 2003]:

1. Extracting a set of information from Pan image.
2. Inference the information that is missing in MS images using the extracted information.
3. Construction the fused images MS_F^H based on the obtained information.

In order to put ARSIS concept into practice, modeling the missing high frequencies information can be handled more sensibly by Fourier or wavelet coefficients or other similar transformations. For example Ranchin and Wald [2000] carried out the Multiscale Model (MSM) as a hierarchical description of the information content relative to spatial structures in an image. In consequent ARSIS concept was addressed which makes use of a multi-scale method for description and modeling of missing information between the multispectral and panchromatic images. Ranchin and Wald [2000] used wavelet transformation for multi-scale ARSIS method over SPOT-XS and Pan images.

Due to the generality of this concept several procedures based on ARSIS can be carried out. For instance the High-Pass Filtering (HPF) [Chavez *et al.* 1991]; wavelet based methodologies like Model-1, Model-2 and RWM (after the names of Ranchin, Wald, and Mangolini), [Ranchin and Wald, 2000 and Ranchin *et al.* 1994] are all procedures that are developed under this concept. In this work two data fusion

techniques based on ARSIS concept as ‘a-trous’ wavelet transform [Aiazzi *et al.* 2002] and the discrete wavelet transform [Ranchin and Wald, 2000] are investigated.

2.1.2.3.1 A Trous Wavelet Transform (ATWT)

A Trous (French: hole) Wavelet Transform (ATWT) [Dulilleux, 1987] is one of the most common wavelet-based image fusion procedures. It is a non-orthogonal wavelet which is a kind of discrete approaches of wavelet transform. After Mallat’s algorithm, this technique is the second popular procedure used in the DWT. ‘A’ Trous’ algorithm has been carried out by several authors e.g. Nunez *et al.* [1999], Gonza’lez-Audicana [2002] and Ranchin *et al.* [2003]. Due to the appeared problems with DWT, the ATWT as an alternative was proposed for image fusion [Aiazzi *et al.* 2002]. The ATWT is a multi-scale decomposition defined formally by a low-pass filter $L = \{l(0), l(1) \dots\}$ and a high-pass filter $H = \delta - L$, where δ denotes an all-pass filter. The high frequency part is then just the difference between the original image and low-pass filtered image. This transformation does not allow perfect reconstruction if the output is downsampled. Therefore downsampling is not performed at all. Rather, at the k^{th} iteration of the low-pass filter, 2^{k-1} zeroes are inserted between the elements of H . This means every other pixel is interpolated (averaged) on the first iteration: $L = \{l(0), 0, l(1), 0, \dots\}$, While on the second iteration $L = \{l(0), 0, 0, l(1), 0, 0, \dots\}$, and so on. The name "A Trous" (with holes) is return to the added 0s which makes holes, (0 value) pixels. The low-pass filter is usually chosen to be symmetric. Cubic B-spline filter [Nunez *et al.* 1999] with $L = \{1/16, 1/4, 3/8, 1/4, 1/16\}$ as a good choice has been used in this work. The carried out procedure (with the assumption that difference in spatial resolution is a factor of two) is similar to the DWT. The main steps of implementations are briefly outlined as

1. $MS_{i=1, \dots, n}^L \xrightarrow{\text{Resampling to Pan resolution}} MS_{i=1, \dots, n}^H$.
2. $MS_i^H \xrightarrow{\text{A Trous transform}} ms \text{ Trous coefficient } s_{h,v,d,\alpha}$.

3. Pan $\xrightarrow{ATrous\ transform}$ Pan Trous coefficient $s_{h,v,d,\alpha}$.
4. Pan high frequency component
normalization to that of ms .
5. Wavelet coefficient $s_{ms\alpha}$ \xrightarrow{Fusion} Fused wavelet
coefficient $s_{ms\alpha+Pan\ h,v,d}$.
6. Fused wavelet coefficients $s_{ms\alpha+Pan\ h,v,d}$ $\xrightarrow{Inverse\ ATWT}$ Fused MS_{Fi}^H .

2.1.3 PLDF using panchromatic band indirectly

In this group of techniques, panchromatic band information is not directly used in the fusion process and it just forms the basis for band specific transformations or estimating procedures [Hill *et al.* 1999]. The mostly used techniques are those that the radiometric similarity of datasets is minimal and input datasets can be called “spectrally inconsistent” e.g. thermal IR bands in fusion with panchromatic band. As an example Price [1987] in order to make a Look Up-Table (LUT) used a crosstabulation between panchromatic and thermal IR datasets after fitting grey values using the High Frequency Modulation (HFM) algorithm [Vrabel, 1996]; the spatial resolution of the IR dataset is increased while their spectral properties are highly smoothed. Tom [1986] developed a technique based on local correlation properties of the input datasets. These techniques showed a good performance to the cases which works based on a single high resolution panchromatic band. Zhukov *et al.* [1995] developed a methodology named MMT after the full name Multi-sensor, Multi-resolution Technique. In this work none of techniques in this category are investigated.

2.2 Pixel level data fusion quality assessment

Ideally, the goal of data fusion is to represent the information contained in input images into a fused image without introducing distortion or information losses. Due to the nature of data fusion and the principals of information theory, it is almost impossible to represent and preserve all input information in a single fused image.

With regard to these facts, the main achievable purpose is to minimize the information loss and distortions in fused images. As a general rule, fused datasets should be suitable for human visual perception and also suitable for machine-based information extraction techniques like object segmentation, data classification, feature extraction, object detection, etc.

Generally, evaluation the quality of a fused image depends on DF application for example when the purpose is enhancing visual properties of data, therefore the definition of the quality maybe different from the case that data are fused for classification purposes. In this regard, as we are looking for the fusion techniques that work for enhancing all aspects of the fused data, therefore the used evaluations are general and global indices that will cover all properties of fused data. From the literature, evaluation procedures in PLDF can be mainly divided into three groups: objective, subjective and Human Vision System (HVS) indicators. The first groups comprise the mathematical and statistical procedures that provide measures to evaluate the accuracy of fused image compare to a reference image. The second group of evaluation are refers to Mean Opinion Score (MOS) that is obtained by averaging some subjective tests where the numbers are ranked based on the visual quality of fused images compare with references. Finally the HVS evaluation techniques are based on the precipitations of human vision systems.

2.2.1 Objective PLDF quality assessment indices

Due to the kind of distortions and the used datasets all properties of fused data must be measured. As the spectral and spatial properties of Pan and MS datasets always do not obey the likeness rules therefore both spectral and spatial resolutions of the fused images must be evaluated. Accordingly, using some quantitative indicators the performance of the used techniques with respect to the spectral and spatial information contents of the fused image in compare to the reference datasets are measured. These indicators are providing measures of the closeness between fused

and reference datasets by utilizing the differences in spectral and spatial statistical distributions of DNs.

With reference to this fact that the number of objective image quality assessment metrics are dramatically high and according to the availability of reference dataset (which the fused dataset is to be compared with [Wang *et al.* 2004]) the developed and applied objective indices are categorized into three main groups.

1. Full-reference image quality assessment techniques that use an available complete reference image.
2. No-reference or blind quality assessment approaches are desirable in cases which reference image is unavailable.
3. Reduced-reference in which the reference image is only partially available. In such a procedure a set of extracted features made available as side information to help in evaluation the quality of fused image.

As in this work the main objective is to evaluate the kind and amount of distortion due to the fusion process accordingly a quality assessment that can offer the whole information is desirable. Therefore here the focus is on full-reference quality assessments. As the reference datasets were not available for second property of Wald, therefore the needed reference datasets are produced.

2.2.1.1 Wald's property indicators

Due to the main rational behind the PLDF procedures that aims at injecting the higher spatial resolution properties of Pan into the MS images while their original spectral content are preserved. Therefore the importance of spectral consistency is very high for almost all applications of satellite imagery especially those that are depend on the spectral properties of data e.g. classification and visual image interpretation. As mentioned above the number of indicators is high and very diverse that make the quality assessment be complicated. In order to make a thorough and global

measurement Wald *et al.* [1997] offered a standard protocol for evaluating quality of fused images. This protocol is formulated by three “properties” of fused images as:

1. Any MS fused image once downsampled to its original spatial resolution should be as identical as possible to the original image;
2. Any MS fused image band should be as identical as possible to the image band that a corresponding sensor would observe with the same high spatial resolution (if available);
3. The fused dataset should be as identical as possible to the dataset that a corresponding sensor would observe with the same high spatial resolution (if available).
4. Any fused image band must be as spatially informative as possible in compare to original panchromatic image.

As three first properties are mostly based on the spectral fidelity of the fused dataset and the spatial fidelity has a minority of importance therefore we added the last property as the complementary to Wald’s protocol. The last added property is return to the spatial homo- or heterogeneity of the fused image which is evaluated in compare to the original Pan image. This parameter helps to know the spatial information contents of the Pan and helps to know “are spatial information properly transferred into the fused dataset?”

2.2.1.2 Wald’s requirements

In order to put the above-mentioned measurements into practice, an indicator must be used that can offer a measurement of similarity between fused image and a proper reference (if available). In this regard as a general framework Wald [2002] numbered three main “requirements” for any image quality assessment indicator.

1. It should be independent of data units, calibration coefficients and instrument gains. Consequently it must be applicable to unitless quantities of DNs or radiances and any other forms of data values.
2. This quantity should be independent from the number of spectral bands under consideration. This is a sine qua non condition to compare results obtained in various conditions.
3. This quantity should be independent of Sharpening Factor (SF) or the scales of Pan and MS datasets. This permits to compare results obtained in different scales and for different image resolutions.

2.2.1.3 Reference image creation

From the literature several methods have been proposed to make a reference image. The routine for reference image creation is adapted from is based on image scale changing. In this procedure it is assumed that an artificially-made reference image quality evaluation can offer the needed quality measurements for assessing the real images:

1. $Pan^H \xrightarrow{\text{Register and downsample to MS resolution}} Pan^L$.
2. $MS^L \xrightarrow{\text{Downsample to very low resolution}} MS^{VL}$.
3. $Pan^H, MS_k^L \xrightarrow{\text{Pixel level data fusion}} MS_k^{HF}$.
4. $Pan^L, MS_k^{VL} \xrightarrow{\text{Pixel level data fusion}} MS_k^{LF}$.
5. $MS_k^L, MS_k^{LF} \xrightarrow{\text{Statistical and visual comparison}} \text{Quality measurement}$.
6. *Artificial quality measurement generalized as real quality measurement of the PLDF technique.*

Where H, L and VL are the High (e.g. Pan, 10 m), Low (e.g. MS, 30 m) and Very Low (Downsampled MS, 90 m) spatial resolutions of real and downsampled datasets, respectively. The mentioned routine for making a reference image and generalize the

quality of the fabricated reference image (MS_k^{VF}) to the real image (MS_k^L) is based on the assumption that the error should increase with the enhancing of spatial resolution. Since the complexities of a scene usually increase as the resolution is getting higher, therefore the above assumption can be reliable. As the amount of sharpening factor for VL to L datasets is the same as for L to H therefore the obtained accuracies using these routines are reliable and can be generalized to the real fused datasets. Regarding to the relationship between object and pixel sizes that will change based on resolution changes therefore it seems the assumption of scale changing is not a comprehensive assumption. But from the literature this procedure is the most acceptable one and has been adapted in this work.

2.2.2 Spectral indices

These indices are mostly concerning the spectral valuates of individual pixels and not about the neighboring pixels. Therefore they are referred to as spectral indices.

1. Correlation between Fused (F) and Reference (R) images

$$\text{Corr}(R, F) = \frac{\sum (r - \mu_R)(f - \mu_F)}{\sqrt{\sum (r - \mu_R)^2 (f - \mu_F)^2}} \quad (2-28)$$

Where r and f are the pixel values of the reference R and fused F images; μ_R and μ_F are the means of R and F, respectively.

2. Relative Difference of Means (RDM)

$$\text{RDM}(R, F) = \frac{(\mu_F - \mu_R)}{\mu_R} \quad (2-29)$$

3. Relative Difference of Variances (RDV)

$$RDV(R, F) = \frac{(\delta_F^2 - \delta_R^2)}{\delta_R^2} \quad (2-30)$$

Where δ_F^2 and δ_R^2 denote the variances of the F and R, respectively.

4. Peak Signal to Noise Ratio (PSNR) [Winkler, 2005]

$$PSNR = 20 \log_{10} \left(\frac{Peak}{\sqrt{MSE}} \right) \quad (2-31)$$

Where peak is the maximum possible radiometric values for dataset, as it is 255 for 8 bit radiometric resolution and 2084 for 11 bit images, and so on. Mean Square Error (MSE) is the measure of radiometric distortion of the fused pixels as

$$MSE = \frac{1}{N} \sum_{i=1}^N (f_i - r_i)^2 \quad (2-32)$$

5. Relative dimensionless global error in synthesis (ERGAS)

Based on the three mentioned “requirements”, Wald [1999] introduced a quality assessment called ERGAS, after its name in French: erreur relative globale adimensionnelle de synthèse, English: relative dimensionless global error in synthesis.

$$ERGAS = 100 \frac{H}{L} \sqrt{\frac{1}{N} \sum_{k=1}^N [RMSE(F_k)^2 / (M_k)^2]} \quad (2-33)$$

Where H and L are the resolutions of the Pan and MS bands; M is the mean of the under investigation band, F; and RMSE is the Root Mean Square Error as the indicator of difference between fused and reference images.

With respect to calibration and changes of units it is reliable. It also obeys the second requirement. The ratio H/L takes into account the various resolutions. For the same error ERGAS, the mean value of the relative RMSE (F_k) increases as the ratio H/L decreases, and it is equal to:

$$RMSE = \sqrt{\frac{1}{N} \sum_{k=1}^N [RMSE(F_k)^2 / (M_k)^2]} \quad (2-34)$$

Where N is the number of pixels in the fused band, F.

6. Universal Image Quality Index (UIQI)

$$UIQI = \frac{\delta_{FR}}{\delta_F \delta_R} \frac{2\mu_F \mu_R}{(\mu_F)^2 + (\mu_R)^2} \frac{2\delta_F \delta_R}{\delta_F^2 \delta_R^2} \quad (2-35)$$

Where δ_{FR} ; δ_F^2 ; and δ_R^2 are the covariance and variances of F and R, respectively. This index is developed by modeling all possible distortions of an image. It is a combination of three important factors of image impairments including loss of correlation, luminance distortion, and contrast distortion [Wang, 2002]. Where the first component is the correlation coefficient between F and R; the second component is the measure of how close the mean luminance; and the third one is the measure of how similar the contrasts of two images are.

7. Structural Similarity (SSIM)

As the mentioned indicators consider the spectral and spatial properties of the fused datasets in almost separate ways therefore the need for a hybrid index that combine

these two are noticeable. The SSIM is the generalized and developed version of the UIQI which has offered promising results on image quality assessment. The philosophy behind is that the luminance of the surface of an object being observed is the product of the illumination and the reflectance, but the structures of objects in the scene are independent from illumination [Wang *et al.* 2004]. In SSIM the structural information of image independently from the influence of the illumination has been calculated. Therefore it is expected that SSIM is one of the best ones which in addition to spectral properties considers some aspects of spatial properties of fused datasets. In order to do that SSIM separates the task of similarity measurement into three comparisons: Luminance L, Contrast C and Structure S.

$$L(f,r) = \frac{2\mu_f\mu_r + C_1}{\mu_f^2 + \mu_r^2 + C_1} \quad (2-36)$$

$$C(f,r) = \frac{2\delta_f\delta_r + C_2}{\delta_f^2 + \delta_r^2 + C_2} \quad (2-37)$$

$$S(f,r) = \frac{\delta_{fr} + C_3}{\delta_f\delta_r + C_3} \quad (2-38)$$

And the combination of the three comparisons provides a general image quality indicator named structural similarity (SSIM).

$$SSIM(f,r) = \frac{(2\mu_f\mu_r + C_1)(2\delta_{fr} + C_2)}{(\mu_f^2 + \mu_r^2 + C_1)(\delta_f^2 + \delta_r^2 + C_2)} \quad (2-39)$$

Where $C_1 = (\kappa_1 D)$ in which D is the dynamic range of the pixel value (e.g. 255 for 8-bit) and $\kappa_1 \leq 1$ is a small constant. Similar considerations C_2 and C_3 also apply to contrast and structure comparisons.

All abovementioned measuring indicators are individual and global indices which supply statistics of similarity between two images. These measures are calculated by utilizing the differences in statistical distortions of pixel values [Eskicioglu, 1995]. In

this work all mentioned spectral indices were evaluated and finally the SSIM has been selected. After statistically evaluation of all techniques and comparing the obtained statistics with the visual appearance of fused images it was realized that SSIM can better shows the amount of distortions. More detailed information can be found in Karathanassi *et al.* [2007].

2.2.3 Spatial indices

As the abovementioned indicators work based on comparing pixel values of the fused and reference images with no care about the pixel neighbors therefore some probable drawbacks are sensible. These problems return to the fact that, it is probable for two compared images with the same statistical parameters (like mean and variance) to have different spatial arrangements of pixels. For example, assume a 5*5 window from an image (Figure 2-4(a)); after fusion process, several possible outputs could be appeared while in all cases statistical properties are the same.

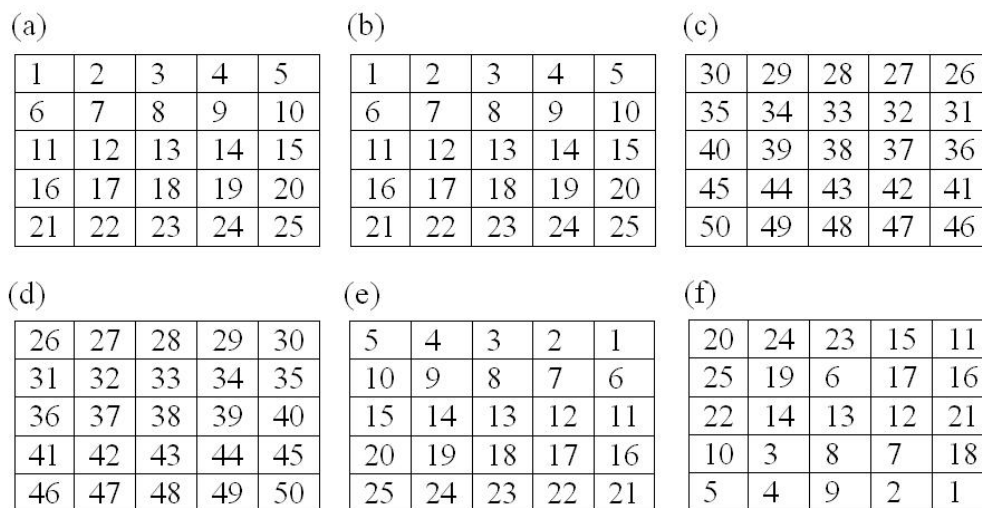


Figure 2-4. 5*5 window from an image: (a) original image and (b-f) different probable results from a pixel level data fusion process.

With reference to figure (2-4(a)) after an assumptive pixel level fusion about five possible spatial arrangements of pixels and consequently different spatial characteristics will be appeared:

1. First (i.e. the best) is the case which pixel values and their spatial arrangements are the same (b);
2. Second (i.e. the worst) is the case where no pixel values and no spatial arrangements are the same (c);
3. Third is the case when one of the data properties i.e. spatial arrangement (d) or spectral pixel values (e) is exactly the same while another property is different.
4. Fourth case could be any possible situation in which the pixel values and their spatial arrangements could partly be the same (f).

With reference to the mentioned possibilities the weakness of spectral based parameters is more sensible. On the other hand the spatial based calculations lonely will also mislead the evaluation process. For example in the case (d) the spatial indicators will show the same value while it is definitely different from the reference data (a). Thus we do believe two spectral and spatial properties must be evaluated and used in a complementary fashion for image quality assessments. Based on the number four property (added property to Wald's properties) which considers the spatial similarity of fused dataset to compare with Pan image the next two indices are evaluated as two considerable spatial indicators.

2.2.3.1 Normalized Difference of Entropies (NDE)

Entropy, as a measure of texture, has been applied in several domains of image processing. The texture-based entropy filter in the form of co-occurrence measure uses a gray-tone spatial dependence matrix to calculate texture values. This is a matrix of relative frequencies with which pixel values occur in two neighboring processing windows separated by a specified distance and direction. It shows the number of occurrences of the relationship between a pixel and its specified neighbor [Anys, 1994]. Thus the normalized differences of the entropy will show the amount of spatial similarity of the fused image in compare to its reference image.

$$RDE(F,R) = \sum_{i=1}^N \frac{(E_{Fi} - E_R)}{(E_{Fi} + E_R)} \quad (2-40)$$

Where E_{Fi} and E_R denotes the entropy of a single fused band from dataset (F) and R is the reference band that here is referred to as Pan image; N is the number of bands of the fused dataset. The NDE as a normalized measurement can get any value between 0 and 1. Therefore NDE=0 is the maximum spatial similarity between fused and Pan image. And with the increment of this value the amount of similarity will get lower. As another possibility the difference of entropies can be measured in absolute difference value.

2.2.3.2 Normalized Difference of Autocorrelations (NDA)

Another robust indicator that can offer some spatial information about an image is autocorrelation. This measurement looks for an overall pattern between contiguous pixels and their similarity in an image. This measurement can be calculated globally across the whole image or locally throughout local filters. Consequently it provides a single global value that describes the spatial dependency of dataset as a whole or can offer an image in which every pixel has a value which shows its spatial dependency in relation to its neighbors. Irrespective of the global or locality of the measurement there are several indicators that calculate autocorrelation e.g. Moran's I, Geary's C and semivariance [Curran, 1988 and Woodcock and Strahler, 1987]. The same as NDE, the amount of NDA is calculated based on the normalized differences of autocorrelation of fused image and reference.

$$RDA(F,R) = \sum_{i=1}^N \frac{(A_{Fi} - A_R)}{(A_{Fi} + A_R)} \quad (2-41)$$

Where A_{Fi} denotes the autocorrelation of a single fused band from dataset (F) and R is the reference band that here is referred to Pan image; N is the number of bands of the fused dataset. The same as NDE this indicator can be calculated as the absolute differences of two datasets.

Here the local Moran's I and Geary's C of Anselin's LISAs [Anselin, 1995] [adapted from Yee Leung *et al.* 2002] are briefly explained and for more dialed discussions readers are referred to related references.

1. Local Moran's I

For illustration purposes let $x_i (x_1, x_2 \dots x_n)^T$ be the vector of observations on random variable X at n locations and $W=(w_{ij})_{n \times n}$ be a symmetric spatial link matrix which is defined by the underlying spatial structure of the geographical units where the observations are made. Based on Moran's I for pixel i, the local Moran's I_i in its standardized form is [Anselin, 1995].

$$I_i = (x_i - \bar{x}) \sum_{j=1}^n w_{ij} (x_j - \bar{x}) / \frac{1}{n} \sum_{j=1}^n (x_j - \bar{x})^2 \quad (2-42)$$

Where

$$\bar{x} = \frac{1}{n} \sum_{j=1}^n x_j, (w_{i1}, w_{i2}, \dots, w_{in}) \quad 2-43$$

\bar{x} is the i^{th} row of the symmetric spatial link matrix W and $w_{ii}=0$ by convention. A large positive value of I_i indicates spatial clustering of similar values (either high or low) around location i and a large negative value indicates a clustering of dissimilar values that is a location with a high value which surrounded by neighbors with low values and vice versa.

2. Local Geary's C

The local Geary's C_i at a reference location i is defined by Anselin [1995]

$$C_i = \frac{\sum_{j=1}^n w_{ij}(x_i - x_j)^2}{\frac{1}{n} \sum_{j=1}^n (x_j - \bar{x})^2} \quad (2-44)$$

With this assumption that, without loss of generality, $W_{ii} = 0$. A small value of C_i suggests a positive spatial association (similarity) of observation i with its surrounding observations, whereas a large value of C_i suggests a negative association (dissimilarity) of observation i with its surrounding observations.

In this work the two mentioned spatial evaluations are calculated and the absolute value of differences has been adapted and used for image evaluation purposes.

2.2.4 Subjective image distortion indicators

Mean Opinion Score (MOS) which is calculated by averaging some subjective tests where the numbers are ranked based on the visual quality of fused image in compare to reference. In these techniques subjects or viewer selected from image interpretation professional and amateurs. A viewer is required to give each fused image a score based on the appearance of fused image in compare with reference image (Table 2-1).

Table 2-1. Scores for a fused image subjective quality assessment

Score	Quality	Image distortion
5	Excellent	Undistorted
4	Good	Perceptible but not irritate
3	Fair	Slightly irritate
2	Poor	Irritating
1	Bad	Very irritating

Finally the MOS score for a fused image is the arithmetic mean of all individual scores and can range from 5 (excellent) to 1 (worst). From the literature, none of these complicated and costly subjective metrics do provide a recognizable superiority over mathematical measures such as SSIM and ERGAS. Because the objective indicators are easy to calculate and need low computational process and also are independent from viewing conditions and individual observers [Wang and Bovik, 2002] therefore here we neglected the subject evaluation and readers for more detailed discussions are referred to Martens and Meesters [1998] and Eskicioglu and Fisher [1995].

2.3 Feature Reduction (FR)

All Earth surface materials have specific spectral behaviors which are related to their physiochemical compositions and temporal and environmental characteristics. For instance vegetation are generally determined and discriminated according to their absorption and reflection properties (spectrally detectable features) which are related to liquid water and chlorophyll contents, respectively [Jensen, 2007]. Also for other surface materials these features are remarkably detectable in the optical remotely sensible portions of Electromagnetic (EM) spectrum (i.e. the regions between 400-2500 nm which covering reflectance spectrum from visible to shortwave infrared) [Bannari *et al.* 2000; Champagne, 2002 and Pacheco, 2004]. The HS imagers which are able to collect a pseudo-continuous reflectance spectrum in the form of narrow channels (almost 10 nm) have high abilities to discriminate surface materials because they provide detectable features for different parts of EM in more details. This beneficial ability of HS image is linked to the data redundancy problem [Motta *et al.* 2006]. Therefore FR is a necessary processing step in some data analysis procedures that DF is one of them.

One of the earliest definitions of feature given by Swain and Davis [1978] “a subset of the original dataset based on an optimal trade-off between probability of error and classification costs”. As this definition is a compromise between classification

accuracy and the data volume, therefore it is imperfect because it does not cover all other applications of image processing. In this regard a broader definition of FR can be “Extraction and/or selection the best representative subset from a dataset”. This subset must have maximum information; the exact definition of maximum information is application and user dependent procedure. For example maximum information for a pixel-based classification is maximum homogeneity of pixels in different bands of spectrum while for a segment-based classification maximum homogeneity of a group of pixels in one band that make a segment is important.

Here, feature is applied to a spectral subset obtained from original dataset. These subsets could be original bands or secondary derivatives of them that are calculated using a data conversion process (e.g. PCT). Therefore a feature must, in one hand, contain the highest amount of information and in another hand has dimension as small as possible. In order to obtain a proper feature two groups of techniques can be carried out: Feature Selection (FS) and Feature Extraction (FE). In the first category the original bands which do not represent important information and can be defined as redundant bands [Lee and Landgrebe, 1992] will be removed by some measures. For example the class distinction criterion which can be calculated using several statistical methods like divergence [Kailath, 1967]; transformed-divergence [Swain and Davis, 1978] and Bhattacharyya distance [Fukunaga, 1990 and Richards and Jia, 1999] are procedures to remove unwanted bands. The second category that is based on the transformation of original dataset into a new data presentation system followed by a procedure that extract a subset which can represent the most informative contents of original dataset while the dimensionality is reduced [Heydorn, 1971 and Lee, 1992]. For example PCT [Keinosuke, 1990] and MNF transformations [Green *et al.* 1988] are mostly linear conversions that are widely used in remotely sensed data analysis. Another aspect of FR which is developed in this work is return to the basis that the FR procedure will be carried out, which named “block based” and “class based” FRs.

2.3.1 Feature reduction levels

In Data Based Feature Reduction (DBFR): the original dataset e.g. EO-1/Hyperion is investigated as a whole and the purpose is finding a subset of features that is the best representative of the dataset. In this regard any used procedure can be called feature reduction. The second level of FR is named Block Based Feature Reduction (BBFR) that, on the contrary to DBFR, which is based on the whole dataset, in this methodology the feature obtaining procedure is limited to some smaller dimensions blocks of bands. The DBFR is a common procedure in remote sensing FR that has been carried out in several works.

2.3.1.1 Block Based Feature Reduction (BBFR)

In hyperspectral datasets due to the narrowness of bandwidths and pseudo-continuity property of datasets, it is assumed that between-neighboring-band correlations are high enough which some bands can be clustered as separate blocks. As can be seen in figure (2-5) the square blocks across the diagonal axis have clearly recognizable values that show the blocks of bands with inter-correlations more than 90 percent.

In a hyperspectral imagery the correlation between adjacent bands are higher than for bands further apart and highly correlated bands appear into separable groups or blocks (Figure 2-5); this statistics can be visualized as an image entitled statistic image [Kim and Swain, 1990]. Based on this assumption, let N denote an n -dimensional dataset representing the n spectral channels. In block based feature reduction procedure the adjacent bands will come together in a block if their correlation is higher than a specific threshold, τ .

$$\text{If } R_{i,i+1} > \tau \text{ then } R_{i,i+1} \in B_k, \quad 0 < R_{i,i+1} < 1 \quad i=1,2,\dots,n \quad k=1,2,\dots,m \quad (2-45)$$

Where $R_{i, i+1}$ is the correlation between band i and its neighboring band $i+1$. B_k is the block with a inter-correlation higher than τ . k subscript denotes the block number. Thus we will have m blocks that each of them will contain a number of highly

correlated bands. τ is a measurement to control the dimension and number of blocks; as the highest amount of τ (i.e. one) will result maximum block numbers as $n=m$ and in contrary the lowest amount (i.e. zero) will allocate all channels to one block. This new feature reduction procedure was performed over EO-1/Hyperion, Indonesia, 2004 dataset. And the obtained results are very effective.

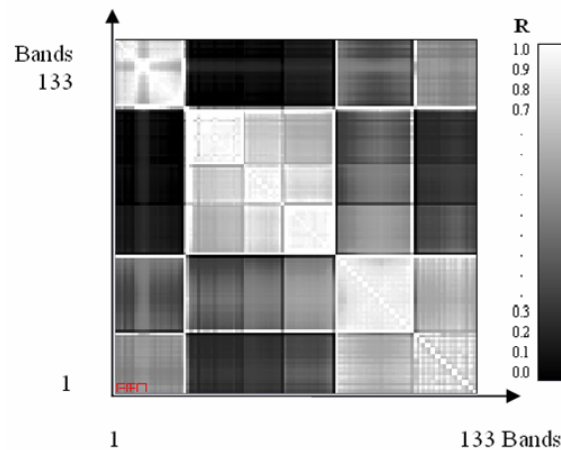


Figure 2-5. Statistic image for EO-1/Hyperion, with 133 spectral bands, Indonesia, 2004.

2.3.2 Feature selection techniques

In this work a new feature selection methodology named Maximum Spectral and Spatial Information Indicator (MSSI) was invented, performed and evaluated in compare to two common feature selection algorithms i.e. Bhattacharyya distance and transformed divergence.

2.3.2.1 Bhattacharyya Distance (BD)

Bhattacharyya distance is a numerical approach that works as a separation factor for two classes in a dataset [Kailath, 1967 and Fukunaga, 1990]. The Bhattacharyya distance is mathematically defined as

$$B = \frac{1}{8}(\mu_i - \mu_j)^T \left\{ \frac{\Sigma_i + \Sigma_j}{2} \right\}^{-1} (\mu_i - \mu_j) + \frac{1}{2} \text{Ln} \left\{ \frac{|\left(\frac{\Sigma_i + \Sigma_j}{2}\right)|}{\sqrt{|\Sigma_i||\Sigma_j|}} \right\} \quad (2-46)$$

Where μ_i and μ_j are mean values and Σ_i and Σ_j are the covariance matrices of i and j classes, respectively. In this measurement the first term is the account of separation due to the class means which is normalized due to the class covariance and the second term measures the class separation based on class covariance [Richards and Jia, 1999]. This FS procedure is documented in Tadjudin and Landgrebe [1998].

2.3.2.2 Transformed Divergence (TD)

In order to understand transformed divergence first divergence that is an operator which measures the separation of two or more spectral classes must be explained. The explored distribution functions of classes are spectral probable at position x (pixel in a multidimensional vector space based on a column and row coordinate system of an image) [Richards and Jia, 1999].

$$d_{ij} = \int_x \left\{ p(x|C_i) - p(x|C_j) \right\} \text{Ln} \frac{p(x|C_i)}{p(x|C_j)} dx \quad (2-47)$$

Where $p(x|C_i)$ and $p(x|C_j)$ are the values of the i^{th} and j^{th} spectral class probability distributions at position x . Therefore the overall divergence in a dataset is calculated using the summation operator as

$$d_{ij}(x) = \sum_{n=1}^N d_{ij}(x_n) \quad (2-48)$$

Where N denotes the number of variables in a multidimensional spectral space e.g. number of bands.

From the literature the divergence is suffering from two drawbacks: (i) it is a summing operator; therefore with increase the number of spectral variables it will never get smaller values. But in reality it is not true and the increased number of bands sometimes will not increase the amount of separation [Richards and Jia, 1999]. (ii) another point is about the somehow nonlinear behavior of divergence as a function of distance between class means. A small distance incensement will sharply grow divergence which in reality is not true. These problems with divergence and also the high ability of Bhattacharyya operator caused to its modification entitled “transformed divergence” which works in a similar way as the Bhattacharyya distance [Swain and Davis, 1978].

$$d_{ij}^T = 2(1 - e^{-d_{ij}/8}) \quad (2-49)$$

Where d_{ij}^T denotes the transformed divergence for i and j classes. Therefore because of the exponential properties it will saturate with increasing class separation [Mausel *et al.* 1990].

Based on two abovementioned distance-based feature selection algorithms a wanted number of features can be selected. Thus the obtained features are the best bands that can separate land cover classes in a dataset.

2.3.2.3 Maximum Spectral and Spatial Information Indicator (MSSI)

Autocorrelation as a geostatistic methodology is applied to a variable if its value in a specific place or time is correlated with its values in other places or times. Based on this definition and from the remote sensing perspective autocorrelation can be measured in spatial [Goodchild, 1986 and Griffith, 1987]; temporal [Georgiou, 2007]; and spectral domains. In this work the spectral and spatial autocorrelations for the intention of hyperspectral feature selection have been developed and evaluated.

MSSI is a mathematical methodology for measuring the similarity or dissimilarity “between” and “within” components of a dataset. For a n-dimensional (component or band) hypothetical dataset this methodology is composed of two parts.

- Within components or spatial autocorrelation and
- Between components or spectral autocorrelation.

Spatial autocorrelation is a statistical measurement of the degree of dependency among observations of a variable in spatial domain. For example DN values in a remotely sensed image (Figure 2-6) have almost similar behavior till specific distance which called “homogeneity distance”. Using this joint property the behavior of a pixel can be predicted using some other ones. In order to calculate these measurements it is considered that if the values of the variable are interrelated and if so, there is a spatial pattern to calculate, therefore there is spatial autocorrelation [Griffith, 1987]. Spatial autocorrelation in an image is mostly computed in a moving window (kernel with different sizes: 3*3, 5*5, etc). It can be computed in global and local scales [Getis and Ord, 1992].

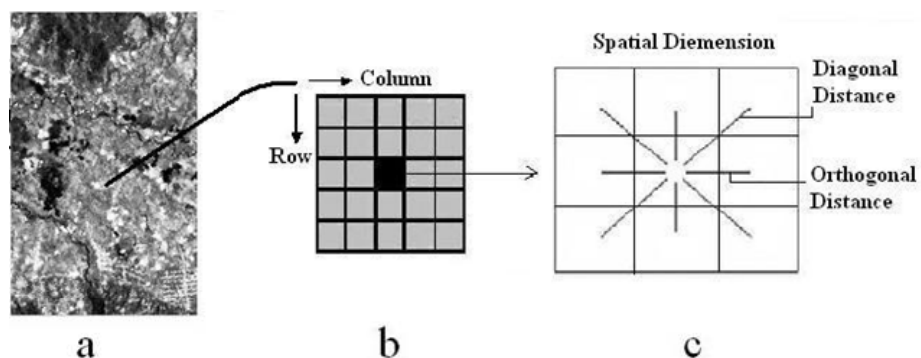


Figure 2-6. Spatial autocorrelation. (a) a monochrome image; (b) spatial domain of a pixel; and (c) adjacency rules.

Similar to spatial definition of autocorrelation, spectral autocorrelation is defined as the degree of dependency or similarity among observations of a variable in spectral

domain. For illustration let assume a hyperspectral dataset with N spectral bands, if we want to find a subset with n members (where $n \subset N$) consequently the amount of spectral autocorrelation is a statistic which measures the spectral similarity (i.e. homogeneity) between these n spectral bands. Therefore spectral autocorrelation based on the rational behind is a statistical measurement of the degree of dependency among observations (e.g. spectral bands) of a variable (e.g. object reflectance in electromagnetic spectrum) which is calculated at the level of pixels (Figure 2-7). In order to make differences clearer, let say spatial is within a band correlation while spectral is between bands correlation.

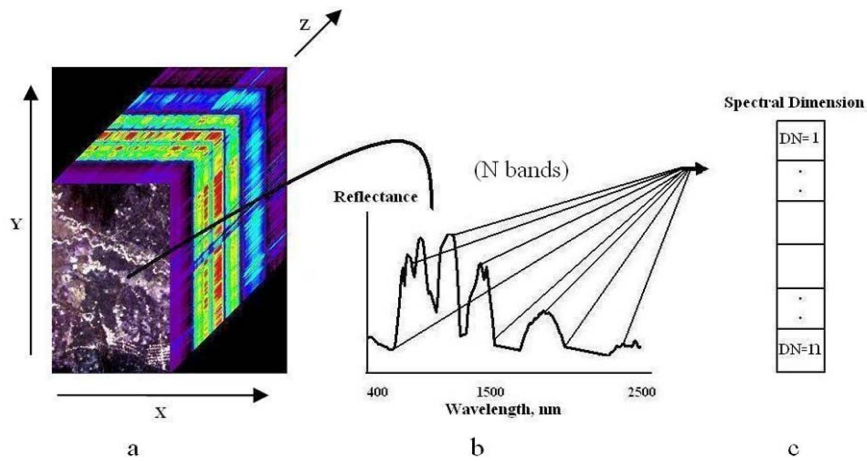


Figure 2-7. Spectral autocorrelation. (a) 3D cube of a hyperspectral dataset with N bands; (b) the spectral response (reflectance) of a pixel as a function of the wavelength; and (c) spectral dimension of a pixel in a selected subset with n bands.

MSSI which is the combination of these two measurements is a comprehensive and informative indicator that can be used as a selection criterion to obtaining the best representative n -bands subset from an N -bands dataset. In order to find the most informative subset from a dataset two scenarios can be carried out.

- Finding the most spectrally and spatially similar components.

- Finding the most spectrally and spatially dissimilar components.

In the first scenario the components with the highest amount of similarity are considered as redundant, therefore the less similar ones are most informative. On the contrary in the second scenario the components with lowest similarity which assumed having the highest amount of information will be selected. These two mentioned scenarios can be carried out based on the purpose of FR procedure; for example in feature selection and classification procedures the second procedure (i.e. spectral and spatial dissimilarity) is needed while on the contrary for the purpose of feature extraction e.g. PCT the similarity procedure (first scenario) is required.

From this background MSSSI is a framework which tries to simultaneously combine maximum spectral and spatial information from a subset. Consequently the obtained subset expectedly will contain the highest possible spatial and spectral information. In this regard a robust framework is needed that ideally have next characteristics:

1. Able to calculate spectral and spatial information contents as precise as possible.
2. Able to combine spectral and spatial information contents in the simplest possible way.
3. Measurable as simple as possible.
4. Independent of unite and scale of datasets.

With reference to the abovementioned restrictions, MSSSI can be handled by using two separate measurements, each for one characteristic of the subset (spatial and spectral information contents) and finally combine these two measurements. As this will be an expensive calculation thus we looked for an index which can be considered as the combination of both. In this regard the image quality indices which work based on the spectral and spatial similarities of two images have been evaluated. With exploration of these indices in a proper way they will garnet these restrictions and can provide the needed spectral and spatial information for the purpose of MSSSI feature

selection. Therefore three of the most famous image quality assessment indices have been evaluated. It should be noted that the MSSSI is a general framework and can be calculated by any other measurements. In the framework of MSSSI the relative dimensionless global error in synthesis (ERGAS) [Wald, 2002]; Universal Image Quality Index (UIQI) [Wang, 2002] and Structural Similarity (SSIM) [Wang *et al.* 2004] were investigated. The SSIM is the generalized and developed version of UIQI which has offered promising results on image quality assessment. In this indicator the structural information of the image independently from the influence of illumination are calculated. Therefore SSIM could somewhat provide the needed conditions for MSSSI.

As in this work the second scenario (Finding the most dissimilar spectrally and spatially components) explored therefore in the practical viewpoint MSSSI is carried out in the next steps.

1. Finding two most dissimilar bands using $SSIM^{-1}$;
2. Finding third most dissimilar band to the two earlier selected bands;
3. Finding fourth most dissimilar band to the three earlier selected bands and so on;
4. Stopping searching procedure when the number of selected bands is enough or the dissimilarity is lower than or equal to a specific threshold.

2.3.3 Feature reduction

In a hyperspectral dataset with more than 100 spectral bands or features which are from different parts of electromagnetic spectrum (e.g. visible; near infrared; and shortwave infrared) in an almost continues form (with a bandwidth about 10 nm). In almost all PLDF this high number of bands can not be fused. Therefore based on some statistical and transformational routines a subset with smaller dimension can be selected [Lee and Landgrebe, 1992] or extracted [Heydorn, 1971 and Lee, 1992]. In

obtaining the best possible bands for fusion purposes three possible scenarios can be carried out: sufficient, under-sufficient and over-sufficient number of bands.

The three mentioned categories are due to data fusion applications, algorithm limitations, logical relationship between input and output and soft- and hardware costs. For example in an IHS transformation for the purpose of visual interpretation, the optimal band number is three MS bands in combination with one panchromatic image. But any three-band subset could not be optimal. In this regard, a mechanism that can offer an optimal three-band subset from a higher dimensional datasets is considered here as the feature selection for data fusion. For the case of over-sufficient as an example using the Brovey transformation any number of bands (let say 100 or more) can be fused with no technical limitations but this over-sufficient number of bands will cause a high rate of spectral distortions. Also using two-band dataset in combination with Pan image using for example PCT is somewhat under-sufficient. Due to the fact that the number of bands in MS is almost higher than the wanted number of bands and especially this problem is more sensible in the HS datasets, therefore in order to overcome these problems a number of band selection strategies can be considered. In this work the new innovated feature selection procedure (i.e. MSSSI) is adapted.

CHAPTER THREE

3 Decision Level Data Fusion (DLDF)

DLDF like other levels of fusion has been contemplated from different points of view. Therefore definitions in the literature are somewhat different. For example Pohl and Van Genderen [1998] modified the Shen [1990] definition as: “Decision or interpretation level fusion represents a method that uses value-added data where the input images are processed individually for information extraction. The obtained information is then combined applying decision rules to reinforce common interpretation and resolve differences and furnish a better understanding of the observed objects”. While based on Benediktsson and Kanellopoulos [1999] “Decision fusion is defined as the process of fusing information from several individual data sources after each data source has undergone a preliminary classification”. Another explanation was offered by Hall and Llinas [2001] that “Decision level combines the decisions of independent sensor detection/classification paths by Boolean (e.g. AND, OR) operators or by a heuristic score (e.g. maximum vote and weighted sum)”. The main important and common point in these definitions is return to the individually processing of different datasets prior to the fusion process. These pre-fusion individual classifications could be a remarkable strength point in fusion process and weakness as well. This property is strength because the maximum ability of different classifiers is explored e.g. parametric and non-parametric classifiers combination provides such a robust fusion frame. And on the contrary it is weakness for the cases for example in the Logarithmic Opinion Pool (LOP) a single zero of membership function or posterior probability (and also very small numbers) can potentially veto decisions from the remaining classifiers [Benediktsson *et al.* 2003]. Benediktsson and Kanellopoulos [1999] used AVIRIS (Airborne Visible Infrared Imaging Spectrometer) dataset in the Volcano Hekla in Iceland with 15 land cover classes; they tried to classify data based on combination of

neural network and statistical classifiers. There are several other works in this field of study which have used fuzzy set as a framework for DLDF. For example Jeon and Landgrebe [1999] used two decision fusion rules to classify multi-temporal TM data. Tupin *et al.* [1999] fused several structure detectors to classify SAR images and Lisini *et al.* [2005] used the combination of several sources according to their class accuracies.

A high number of decision level data fusion (also called post-decision, post-detection or post-classification fusion [Hall and Llinas, 2001]) methods have been proposed in the data fusion literature. These methods are based on the fusion of classifier results by a proper fusion algorithm.

The classifiers can be categorized from different points of view. One of the very elementary categorizations of classifiers is return to the statistical hypotheses of classifier in which parametric such as Maximum Likelihood Classifiers (MLC) [Richards, 2007] and non-parametric classifiers such as Neural Network Classifier (NNC) [Benedickson, 1990] and Support Vector Machine (SVM) [Varshney and Arora (Ed.), 2004] are remarkable. In all classifiers the final results will be obtained based on a decision to allocate a pixel to a class, therefore the obtained results are called decisions. From the literature there are two general methodologies to decision producing: (i) hard decisions in which the belonging of a pixel to a class is unique e.g. the Boolean logic with 0 and 1 values, where 1 is for pixel belongs to a class and 0 when it does not and (ii) soft decisions which the belonging of a pixel to a class is a value between 0 and 1 e.g. fuzzy logic. With regard to these two different kinds of decisions, decision level fusion can be carried out at class label level (hard fusion), or at the posterior probability or membership levels (soft fusion). Irrespective of the fusion methodology, from the applicability viewpoint DLDF can be applied in next cases.

1. In cases which a classifier has differentiated some classes while others have not.
2. When border of classes is not sharply clear.

3. When priori knowledge about dataset reliability is incomplete.
4. In the cases that intention is in introducing some priori knowledge to the fusion process.
5. When classifier(s) offers precise information concerning some classes and on the contrary other classifier(s) does for other classes.

In such circumstances using a diversity of approaches a fusion framework will take advantages and strengths of each individual classifier therefore a new concept in data processing entitled post-classification decision fusion are introduced.

3.1 Data fusion for classification

As a practical matter, it is striking to note that DF techniques for mapping purposes can be heading into two main groups: Fusion-Then-Classification (FTC) [Schackelford, 2003] and Classification-Then-Fusion (CTF) [Foody, 1998]. FTC is based on PLDF and CTF is obtainable by DLDF. These procedures have their characteristics and limitations that studied and evaluated by several authors, for example Robinson *et al.* [2000] evaluated two approaches by a linear mixing model and they came to this conclusion that classification-then-fusion is preferable in term of accuracy. In this regard and in order to get true land cover maps using different classifiers, they must be flexibly comparable and combinable. As mentioned by Foody *et al.* [2002] the comparability of measurements requires some common understanding of their accuracy, some way of measuring and expressing the uncertainty in their values and the inferential statements derived from them [Stigler, 1986]. Concerning the inputs of fusion process i.e. decisions and their accuracy or performance two main aspects must be measured: (i) global precision (the accuracy of the classifier) and (ii) local precision e.g. the accuracies of class in the form of spectral and spatial characteristics of dataset [Benediktsson *et al.* 2006]. Because of the variety of data sources, applications, and different properties of classifiers, the

most robust fusion methodology is the procedures which can model and measure these two aspects as precise as possible.

Due to the fact that in a high number of DLDF techniques the main emphasis is in after classification fusion process therefore one of main aspects that are less concerned is return to how chose data and classifier. As in this work these aspects are more concerned and the used dataset is a hyperspectral image thus we have developed our procedures in the frame of hperspectral DLDF.

3.1.1 DLDF for image classification

In the literature numerous researches and studies over hyperspectral data classification has been undertaken that predominantly are in visible to infrared (400-2500 nm) parts of electromagnetic spectrum. As an example Jensen [2007] mentioned that majority properties of land surface materials can be investigated by the help of high dimension remotely sensed imagery which use mostly the spectrum in visible and NIR regions of EM. For instance the vegetation properties like variation in vegetation species, community distribution patterns, alteration in vegetation phenological (growth) cycles, modifications in plant physiology and morphology are easily obtainable. Also for other materials of the land surface and the related aspects of hyperspectral exploitation Harsanyi [1994]; Varshney and Arora [2004]; Chang [2006]; and Liang [2004] have offered good discussions.

The collected data by remote sensors are functions of the interaction of electromagnetic radiation with earth surface materials, which is evidently fundamental to remote sensing [Ress, 2001]. Based on very elementary principals of physics the reflected energy from any object is equal to the incident radiance flux minus the absorbed and transmitted fluxes.

$$\Phi_{\rho\lambda} = \Phi_{i\lambda} - (\Phi_{\alpha\lambda} + \Phi_{\tau\lambda}) \quad (3-1)$$

Where $\Phi_{\rho\lambda}$ is the flux reflected from the object and quantized by the sensor to make a pixel in an image; $\Phi_{i\lambda}$ is the flux radiant incident come from the sun or diffused from the neighboring objects; $\Phi_{\alpha\lambda}$ the absorbed energy by the object; and $\Phi_{\tau\lambda}$ is the transmitted flux through the object to the underneath parts and layers. Therefore based on these properties of reflected parts of the EM spectrum, different types and identities of objects can be detected. For instance the spectral response characteristics of a green vegetation (Figure 3-1) is depicted which is mainly due to three important parameters: leaf pigments in Visible (Vis) from 0.4 to 0.7 μm ; cell structure in Near Infrared (NIR) from 0.7 to 1.3 μm ; and vegetation water contents in Short-Wave Infrared (SWIR) from 1.3 to 2.6 μm .

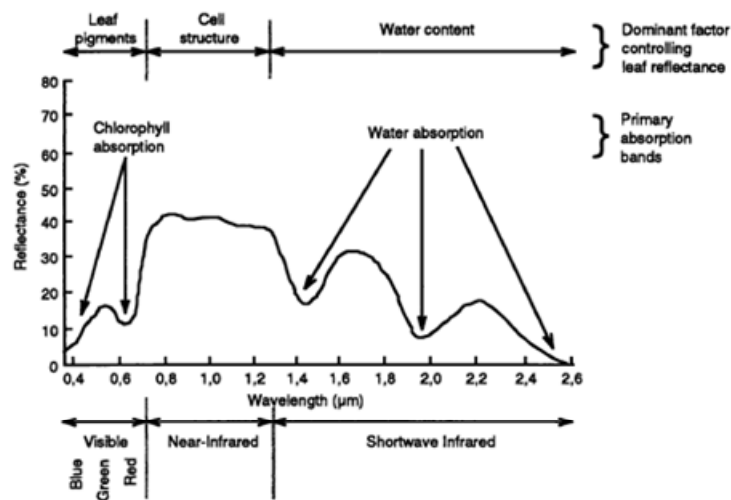


Figure 3-1. Spectral response characteristics of green vegetation, as resultant of absorption, reflection and transmittance of light. After Hoffer [1978].

Based on these parameters, it is clear that the chlorophyll absorptions are located about 0.43-0.45 and 0.65-0.66 μm in the visible region and water absorptions occur at 0.97, 1.19, 1.45, 1.94 and 2.7 μm in the SWIR.

Therefore, the hyperspectral imagery can be investigated as a simultaneous multi-source dataset for the purposes of image classification and fusion. Accordingly we have developed two DLDF strategies for hyperspectral image classification.

1. Wavelength Based Decision Fusion (WBDF). and
2. Class Based Decision Fusion (CBDF).

Both procedures work based on breaking down source hyperspectral dataset into smaller subsets which followed by classification processes for any subset individually. Finally a decision level fusion over the obtained decisions from classifiers will be carried out, while the difference of techniques returns to different mechanisms that can be used to selecting subsets. In the first methodology which is depicted in figure (3-2) input dataset is divided into some distinct parts of electromagnetic. The basis for separation is the material's spectral response to the incident solar flux. As for all objects in a scene there is a spectral curve therefore based on the purpose of classification and the land surface classes, different subsets are extractable.

As in this work the main land covers are agricultural fields therefore based on the behavior of vegetations the Hyperion dataset is divided into independent subsets including (i) visible (400-700 nm); (ii) Near Infra Red (NIR) (700-1000 nm); and (iii) Middle Infra Red (MIR) (1000 – 2500 nm). After individual classification of subsets, using the explored DLDF algorithms obtained decisions fused to making the final land cover map.

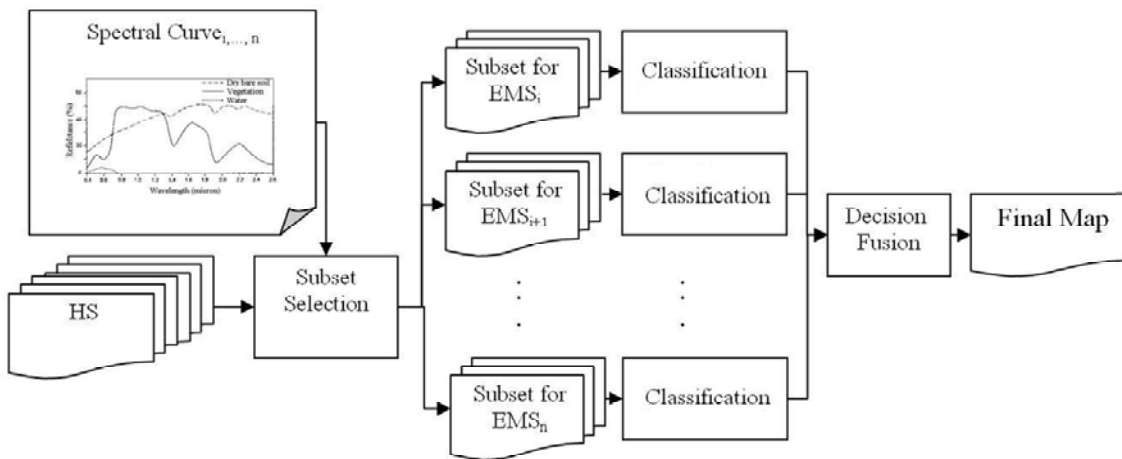


Figure 3-2. Block diagram of Wavelength Based Decision Fusion (WBDF)
 Where EM is the Electromagnetic spectrum.

In the second routine (Figure 3-3) subsets are selected based on the rule of maximum spectral and spatial information contents of dataset. Irrespective of the band location in the EM and based on the assumption that each class can precisely be classified using a specific subset therefore in this procedure the goal is finding the most comprehensive subset for each class. In the following and after classification procedure the obtained decisions will be fused in a DLDF framework. In order to obtain these class-based subsets the MSSI feature selection procedure is adapted.

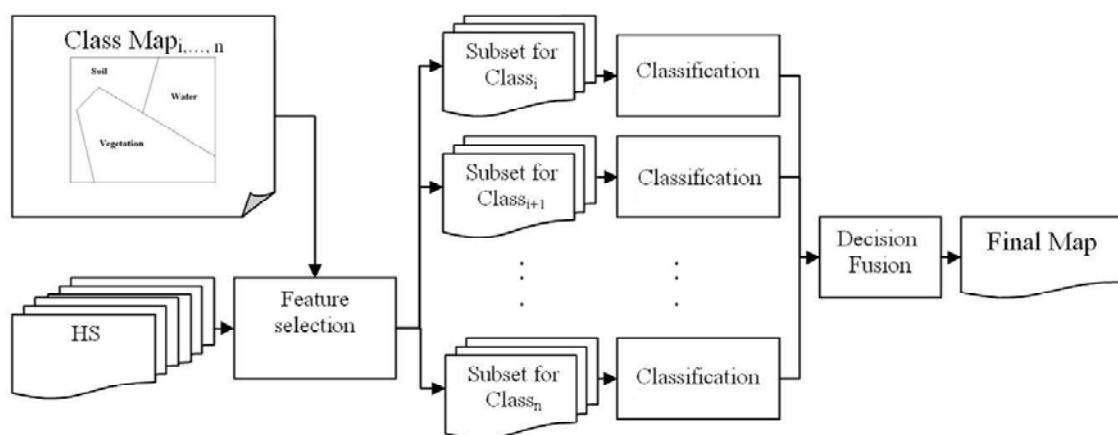


Figure 3-3. Block diagram of Class Based Decision Fusion (CBDF).

The two abovementioned procedures work based on one classifier and different subsets (Figure 3-2 and 3-3). In order to make a comparison and evaluation, a

common decision fusion methodology as Multi Classifier Decision Fusion (MCDF) is carried out. This procedure works based on combination of several classifiers over the original dataset or one selected subset (Figure 3-4).

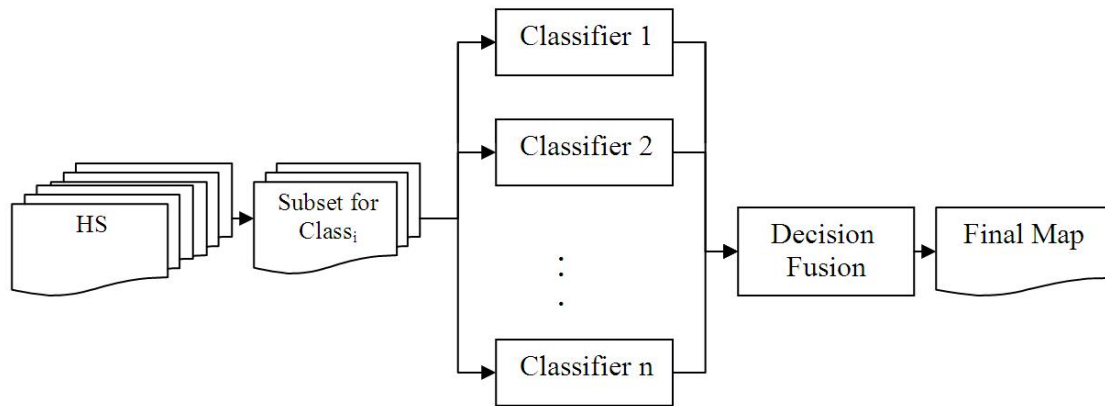


Figure 3-4. Block diagram of Multi Classifier Decision Fusion (MCDF).

All three introduced mechanisms for DLDF have their strengths and weaknesses. For example WBDF works based on the behavior of material in the electromagnetic spectrum which will offer good results for the areas with more similar land cover classes. And also for CBDF it can be mentioned that this procedure is powerful for the cases which classes can be separated with few bands. The weakness of these two procedures is their limitations to explore just one classifier, which is not the case in MCDF procedure.

3.2 DLDF techniques

In order to put any procedure of DLDF into practice a mathematical statistical frame is needed. From the literature several techniques are discussed and evaluated. If the techniques based on their abundance of application be listed probably Bayesian Theorem (BT) is the first which followed by Dempster-Shafer Theory (DST); Fuzzy Set Theory (FST) and Neural Network (NN). In this work DST has been adapted to evaluate the WBDF, CBDF and MCDF procedures.

3.2.1 Dempster-Shafer Theory (DST)

The Dempster-Shafer theory owes its name to work by Dempster [1968] and Shafer [1976]. In the early 1980s, when experts wanted to adapt probability theory to expert systems, the theory came to the attention of researchers [Shafer, 2002]. The DST, as a generalization of Bayesian theory, is a mathematical theory of evidence which works on the basis of belief function and plausible reasoning which are used to combine separate pieces of information (evidences) to calculate the probability of an event.

Unlike Bayesian probability theory, in DST the lack of evidence for a hypothesis will not be the evidence against that hypothesis. DST measures the uncertain situations by Belief (Bel.) and Plausibility (Pls.) definitions. Therefore, uncertainty (θ) represents both imprecision and uncertainty. Based on DST, the degree to which evidence provides concrete support for a hypothesis is known as belief and the degree to which the evidence does not refute that hypothesis is known as plausibility. The difference between these two is then known as a “belief interval”, which acts as a measure of uncertainty about a specific hypothesis. In addition to the concepts of belief and plausibility, the logic of Dempster-Shafer theory expresses the degree to which the state of one’s knowledge does not distinguish between the hypotheses. This is known as “ignorance”. Ignorance expresses the incompleteness of one’s knowledge as a measure of the degree to which we cannot distinguish between any of the hypotheses (i.e., land cover classes) [IDRISI Manual version 15, 2006]. In addition to the high strength of DST in soft classification procedure, it also has shown good ability to combine several kinds of data sources in DLDF. For instance Le Hégarat *et al.* [2000] mentioned good results for fused ERS multi-temporal and Landsat-MS images for two consecutive agricultural years (1995–96 and 1996–97). One of the main advantages of DST is return to the ability of evidence theory which represents both uncertainty and imprecision with two functions: plausibility and credibility (or belief) [Shafer, 2002]. The mentioned property results to a flexible modeling ability to fit a high number of almost incomplete and inconsistency datasets. Based on the rational

behind the decision level data fusion which trays to combine final results of several classifications, DST is a proper technique to carry out this procedure. The applicability of this technique in data fusion has been explained in more details in Pearl [1990].

3.3 Image classifiers

As in DLDF any dataset must be classified priory to the fusion process and also the most power of DLDF is based on the flexibility of classified results, therefore in this work three of the most powerful soft classifiers are introduced. On contrary to hard classifiers, the results for any pixel are a degree of membership with regards to all possible classes. Another different is that in hard classifiers the final result is a single classified map, but in soft classifications the results are a set of images (one per class) which express for each pixel the degree of membership based on all under investigation classes. In this work three of the most famous soft classifiers for DLDF procedure evaluations are carried out and Spectral Angle Mapper (SAM) as a non-fusion hard classifier was explored for evaluation the results.

3.3.1 Fuzzy classification

Fuzzy sets theory whose elements defined based on the degrees of membership is the extension of the works of Zadeh [1965]. In the classical set theory, the membership of elements in a set is in the form of binary values that an element either belongs will get the value of [1] or does not belong that gets the value of [0]. On the contrary, fuzzy set theory makes a gradual assessment of the memberships of elements in a set therefore a set of memberships will be introduced that have a value in between [0-1] [Zadeh, 1965]. Similar to classical sets, the fuzzy sets also take advantages of logical and mathematical operators. For example the fuzzy intersection, fuzzy union and fuzzy complement operators, etc. It is remarkable to note that because of fuzzy flexibility and its operators it can make an appropriate framework to fuse the output of several classifiers for supplementary processing.

In order to make a general outline of fuzzy classification a very short mathematical description is adapted from Fauvel *et al.* [2006].

Definitions:

Fuzzy subset: A fuzzy subset F of a reference set U is a set of ordered pairs $F = \{(x, \mu_F(x)) | x \in U\}$; where $\mu_F : U \rightarrow [0, 1]$ is the membership function of F in U .

Normality: A normal fuzzy set is a set, which if and only if $\max \mu_F(x) = 1$.

Support: The support of a fuzzy set F is $\text{Supp}(F) = \{x \in U | \mu_F(x) > 0\}$.

Core: The core of a fuzzy set is the (crisp) set containing the points with the largest membership value ($\mu_F(x) = 1$). It is empty if the set is nonnormal.

Logical operations:

Union: The union of two fuzzy sets is defined by the maximum of their membership functions, i.e., $\forall x \in U, (\mu_F \cup \mu_G)(x) = \max \{\mu_F(x), \mu_G(x)\}$.

Intersection: The intersection of two fuzzy sets is defined by the minimum of their membership functions, i.e., $\forall x \in U, (\mu_F \cap \mu_G)(x) = \min \{\mu_F(x), \mu_G(x)\}$.

Complement: The complement of a fuzzy set F is defined by $\forall x \in U, \mu_{F^c}(x) = 1 - \mu_F(x)$.

Measures of fuzziness:

Fuzziness is an intrinsic property of fuzzy sets. To measure how fuzzy a fuzzy set is, and thus estimate the ambiguity of the fuzzy set, Ebanks [1983] proposed to define the degree of fuzziness as a function f with the following properties. $\forall F \in \mathcal{F}(U)$, if $f(\mu_F) = 0$, then F is a crisp set.

$f(\mu_F)$ is maximum if and only if $\forall x \in U, \mu_F(x) = 0.5$.

$\forall (\mu_F, \mu_G) \in U^2, f(\mu_F) \geq f(\mu_G)$ if

$$\forall x \in U \begin{cases} \mu_G(x) \geq \mu_F(x), & \text{if } \mu_F(x) \geq 0.5 \\ \mu_G(x) \leq \mu_F(x), & \text{if } \mu_F(x) \leq 0.5 \end{cases} ! \cong F \approx U, f(\mu_F) = f(\mu_{\bar{F}}). \quad \text{A set and its}$$

complement have the same degree of fuzziness. $\cong (\mu_F, \mu_G) \approx U^2, f(\mu_F \succ \mu_G) + f(\mu_F \cap \mu_G) = f(\mu_F) + f(\mu_G)$.

For the classification purpose after training data selection, the fuzzy membership is calculated based on the mechanism of supervised classifier. The fuzzy set membership is based on the standard distance of each pixel to the mean reflectance on each band for a signature. Therefore based the number of classes for any pixel there are membership values. These membership values will be treated with the same procedures like MLC hard classifiers for obtaining the final classification map.

3.3.2 Bayesian Theorem (BT) classification

Bayes theorem (also known as Bayes' rule) introduced by Thomas Bayes [1763] is a result in probability theory, which relates the conditional and marginal probability distributions of random variables [Sivia, 1996]. In probability theory with a few strict hypotheses the Bayesian probabilistic theory can be used as a modeling and reasoning tool to dealing with uncertainty of the real world phenomena. This theorem is a tool for transforming prior probability into posterior probability. Equation (3-2) gives the Bayes theorem that relates the conditional probabilities of random events M and D.

$$P(M|D) = \frac{P(D|M)P(M)}{P(D)} \quad (3-2)$$

Where $P(M|D)$ is the conditional probability of M, given D. It is also called the posterior probability because is derived from or depends upon the specified value of D; $P(D|M)$ is the conditional probability of D, given M; $P(D)$ is the prior or marginal probability of D and acts as a normalizing constant and $P(M)$ is the prior probability

of M , it is prior in the sense that it does not take into account any information about D .

In remotely sensed imagery analysis, Bayes' theorem is used to allocate a pixel in an image to a spectral class; therefore if x is a pixel vector, $P(x)$ is the probability that the pixel can be found at position x in multispectral space [Richards and Jia, 1999]. Characteristics and advantages of this procedure have been described by several authors [Sivia, 1996; Box et al, 1992; and Bernardo *et al.* 1994].

The same as fuzzy classifier, Bayes works similar to maximum likelihood hard classifier. Based on Bayes' theorem the posterior probability for every pixel will be calculated with the number of classes. Using the training data, the variance/covariance matrix is derived which is a basis for the multivariate conditional probability $p(e|h)$ assessment. This quantity is then modified by the prior probability of the hypothesis being true and then normalized by the sum of such considerations over all classes. This latter step is important because it makes the assumption that the classes considered are the only classes that are possible as interpretations for the pixel under investigation. Thus even weak support for a specific interpretation may appear to be strong if it is the strongest of the possible choices given [DRISI Manual version 15, 2006].

3.3.3 Spectral Angle Mapper (SAM) classifier

The spectral angle mapper algorithm works based on the assumption that data have been correctly calibrated to apparent reflectance with dark current and path radiance removal. SAM determines the similarity between two spectra by calculating the spectral angle between them, treating them as vectors in a space with dimensionality equal to the band numbers [Kruse *et al.* 1993]. The amount of spectral similarity is expressed in term of average angle (Ω) between Image Spectrum (IS) and Library Spectrum (LS) (Equation 3-3 and 3-4).

$$\Omega = \cos^{-1} \left(\frac{\vec{IS} \cdot \vec{LS}}{\|\vec{IS}\| \|\vec{LS}\|} \right) \quad (3-3)$$

This can also be written as

$$\Omega = \cos^{-1} \left[\frac{\sum_{i=1}^{nb} I_{s_i} L_{s_i}}{\left(\sum_{i=1}^{nb} I_{s_i}^2 \right)^{1/2} \left(\sum_{i=1}^{nb} L_{s_i}^2 \right)^{1/2}} \right] \quad (3-4)$$

SAM uses only the direction of the spectra, not their length, this method is insensitive to the unknown gain factor and all possible illuminations are treated equally. Poorly illuminated pixels will fall closer to the origin. The length of the vector relates only to how fully the pixel is illuminated. For each library spectrum chosen in the analysis of a hyperspectral image, the spectral angle is determined for every image spectrum (pixel). After making spectral angle maps gray-level threshold is typically used to empirically determine those areas that most closely match the library spectrum while retaining spatial coherence. Thus based on the measured distances any pixel will be allocated to a specific prior-defined class.

3.4 DLDF accuracy assessment

On the contrary to the PLDF which the accuracy is mostly evaluated based on the comparison of fused image with reference, the accuracy in DLDF is considered in the form of final obtained map accuracy. Thus the used evaluation parameters are the classification accuracy indicators e.g. overall accuracy, user accuracy, producer accuracy and kappa coefficient [Russell and Congalton, 1999]. Confusion or error matrix and its derivatives e.g. commission and omission are the frame to calculate these accuracy indicators.

Overall Accuracy (OA) or the percent of correct allocation is calculated by summing the number of pixels classified correctly and dividing by the total number of pixels (Equation 3-5). The pixels classified correctly are found along the diagonal of the confusion matrix which lists the number of pixels that are classified into the correct ground truth class. The total number of pixels is sum of all pixels in all ground truth classes.

$$OA = \frac{\text{Total number of correctly classified samples}}{\text{Total number of sample}} \quad (3-5)$$

User's Accuracy (UA) is the probability (Equation 3-6) that the ground truth class is x given a pixel is put into class x in the classification image.

$$UA = \frac{\text{Number of correctly classified samples of a class}}{\text{Number of samples classified as that class}} \quad (3-6)$$

Producer's Accuracy (PA) is the probability (Equation 3-7) that a pixel in the classification image is put into class x given the ground truth class is x.

$$PA = \frac{\text{Number of correctly classified samples of a class}}{\text{Number of samples of a class}} \quad (3-7)$$

Respective of the fact that the OA, UA and PA are offering an overestimation of classification accuracy. Because the agreement between classified and reference datasets which is due to chance, has not been taken into account. In this regard some other indicators must be carried out. For example Kappa coefficient of agreement can bring the chance agreement into account. The proportion of chance agreement that is due to the misclassification represented by off-diagonal elements of the error matrix. [Russell and Congalton, 1999]. Kappa Coefficient (KC) or κ (Equation 3-8) is a

discrete multivariate technique of use in accuracy assessment that shows the agreement of classified with reference data [Jensen, 2005].

$$\kappa = \frac{N \sum_{i=1}^k x_{ii} - \sum_{i=1}^k (x_{i+} \times x_{+i})}{N^2 - \sum_{i=1}^k (x_{i+} \times x_{+i})} \quad (3-8)$$

Where k is the number of rows (e.g. land cover classes) in the matrix; x_{ii} is the number of observations in row i and column i ; x_{i+} and x_{+i} are the marginal total for row i and column i , respectively; and N is the total number of observations.

CHAPTER FOUR

4 Data sources and test areas

This PhD work is performed based on the evaluation of different DF techniques for all possible kinds of optical remotely sensed images. Therefore the Earth Observing-One (EO-1) was selected as a proper satellite imager that collects all needed data for the purposes of this work. As the investigated and developed techniques are data-independent and also the assessment and validation of fused EO-1/Hyperion and ALI for land cover mapping is one of purposes of this work therefore, we have selected two EO-1 datasets from two different parts of the world: Iran and Indonesia. The first dataset is covering an area in Ahmadabad village, south Tehran, Iran (21st May, 2005) where the land cover classes are mainly agricultural fields. The second test area is located at the Palolo Valley, Sulawesi, Indonesia (20th September, 2005) in a humid tropical environment.

NASA New Millennium Program's Earth Observing-1 Mission (NMP/EO-1) started on 21st November 2000. The central point of EO-1 mission is to assess the space-validate advanced technologies [Ungar *et al.* 2003]. The mounted sensors are Advanced Land Imager (ALI) with a multispectral sensor with 9 spectral bands at 30 meter spatial resolution fashion and a panchromatic band with 10 meter spatial resolution and Hyperion hyperspectral sensor, with 242 spectral bands in the Visible (Vis); Near Infrared (NIR); and Short-Wave Infrared (SWIR) wavelengths with 30 meter spatial resolution.

As a general rule in remote sensing making any use of satellite images is related to some preprocessing steps: noise reduction, radiance to reflectance conversion, geometric correction and image orthorectification.

4.1 Satellite imagery

EO-1 is a very sophisticated multi-sensor land imager which is equipped by Hyperion hyperspectral imager; Advanced Land Imager multispectral and panchromatic (ALI/MS and Pan); and the Linear Etalon Imaging Spectral Array (LEISA) Atmospheric Corrector (LAC) [Ungar *et al.* 2003]. EO-1 has opened a new perspective for remote sensing and subsequently for data fusion research and applications. Therefore, the temporal integration between datasets which was an inevitable restriction in multi-source data fusion is going to be eliminated or moderated in the future. The EO-1 is in altitude 705 km has a sun-synchronous orbit and a 10:01 AM descending mode. The orbit inclination is 98.2 degree; the orbital period is 98.9 minutes and its equatorial crossing time is one minute behind Landsat-7. The velocity of the EO-1 nadir point is 6.74 km/sec. [EO-1/ Hyperion science data user's guide, 2001] (Figure 4-1). Table (4-1) lists the spectral and spatial resolutions of the EO-1 satellite imager.

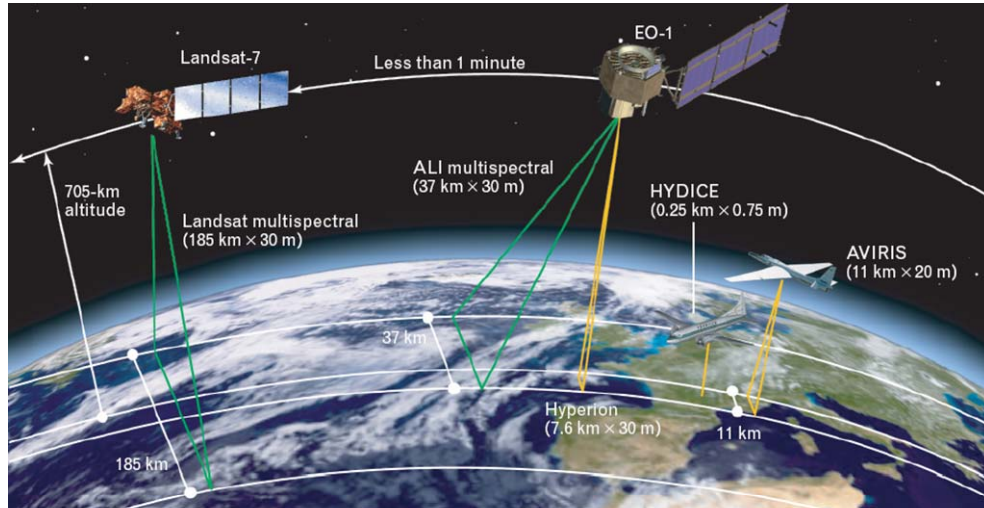


Figure 4-1. EO-1 land sensing mode. After Shaw and Burke [2003].

Table 4-1. EO-1 sensor characteristics. After Richards [2006]

Instrument	Spectral Bands (μm)	IFOV (m)	Swath (km)	Dynamic Range (bits)
------------	-------------------------------------	-------------	---------------	-------------------------

Hyperion	0.4–2.4	30 × 30 (220 bands @ 10 nm bandwidth)	7.7	12
ALI/Multispectral	0.433–0.453	30 × 30	37	12
	0.450–0.515	30 × 30	37	12
	0.525–0.606	30 × 30	37	12
	0.639–0.690	30 × 30	37	12
	0.775–0.805	30 × 30	37	12
	0.845–0.890	30 × 30	37	12
	1.200–1.300	30 × 30	37	12
	1.550–1.750	30 × 30	37	12
	2.080–2.350	30 × 30	37	12
ALI/panchromatic	0.480–0.690	10 × 10	37	12

4.1.1 Hyperion

The Hyperion sensor was designed as a technology demonstration which provides high-quality calibrated data for hyperspectral application evaluation [Pearlman *et al.* 2003 and Ungar *et al.* 2003]. As the first hyperspectral space-born imager acquires images in visible (400-700 nm), near infra red (700-1000 nm) and shortwave infrared (1000-2500 nm) spectra [Datt *et al.* 2003]. Hyperion, which acquires data by VNIR sensor in 70 bands and SWIR in 172 bands that provides images in 242 bands with 10 nanometer bandwidth from 0.4 to 2.6 micrometers. 44 bands of 242 bands are intentionally not illuminated by TRW. The 198 rest bands are illuminated and deliver to customers. The 44 non-illuminated bands includes: 1-7, 58-76 and 225-242 that have been set to null in the pre-delivery pre-processing step by TRW [EO-1/Hyperion science data user's guide, level 1_B, 2001].

4.1.1.1 Pre-processing

An almost cloud free and clear EO-1/Hyperion scene was acquired over the Palolo Valley, study site, Indonesia on the 20th September 2005. The delivered data are

already radiometrically calibrated into Level-1A product at Thompson Ramo Woolridge (TRW). Despite the performed radiometric correction there are still rooms to do some more preprocessing. In this part of work two main preprocessing includes noise reduction and radiance to reflectance conversion were carried out.

In the delivered data there are 20 almost overlap bands between VNIR (from 50-70) and SWIR (71-91) sensors; the spectral overlap between them is about 80% (Table 4-2). As 58-76 bands of VNIR has been set to null only band numbers from 50 to 57 are overlapped with 71 to 79 from SWIR. To eliminate these 8 remained overlapped bands we used Signal to Noise ratio (SNR) [Van der Meer, 2001] and visual inspection as well.

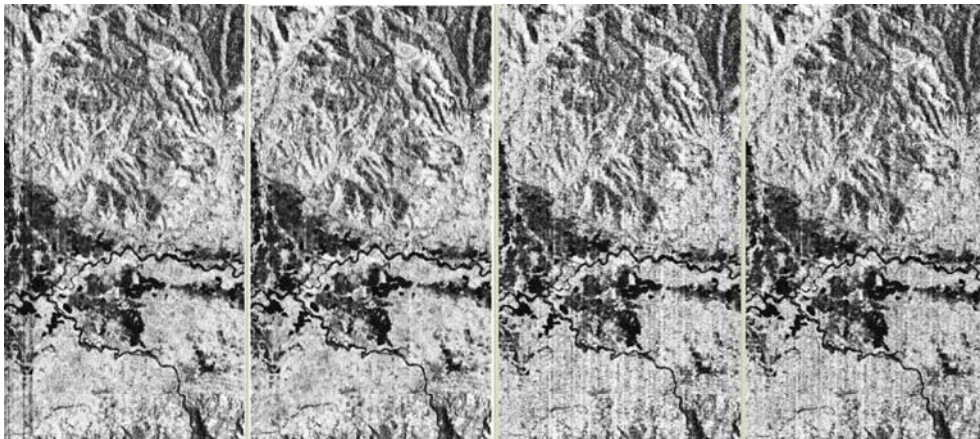
Table 4-2. Spectral overlap bands between VNIR (50-57) and SWIR (71-78).

Overlap Hyperion Band	Average Wavelength (nm)	Overlap Hyperion Band	Average Wavelength (nm)
B71	851.9200	B75	892.2800
B50	854.1800	B54	894.8800
B72	862.0100	B76	902.3600
B51	864.3500	B55	905.0500
B73	872.1000	B77	912.4500
B52	874.5300	B56	915.2300
B74	882.1900	B78	922.5400
B53	884.7000	B57	925.4100

In the statistical properties comparison of Signal-to-Noise Ratio (SNR) for 4 overlapped bands no meaningful differences were observed (Table 4-3). Therefore, in visual inspection bands 56 and 77 were eliminated (Figure 4-2).

Table 4-3. Statistic: Signal-to-noise ratios for four overlap bands.

Overlap Band	Min	Max	Mean	St. dev.
Band 56	23	255	124.3379	54.56559
Band 57	13	255	124.596	55.97276
Band 77	0	255	124.6024	55.73756
Band 78	0	255	124.5716	55.60398



(a) (b) (c) (d)

Figure 4-2. Visual inspection of bands where (a) band 56 and (c) band 77 were eliminated; (b) band 57 and (d) band 78 were selected.

4.1.1.1.1 De-striping

Striping in Hyperion dataset is apparent, especially in the first 12 visible and near Infrared bands and many SWIR bands. For pushbroom [Jensen, 2007] characteristic of Hyperion which has a separate detector for each column of each band any improper calibrated detector in both VNIR and SWIR sensors can cause an undeniable striping artifacts.

Based on the sources of striping phenomenon the bands with striped columns are separated and ratified in which abnormal or striping pixels are classified into four categories (1) continuous with atypical DN values; (2) continuous with constant DN values; (3) intermittent with atypical DN values; and (4) intermittent with lower DN values [Goodenough *et al.* 2003]. Based on this ratification 30 band with strip

problem have been chosen. A band de-stripping algorithm using a local averaging algorithm was carried out (Equation 4-1). After the de-stripping process over these bands they were visually inspected and 13 bands of them were chosen and the rest were leaved out (Table 4-4).

Local averaging de-stripping algorithms alleviate striping phenomenon without causing any unwanted effects on the image [Datt, 2003]. Therefore local averaging algorithm was carried out using right and left columns. For example figure (4-3) shows band 94 before and after de-stripping by equation (4-1).

$$DN_{new} = \frac{\sum_{i=i-1}^{i=i+1} DN_i}{3} \quad (4-1)$$

Where DN_i is defined as abnormal pixel and DN_{new} is calculated using DNs of left and right neighbors.

Table 4-4. Bands with defected columns.

Band	Column
10,11	6, 114, 199
12, 13, 14, 15, 16, 17, 18	114
27, 28	47
94	92
116	156

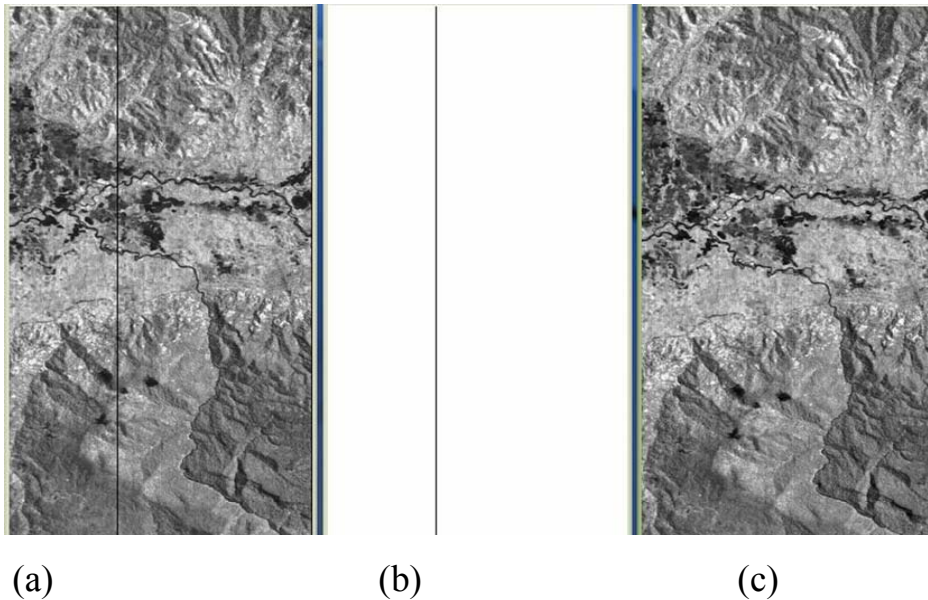


Figure 4-3. (a) Stripped band 94 continuous with constant zero DN value; (b) Stripped column 92; and (c) De-stripped band.

4.1.1.1.2 Radiometric transformation

As the purchased dataset are in Level 1Gst (L1Gst) that radiometrically corrected and resampled for geometric correction and registered to a geographic map projection. The images are ortho-corrected using digital elevation models (DEM) by the Shuttle Radar Topography Mission-Two (SRTM-2) [Rodriguez *et al.* 2005] to correct parallax error due to local topographic relieves.

The amount of reflected solar energy by the earth surface materials provides information about the objects in the earth surface through the spectral material property measurements by satellite imagers. The measured radiance also contains three main unwanted mixtures caused by atmospheric aerosols such as absorption and scattering [Pat and Chavez, 1996]; topographic effects; and the solar wavelength based illumination effects [Jensen, 2005].

In order to get the real object reflectance that is free from the atmospheric effects [Chander and Markham, 2003] and solar illumination causes, the calculated spectral radiances L_{λ} was transferred by equation (4-2) to effective at-satellite exoatmospheric reflectance [Markham *et al.* 1987] or at-sensor reflectivity [Griffin, 2005].

$$\rho_p = \frac{\Pi * L_\lambda * d^2}{ESUN_\lambda * \text{Cos } \theta_s} \quad (4-2)$$

Where ρ_p is unitless planetary reflectance or at-sensor reflectance; L_λ is spectral radiance at the sensor's aperture; d is earth-sun distance ($d_{\text{Earth-Sun}}$) in astronomical units [Landsat-7 handbook, 2007]; $ESUN_\lambda$ is mean solar exoatmospheric irradiances [Griffin, 2007]; and θ_s is the solar zenith angle in degrees.

The solar zenith angle for EO-1 that have been used for both sensors, ALI and Hyperion, were calculated from the site geographical location measurement date by the help of NASA solar position calculator. In equation (4-2) the earth-sun distance measure (d) is for the mean solar flux correction caused by orbital radius changes. The used incident solar flux, as a function of wavelength, was calculated in Massachusetts Institute of Technology (MIT)-Lincoln laboratory [Griffin *et al.* 2005] using the MODTRAN Radiative Transfer Model (RTM) [Berk *et al.* 1988].

For the purpose of making the same set of reflectance images for each band, at-satellite reflectance was calculated. As the Hyperion radiances are delivered in $\text{W/m}^2\text{-sr-}\mu\text{m}$ units, therefore to make a popular unit of radiance, the at-satellite reflectance (ρ_p) were converted to μflick ($\mu\text{W/cm}^2\text{-sr-}\mu\text{m}$) through multiplying by 100.

More than the mentioned pre-processing steps, visual inspection was also adapted for bands with high amount of atmospheric water vapor absorptions and also bands with very high levels of noise.

4.1.2 Advanced Land Imager (ALI)

ALI, as the primary land imager instrument for NASA's NMP was designed and developed by Lincoln laboratory [Mendenhall *et al.* 2002]. ALI's operation is in pushbroom fashion that provides Landsat type panchromatic and multispectral bands [Forman, 2005]. ALI bands have been designed as the continuation of Landsat multispectral. It also furnished with three additional bands covering 0.433-0.453,

0.845-0.890 and 1.20-1.30 μm (Table 4-5). The wide-angle optics provides a continuous $15^\circ * 1.625^\circ$ field of view for focal plane [Lencioni *et al.* 2005].

Table 4-5. Spectral and spatial resolutions of ALI. After USGS, EO-1 user's guide [2007].

Band	Wavelength (μm)	Ground Sample Distance (m)	Spectral Irradiance ($\text{W}/\text{m}^2 * \mu\text{m}$)
Pan	0.48 - 0.69	10	1747.8600
MS - 1'	0.433 - 0.453	30	1851.8000
MS - 1*	0.45 - 0.515	30	1967.6000
MS - 2	0.525 - 0.605	30	1837.2000
MS - 3	0.63 - 0.69	30	1551.4700
MS - 4	0.775 - 0.805	30	1164.5300
MS - 4'	0.845 - 0.89	30	957.4600
MS - 5'	1.2 - 1.3	30	451.3700
MS - 5	1.55 - 1.75	30	230.0300
MS - 7	2.08 - 2.35	30	79.6100

* Highlighted bands are those used in PLDF.

The same as for Hyperion, ALI dataset at-sensor reflectance were achieved through normalization for solar irradiance by converting spectral radiance to planetary reflectance using equation (4-2).

4.1.3 Explored EO-1/ALI and Hyperion datasets

As in different parts of this work we have explored different datasets for different purposes therefore after general pre-processing routines the used and explored hyperspectral datasets are listed in table (4-6).

- EO-1/Hyperion, Palolo, Indonesia, 2004.
- EO-1/Hyperion and ALI, Palolo, Indonesia, 2005.
- EO-1/Hyperion, Ahmadabad south Tehran, Iran, 2002.

Table 4-6. Selected bands from three Hyperion datasets after pre-processing.

Palolo, Sulawesi, Indonesia, 2004.		Palolo, Sulawesi, Indonesia, 2005.		Ahmadabad south Tehran, Iran, 2002.	
Band	Wavelength (nm)	Band	Wavelength	Band	Wavelength
11-93	455-1073	14 – 26	487 – 610	8 – 57	427 – 926
95-96	1093-1103	28 – 55	630 – 905	83 –119	973 – 1336
101-119	1153-1335	83 – 96	972 – 1104	130 – 164	1447 – 1790
135-163	1497-1780	102 – 118	1164 – 1326	181 – 184	1962 – 1992
191-213	2062-2284	136 – 162	1507 – 1770	187 – 220	2022 – 2355

4.2 Test areas

4.2.1 Palolo valley, Indonesia

The study area was chosen as one of the main important agricultural areas in Sulawesi, Indonesia. Palolo valley is located within the Sunda islands where still 60.6% of the area are forested land (4.1 million ha), whereby 32% of this area are under a special level of protection and 4% are officially opened to conversion. The Lore-Lindu National Park, covering an area of 229.000 hectares is placed in the centre of the study region of the STORMA project. The Palolo valley which comprises the study area for this investigation is situated at the northeastern border of the Lore Lindu National park, Central Sulawesi, Indonesia (1° 8' 31.68" S, 120° 3' 53.78" E and 1° 11' 16.75" S, 120° 6' 21.63" E). Land cover classes for the research area comprise closed tropical rain forest, open tropical rain forest, cacao and coffee plantations, paddy rice, maize, river vegetation, mosaic of crops, trees and natural vegetation, bare soil, river, and urban areas [Rohwer, 2006] (Figure 4-4).

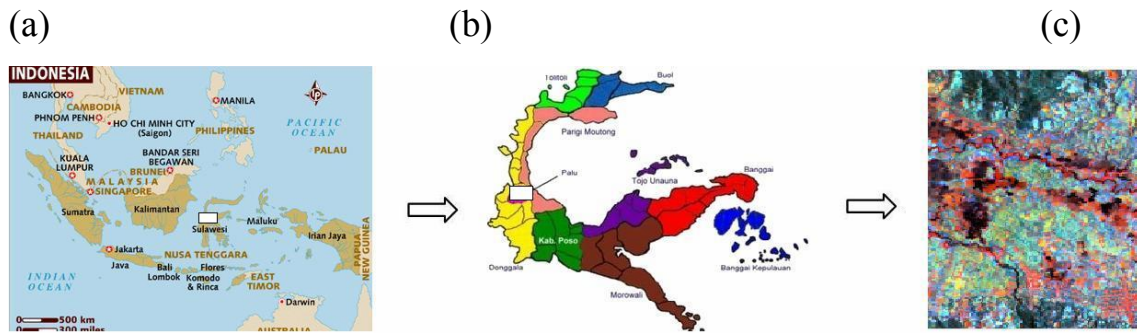


Figure 4-4. Study area 1: (a) Indonesia; (b) Solawesi province; and (c) RGB 210, 60 and 20 bands for the study area, Palolo valley.

4.2.2 Ahmadabad, south Tehran, Iran

Hyperion data were acquired over an agricultural area in Ahmadabad village, south of Tehran, Iran on May 21, 2002 at 06:57:56 GMT (Figure 4-5). The dataset is at 1B1 level of preprocessing. More preprocessing was performed by Fahimnejad *et al.* [2007] includes correction for bad lines, striping pixels and smile, atmospheric correction. Finally a subset for the purpose of this work has been selected (Table 4-6).

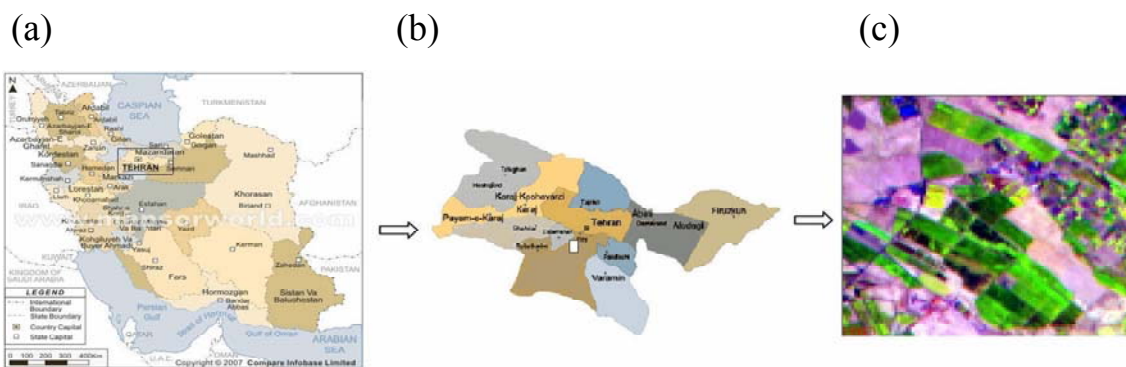


Figure 4-5. Study area 2: (a) Iran; (b) Tehran province; and (c) the RGB 110, 43 and 11 bands, Ahmadabad village.

CHAPTER FIVE

5 Results

As the whole thesis is composed of two main aspects of remotely sensed data fusion, thus the obtained results follows this structure and this chapter is mainly divided into pixel and decision level DF results. In addition, some other aspects like developed feature reduction algorithm for DF purposes and spatial evaluation of PLDF results have been discussed.

5.1 PLDF results (EO-1 Hyperion and ALI datasets, Indonesia, 2005)

The effect of pansharpening on spectral and spatial qualities of the fused datasets was investigated by Wald's protocol and full-reference image quality assessment (Chapter 3). As the number of bands was high, thus using the developed feature selection algorithm, MSSSI, three bands that as the most informative ones were selected for evaluation purposes. The evaluated bands of the ALI/MS (Bands 4, 3, 2 RGB) and Hyperion (30, 21, 14 RGB) which have been selected based on spectral overlap with Pan and maximum amount of information in which MSSSI feature selection was adapted. Therefore the selected bands are the most informative representative of the original datasets. In some cases there is conflict between evaluated properties (for example between Wald's spectral properties 1 and 2 and also between spatial and spectral properties). Therefore in such conflict situations for some applications the spatial accuracy is important while in some others the spectral fidelity is important. In this work both are considered and evaluated.

5.1.1 Objective evaluation

From the mentioned evaluation indices the SSIM (which models almost all possible aspects of image distortions) was selected as the basis for full-reference data quality evaluation. The quality measurements of the fused images are given in tables (5-1, 5-2 and 5-3).

5.1.1.1 Spectral distortion evaluation

In the following the spectral fidelity of the fused images were calculated by SSIM. The measured properties are referred to as Wald’s protocol properties 1 and 2. Wald’s property 1 measures how similar the fused image is to the original low spatial resolution MS image, while properties 2 and 3 measure how similar the fused image is to the assumptive high spatial resolution MS image.

After evaluation of the fused images it was found that in some cases there is a conflict between first property with second and third ones. And as the third one is return to the subjective properties of fused images thus is not measured in this research and the fused images are showed for illustration of visual evaluation purposes (for subjective evaluation as complementary for objective evaluations). As a matter of fact good results for a technique based on property 2 will also offer good results for property 3 [Lemeshevsky, 1999]; thus the third property was not calculated. Tables (5-1 and 5-2) show the Wald’s properties 1 and 2 metrics for different fused images. The values in each cell are the values of spectral fidelity of bands which calculated for ALI-MS bands 2, 3, 4 and Hyperion bands 14, 21, 30.

Table 5-1. Spectral quality metrics. Wald’s properties 1 and 2 for MS dataset.

Band/Technique	Wald’s Property 1				Wald’s Property 2			
	B. 1	B. 2	B. 3	ALL	B. 1	B. 2	B. 3	ALL
PCT	0.75	0.75	0.77	2.57	0.85	0.85	0.87	2.27
IHS	0.65	0.65	0.80	2.11	0.67	0.65	0.79	2.1
Brov.	0.050	0.038	0.028	0.12	0.05	0.04	0.03	0.11

ARSIS_DWT	0.72	0.73	0.69	2.31	0.71	0.79	0.81	2.14
ARSIS_ATWT	0.80	0.81	0.80	2.22	0.74	0.73	0.75	2.41
FB	0.73	0.71	0.78	2.15	0.71	0.71	0.73	2.22
RT	0.81	0.83	0.79	2.43	0.82	0.80	0.81	2.43
GST	0.75	0.75	0.77	2.58	0.86	0.85	0.87	2.27
DWT_Haar	0.83	0.86	0.86	2.49	0.82	0.84	0.83	2.55
DWT_Symlet	0.83	0.86	0.86	2.49	0.82	0.84	0.83	2.55
HPF	0.78	0.81	0.80	2.59	0.86	0.87	0.86	2.39
CN	0.53	0.74	0.84	1.94	0.51	0.71	0.72	2.11

Table 5-2. Spectral quality metrics. Wald's properties 1 and 2 for HS dataset)

Technique/Band	Wald's Property 1				Wald's Property 2			
	14	21	30	ALL	14	21	30	ALL
PCT	0.64	0.70	0.71	2	0.66	0.62	0.72	2.05
HIS	0.33	0.49	0.70	1.49	0.35	0.48	0.66	1.52
Brov.	0.00	0.00	0.00	0	0.00	0.00	0.00	0
ARSIS_DWT	0.74	0.78	0.79	2.15	0.71	0.73	0.71	2.31
ARSIS_ATWT	0.77	0.79	0.80	2.16	0.71	0.71	0.74	2.36
FB	0.71	0.77	0.79	2.17	0.71	0.72	0.74	2.27
RT	0.78	0.81	0.80	2.16	0.73	0.72	0.71	2.39
GST	0.65	0.69	0.71	2	0.66	0.63	0.71	2.05
DWT_Haar	0.67	0.74	0.83	2.23	0.68	0.73	0.82	2.24
DWT_Symlet	0.67	0.74	0.83	2.23	0.68	0.73	0.82	2.24
HPF	0.75	0.81	0.78	2.41	0.78	0.80	0.83	2.34
CN	0.54	0.64	0.72	1.78	0.52	0.61	0.65	1.9

As can be seen from above tables these two properties almost do not offer the same results. For example based on first property HPF is the best one while based on the second property the RT is the best. As a consequence, for measuring the spectral constancy of a fused image, one of these properties must be used. In the literature also this matter has been proved by some authors. For example Li *et al.* [2002] and Shi *et al.* [2003] used first property while Aiazzi *et al.* [1999]; Lemeshefsky

[1999]; and Wald *et al.* [1997] preferred the second one for evaluate their works and techniques.

5.1.1.2 Spatial distortion evaluation

The same as spectral properties, the spatial quality of the fused images is also important. In the literature there are few papers that offered the spatial quality of the Pan sharpened imagery. Here we evaluated the spatial properties based on the spatial autocorrelation of fused images. After some elementary investigations and comparisons the Moran's I (indicator of spatial clustering of similar values) and Geary's C (indicator of spatial dissimilarity of observations) local autocorrelations were selected for spatial distortion evaluation. As can be seen in table (5-3) the image comparisons were performed based on the Coefficient of Variances (C.V.) of autocorrelations. C.V. is the ratio of the standard deviation to the mean. C.V. is a useful statistic for comparing the degree of variation from one image to another, even if the means are drastically different from each other. After comparing the obtained results with the visual properties of fused data it was clear that these developed indicators are almost reliable for spatially fused image evaluation. For example RT and FB are the most weak fusion techniques based on Geary's C while PCT is the best one that is provable in compare to visual comparisons of fused images (Figure 5-1). From these two spatial evaluation techniques Geary's C offered reliable results while the ability of Mora's I was not acceptable. For example for Radon and Fanbeam that the spatial properties of fused images are very dissimilar to Pan therefore Geary's C has measured this dissimilarity very precisely, therefore the absolute different between pan and fused bands is the highest (Table 5-3). On the contrary, based on the Moran's I the Fanbeam and Radon have gotten the same scores as other fused images that, in reality, is not true.

Table 5-3. Spatial quality metrics.*

Geary's C	Moran's I
-----------	-----------

Technique	Band	C.V.	ABS(Pan- Fused)	C.V.	ABS(Pan- Fused)
PCT	Pan	7,56		2,96	
	14	7,19	0,37	3,25	0,29
	21	6,96	0,60	2,67	0,29
	30	7,47	0,09	2,88	0,08
HIS	14	2,47	5,09	2,18	0,78
	21	2,20	5,36	1,92	1,03
	30	2,93	4,63	2,62	0,34
Brov.	14	8,00	0,44	3,29	0,33
	21	7,00	0,56	2,67	0,29
	30	9,00	1,44	2,71	0,24
ARSIS_DWT	14	8,23	0,67	3,23	0,27
	21	7,74	0,18	2,53	0,43
	30	7,23	0,33	2,62	0,34
ARSIS_ATWT	14	7,11	0,45	2,99	0,03
	21	7,10	0,46	2,48	0,47
	30	6,82	0,74	2,57	0,38
FB	14	2,97	4,59	2,86	0,09
	21	2,89	4,67	2,36	0,60
	30	2,71	4,84	2,46	0,49
Rad	14	3,21	4,35	2,82	0,14
	21	4,00	3,56	2,33	0,63
	30	3,04	4,52	2,52	0,44
GST	14	7,23	0,32	3,22	0,26
	21	7,03	0,53	2,67	0,29
	30	7,42	0,14	2,84	0,12
DWT_Haar	14	6,85	0,71	3,78	0,82
	21	6,51	1,04	2,92	0,04
	30	5,00	2,56	2,54	0,42
DWT_Symlet	14	6,85	0,71	3,78	0,82
	21	6,51	1,04	2,92	0,04
	30	5,00	2,56	2,54	0,42
HPF	14	7,07	0,49	3,34	0,38

CN	21	6,99	0,57	2,80	0,16
	30	7,07	0,49	2,89	0,07
	14	5,90	1,65	3,87	0,91
	21	5,93	1,63	3,36	0,40
	30	5,72	1,84	2,64	0,32

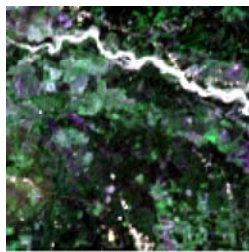
*C.V. is the Coefficient of Variation. ABS (Pan-Fused) is the absolute value of differences which is the measure of similarity of two datasets. The smaller value the more similar images the more spatially property preservation.

5.1.2 Subjective evaluation

In order to make the fused images be more familiar for subjective evaluator (person who visually evaluate the quality of fused image in compare to reference) the original EO-1/ALI-multispectral bands 4, 3, 2 RGB; ALI/ panchromatic; and Hyperion bands 30, 21, 14 RGB datasets and the fused images are showed in figure (5-1). After visual inspection it was concluded that visual properties of results are almost in agreement with spectral and spatial objective evaluations. As these subjective evaluations are very expensive and time consuming therefore must be carefully and effectively carried out. Also as these evaluations are depend to several other parameters than the fused image itself e.g. visual ability of subjective, used colors, illumination conditions, etc therefore they can be used as complementary for objective evaluators. For example using the subjective investigation for RT while spatial properties is not good but the spectral fidelity is high and based on the results of objectives these results are clearly provable. The visual comparison of fused images carried out and the results were almost in agreement with mostly the first measured spectral property of Wald (Table 5-1 and 5-2).



ALI Panchromatic



Hyperion Bands 30, 21, 14



ALI MS Bands 3, 2, 1



HS Brov.



MS Brov.



HS PCT



MS PCT



HS GST



MS GST



HS DWT_Haar



MS WDT_Haar



HS DWT_Symlet



MS WDT Symlet



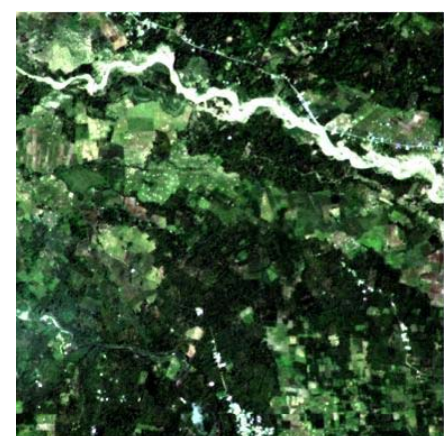
HS HPF



MS HPF



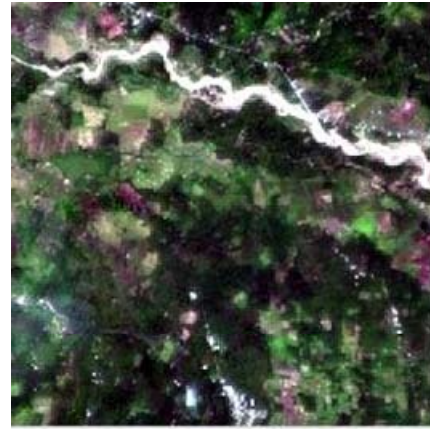
HS IHS



MS IHS



HS ARSIS-DWT



MS ARSIS-DWT



HS ARSIS-ATWT



MS ARSIS-ATWT



HS Fanbeam



MS Fanbeam



HS Radon



MS Radon



HS CN



MS CN

Figure 5-1. EO-1/Hyperion (HS), ALI-Multispectral (MS) and ALI-Pan images of Palolo valley, Indonesia. First row: ALI-Pan image; second row: left column HS and right column MS images. The rest are fused images which named based on fusion techniques (see acronym list).

5.1.3 Histogram comparison

Histogram comparison could be evaluated subjective or objectively. The histogram describes the statistical distribution of pixels in terms of the number of pixels at each DN [Schowengerdt, 1997]. The histograms of the original MS or HS and the fused bands were evaluated separately. In this regard if the spectral information of one band

of a fused image is preserved, thus its histogram will closely resemble the histogram of its original band. As an evaluation factor, it has been used subjectively (visually) by Vijayaraj *et al.* [2004] and also objectively by the help of mean shift computation [Parcharidis, 2000]. As the mean shift is a comparison that is covered by MSSI objective evaluation thus here we just consider histogram comparison in visual appearance. Due to limitation of space just the histogram of two techniques: Brovey and DWT-Haar are shown (Figure 5-2). Brovey's results in compare with the original ones have shown the highest amount of differences (as proved by spectral evaluations (Tables 5-1 and 5-2)). On the contrary the DWT-Haar has offered results that are more similar to their original therefore the histogram comparison is in agreement with image spectral quality evaluation. As a general conclusion, irrespective to the amount of shifts and concerning to the shape of histograms it is clear that the results of the DWT-Haar methodology are more similar to the original than the Brovey. After several datasets comparisons and as stated by Wald [2002] the behavior of the histogram depends upon the observed type of landscape and the sharpening factor (SF). Therefore the higher the SF will cause the more dissimilar statistics of fused bands to the reference. Thus this evaluator must be carefully carried out where datasets have different SFs. As the evaluated datasets (i.e. EO-1/Hyperion and ALI-MS) have the same spatial resolution (30 meter) thus it is a reliable indicator for our datasets.

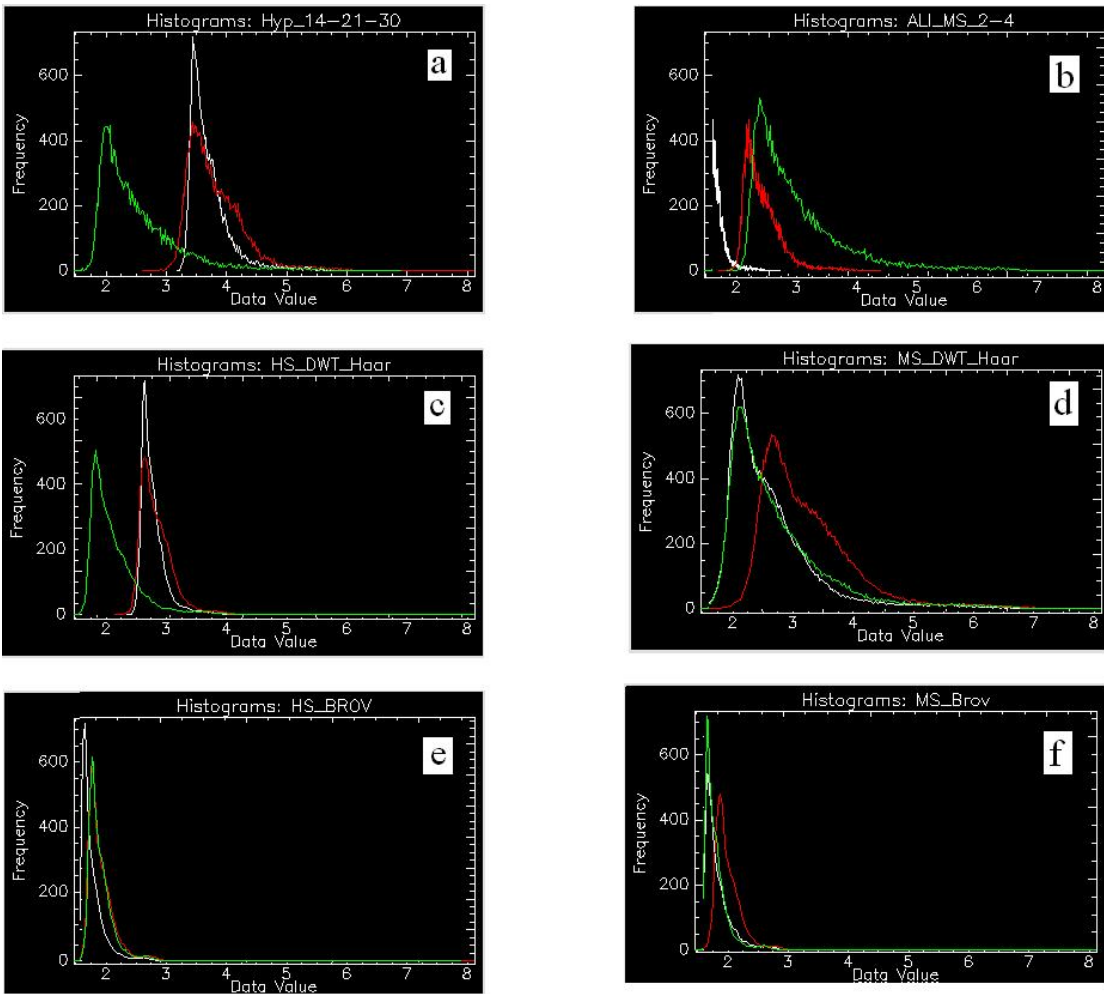


Figure 5-2. Histograms comparison. (a) Hyperion bands 14, 21, 30; (b) ALI bands 2, 3, 4; (c) Hyperion fused by DWT-Haar; (d) ALI fused by DWT-Haar; (e) Hyperion fused by Brovey; (f) ALI fused by Brovey.

5.2 DLDF results (EO-1- Hyperion, Iran dataset, 2005)

The accuracy in DLDF is measured in the form of final obtained map accuracies. Thus the used evaluation parameters are the classification accuracy indicators including Overall Accuracy (OA) and Kappa Coefficient (KC) [Russell and Congalton, 1999]. The mentioned indicators are calculated based on confusion or error matrix.

As mentioned before, three procedures i.e. WBDF; CBDF and MCDF for hyperspectral DLDF has been adapted. All of these procedures are carried out using Dempster-Shafer theory. In order to perform these procedures first subsets were selected, followed by classification processes and finally Dempster-Shafer decision

fusion was carried out. The results have been evaluated based on overall accuracy and kappa coefficient.

In the WBDF and CBDF procedures all selected subsets were classified by Dempster-Shafer classifier. But in the MCDF procedure three soft classifiers: Bayes; Dempster-Shafer; and Fuzzy were performed.

As seen in table (5-4) the triple used bands for CBDF were selected using MSSSI feature selection procedure. And for WBDF, the listed bands were selected based on their location in electromagnetic spectrum. In WBDF the three selected band for e.g. Red (400-500 nm) are bands 8, 12 and 15 which are the most informative bands from that spectrum which are located at first, middle and end of red spectrum of electromagnetic. Also for the rest spectrums the same procedure as for the red spectrum was carried out.

Table 5-4. Selected bands based on two explored feature selection procedures.

WBDF			CBDF	
Wavelength (nm)	Selected bands	Spectral class	Selected bans	
Red 400-500	8, 12, 15	1	8, 36, 117	
Green 500-600	16, 20, 25	2	10, 98, 211	
Blue 600-700	26, 31, 35	3	113, 182, 214	
NIR 700-1000	36, 49, 85	4	93, 101, 149	
MIR 1000-1300	86, 101, 115	5	8, 90, 220	
SWIR1300-2500	116, 199, 220	6	8, 56, 96	

Table 5-5. Accuracy of DLDF techniques in compare to SAM classifier*.

Procedure	OA (%)	KC
Wavelength-based decision fusion	72.7	64.0
Class-based decision fusion	73.5	65.5
Multi classifier decision fusion	76.0	70.2

*Overall Accuracy (OA) and Kappa Coefficient (KC).

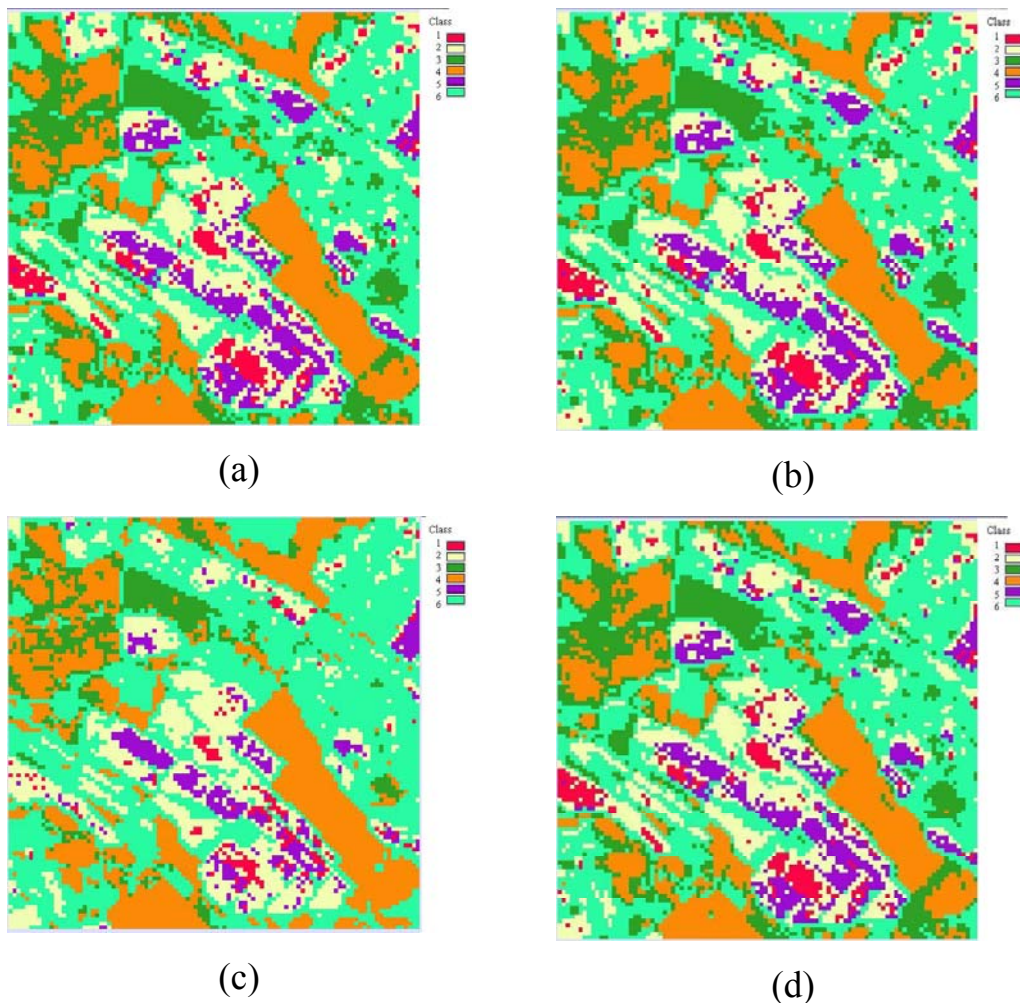


Figure 5-3. Final maps of DLDF procedures and SAM classification.
(a) WBDF; (b) CBDF; (c) MCDF and (d) SAM.

Despite differences in the measured accuracies are almost imperceptible, but the general performance of all procedures is higher than SAM, while MCDF has offered the best results. As the new developed procedures in this work WBDF and CBDF are still under investigation and need to be improved and more evaluated by several other data sources thus definitely it can not be clarify which of them is preferable over other (Figure 5-3 and Table 5-5).

5.3 MSSI feature reduction evaluation

To assess the ability of MSSI methodology a post classification accuracy assessment procedure was carried out. For this purpose the Iran Hyperion dataset was evaluated in the next steps. First a 5-band subset for the under investigation area were selected (Table 5-6). As the selected features must contain maximum spectral and spatial information and also the best visual characteristics, therefore two aspects of obtained subsets are calculated and compared: spatial image entropy and spectral classification accuracy. The Support Vector Machine (SVM) classification methodology was performed and using a confusion matrix the accuracies of land cover maps were evaluated (Table 5-7). The spatial properties calculated by image entropy comparison. Entropy is a convenient measure of information content of remotely sensed imagery that has been used in several works [Malila, 1985 and Masek, 2001]. This indicator could have any value which entropy = 0 is the lowest possible information content and the higher values the higher information contents. The obtained results from MSSI are compared to the results from two common techniques includes: Transformed Divergence (TD) and Bhattacharyya Distances (BD) (Table 5-7). From these evaluated aspects and using this dataset the obtained results show not noticeable superiority of one feature selection algorithm over others. The ability of MSSI must be investigated with more different datasets and for different applications in the future.

Table 5-6. Selected bands using three different feature selection methodologies (Iran dataset).

MSSI	8, 56, 90, 149, 214
BD	8, 38, 87, 154, 212
TD	8, 37, 84, 196, 197

Table 5-7. The spatial and spectral accuracies of selected subsets*.

MSSI	BD	TD
------	----	----

Overall Entropy	Post classification accuracies		Overall Entropy	Post classification accuracies		Overall Entropy	Post classification accuracies	
	Overall Accuracy	Overall Kappa		Overall Accuracy	Overall Kappa		Overall Accuracy	Overall Kappa
1.9	0.87	0.83	1.9	0.88	0.85	1.9	0.88	0.85

*Maximum Spectral and Spatial Information Indicator (MSSI); Bhattacharyya Distances (BD) and Transformed Divergence (TD).

5.4 Block based feature selection evaluation

In order to evaluate the block based feature reduction Hyperion dataset, Indonesia, 2004 was used. As stated in (Chapter 3) the amount of τ (as a measurement to control the dimension and number of blocks) is due to several parameters includes data dimension; desired band numbers in blocks; purpose of data processing; etc. The specification of τ could be any calculation that can help to find homogeneity blocks as high as possible. In this work amount of τ was investigated based on standard deviation of $R_{i, i+1}$. Consequently, as shown in table (5-8) the dimensions of the blocks are fluctuating across the whole dataset and do not follow a specific pattern. As here the statistic image is obtained from the whole dataset therefore the dimension of blocks are from 1 to 20. One-dimension blocks are single uncorrelated bands and 20 is a group of bands with highest correlations.

After obtaining blocks with maximum spectral homogeneity the within-block bands can be treated using any feature extraction or selection procedure. In this work we used PCA feature extraction over all blocks and PC1s from every block were picked up as the representative with maximum information content from any block. Consequently a new dataset with 16 bands which contains first PCs from all blocks is selected. This 16-component subset has more than 90 percent of the information from the whole dataset with 133 bands (Table 5-8). As can be seen this technique is very effective to reduce the dimension of images while the main information contents is still high and comparable with the original image. The obtained blocks and included bands can be used for any further processing like PCT feature extraction or MSSI feature selection.

Table 5-8. Block based feature reduction. Selected bands and their statistical properties. Hyperion dataset, Palolo valley, Indonesia, 2004.

Block Number	Band number in blocks	The number of bands per block	Blocks spectral range (nm)	Mean correlation Per block	Std.Div of blocks
1	11-17	7	455-516	0.98	0.0087
2	18-25	8	526-597	0.98	0.0113
3	26-34	9	607-689	0.99	0.0055
4	35-38	4	699-729	0.64	
5	39-56	18	740-913	0.99	0.0085
6	57, 82	2	923, 962	0.96	
7	83-93, 95-96	13	972-1073, 1093-1103		0.0142
8	96, 97, 101	1 (3)	1114		
9	101-117	17	1153-1315	0.99	0.0089
10	118-119	2	1325-1335		
11	135-142	8	1497-1568	0.98	0.0114
12	143-162	20	1577-1769	0.99	0.0090
13	163, 191- 192	3	1780, 2062- 2072		
14	193-207	15	2082-2224	0.96	0.0091
15	208-210	3	2234-2254	0.97	
16	211-213	3	2264-2284	0.97	

CHAPTER SIX

6 Conclusions, recommendations and future works

Here, conclusions are drawn based on experiments performed in this PhD. work and also several other works (Appendix II) that have been done during these four years of PhD study in relation to data fusion. Also, some comments that are very useful for data fusion implementation are drawn. Finally some recommendations and further investigations are suggested. To better understanding this part of work, chapter 2 and 3 shall be studied before. Also this chapter is almost written briefly because in some other parts of the work some conclusions and recommendations are mentioned and discussed. Based on the main objectives of this work that were image spatial enhancement by PLDF and classification accuracy improvement by DLDF the conclusions and recommendations are put into two separate parts as pixel and decisions levels.

6.1 Comparing the evaluated techniques

6.1.1 Pixel level data fusion

Ten of the most common PLDF techniques and two new ones (i.e. Fanbeam and Radon fusions) were evaluated and it was found that in general the techniques that use high frequencies (e.g. Wavelet-based techniques) from the panchromatic image have done better than those that use the whole Pan image information (e.g. IHS). While techniques that work based on color normalization (e.g. Brovey) offered the weakest results. It also must be noted that one of the main objectives of this work was the investigating the spatial enhancements properties by objective fused image evaluation. Therefore the subjective evaluations were performed as complementary and compared with objective quality measurements.

In order to make more detailed illustrations based on the earlier mentioned spectral and spatial accuracy assessments the evaluated PLDF techniques have been ranked in table (6-1). This ranking is from 1 to 11 which 1 is the best and 11 is the worst.

Table 6-1. PLDF techniques ranked based on the ability of techniques to preserve the spatial and spectral properties of fused images.

Ranking	Wald's property 1 for MS	Wald's property 2 for MS	Wald's property 1 for HS	Wald's property 2 for HS	Geary's C for HS	Moran's I for HS
1	HPF	Haar and Symlet	HPF	RT	GST	HPF
2	GST	RT	Haar and Symlet	ARSIS-ATWT	PCT	PCT
3	PCT	ARSIS-ATWT	FB	HPF	ARSIS-DWT	GST
4	Haar and Symlet	HPF	ARSIS-ATWT and RT	ARSIS-DWT	HPF	Brov.
5	RT	PCT and GST	ARSIS-DWT	FB	ARSIS-ATWT	ARSIS-ATWT
6	FB	FB	PCT and GST	Haar and Symlet	Brov.	ARSIS-DWT
7	ARSIS-DWT	ARSIS-DWT	CN	PCT and GST	Haar and Symlet	FB
8	ARSIS-ATWT	IHS	IHS	CN	CN	RT
9	IHS	CN	Brov.	IHS	RT	Haar and Symlet
10	CN	Brov.		Brov.	FB	CN
11	Brov.				IHS	IHS

Based on the above ranking and from this overview, some remarkable conclusions are drawn.

1. From the first introduced spatial property evaluator (NDA based on Geary's C) it can be concluded that in techniques which work based on the whole Pan

injection into the fusion process Like PCT and GST, the influence of Pan is completely clear in compare to the techniques which work base on high frequencies of Pan injection into the fusion process for instance DWT-Haar and Symlet. Therefore the spatial evaluation helps to understand the influence of Pan in the fusion process.

2. Techniques that work based on selected panchromatic band frequencies (see chapter 3) e.g. DWT and HPF offered better results in the spectral fidelity point of view.
3. Techniques that work based on color transformations and normalization like IHS and CN offered weak results almost in both spectral and spatial evaluation accuracies.
4. The novel PLDF techniques i.e. FB and RT, despite almost good spectral results but they have gotten lower positions in spatial properties evaluation due to their poor spatial preservation abilities.
5. Different behavior of techniques over multispectral and hyperspectral imagery is also noticeable. In general the obtained results for MS are better than for HS dataset. This phenomenon returns to the fact that MS bandwidths are wider than HS bands (for example ALI band 3 has a bandwidth about 80 nm while Hyperion band 30 is about 10 nm) therefore the amount of energy for illumination a MS band is more similar to Pan than HS bands.
6. The obtained results from measured spectral properties of fused images sometimes are incompatible for example in Wald's property 1 the HPF has gotten the best rank while based on the Wald's property 2 it has gotten ranking 4 (Table 6-1). Therefore these properties must be carefully selected and interpreted.
7. The measured spectral and spatial properties in some cases are incompatible and in some others are complementary as well. For example Brovey has gotten the lowest rank in the spectral properties while based on its spatial properties it has gotten the ranks of 4 and 5. Consequently these properties are complete frameworks which help to know all facts about a fused image.

8. For some techniques e.g. CN and Brovey, notwithstanding the weak results for spatial and spectral objective quality measurements, the visual appearance of them is fine. On the contrary for example DWT-Haar or Symlet the visual appearance of fused images may not be fine but the measured qualities show better results. Therefore due to the application of data fusion different quality assessments can be applied. For instance while CN and Brovey are better for visual image interpretation (with consideration for color distortion and probable misleading), the DWT-Haar and Symlet are more better for other applications of image analysis e.g. classification. In this regard subjective and objective image accuracy evaluations are complementary and one can not be replaced by another.
9. The histogram comparison is also a good image quality measurement and the obtained results are in the direction of spectral assessments of fused images.
10. It is noticeable that for the new introduced spatial evaluation measurements, the autocorrelation comparison based on Geray's C offered acceptable measurements while the comparison based on Moran's I was not reliable.

6.1.2 Decision level data fusion

Of course this level is a classification based DF therefore the comparison is meaningful when the objective is data classification. Therefore the next remarks are partly based on earlier experiments in Darvishi Bolorani *et al.* [2005¹]. Based on the evaluated and introduced algorithms for this level of fusion the following conclusions can be drawn.

1. Referencing to the evaluated hyperspectral dataset e.g. Iran dataset, both developed DLDF techniques i.e. WBDF and CBDF offered the same classification accuracies, While MCDF obtained the highest accuracy.
2. The evaluated procedures offered higher accuracies than classification procedures without fusion.

6.1.3 Feature selection

Feature selection has a very crucial importance in almost all data fusion procedures. This importance is higher when the dimension of data is higher such as for hyperspectral datasets. In this work a novel feature selection technique i.e. MSSSI has been evaluated and compared to two common feature selection techniques i.e. BD and TD. Despite the fact that MSSSI did not offer better results than other feature selection algorithms, but the rationale behind it is strong and needed to be more evaluated and improved. Also the evaluated block level feature reduction procedure had a good ability to reduce the dimension of datasets.

6.2 Strengths and limitations of data fusion

6.2.1 Data fusion strengths

The ideal of data fusion is getting the highest possible information content from raw or pre-processed datasets. The highest possible information potentially could be spectral, spatial, radiometric, and temporal resolutions, highest possible classification accuracy, etc. The literature of data fusion covers a high variety of data, techniques and applications; therefore no rule of thumb exists for discrete description of data fusion strengths. Data fusion, like any other procedure is composed of (i) information sources; (ii) means of information acquisition; (iii) information exchange communication; and (iv) intelligence for information processing into higher content of presentation [Wald, 2002]. Therefore, any categorization concerning the pros and cons of DF should consider it as a whole process. Based on the obtained experiences from this work and other related studies (see appendix II) as well as from the literature, strengths are illustrated at pixel and decision levels of fusion.

6.2.1.1 Pixel level

1. *Improvement image resolutions:* Indeed the ideal of DF is obtaining the highest possible resolution from input datasets. For example in our dataset the spatial resolution improvement was the main objective. More than this, other kinds of resolution can be improved. For example in Darvishi Bolorani *et al.* [2006²] the temporal resolution was improved using the combination of multi-temporal ENVISAT/ASAR satellite Synthetic Aperture Radar (SAR) images and also in Darvishi Bolorani *et al.* [2005²] the spatial resolution improved the ability of Landsat/ETM+ datasets to extract urban road networks.
2. *Data volume, storage and transformation:* Data volume is a very important aspect of RS datasets. Using a good sophisticated fusion, raw images (e.g. HS and Pan) can be separately stored and just according to requirement be fused. For example the volume of a Hyperion-hyperspectral image with 242 spectral bands and 30 meter spatial resolution and an ALI-panchromatic image with 10 meter spatial resolution is about 9 times lesser than an assumptive Hyperion-hyperspectral image with 242 spectral bands and 10 meter spatial resolution. Therefore storage raw datasets and fuse them and according to requirement is an effective policy which facilitates data storage and transformation.
3. *Very high number of applications:* On the contrary to DLDF which mostly limited to data classification, but in the PLDF there is not limitation for applications. For example the fused datasets can be used to a variety of applications e.g. Zhang [1999], Ranchin and Wald [2000], Li *et al.* [2002], Cakir and Khorram [2003], Chen *et al.* [2005] and Zhang and Hong [2005] used fused images for a variety of applications.

6.2.1.2 Decision level

1. *Complementary of different classifiers:* In this level the advantages of different classifiers are exploited while their weaknesses are mostly compensated. The obtained results from DLDF proved that the MCDF offered better results than

WBDF and CBDF. Therefore combination of several classifiers is still a powerful tool in DLDF.

2. *Eliminating the effects of data resampling*: Almost all PLDF techniques include at least one resampling process that causes spectral distortions in fused datasets. But in DLDF which datasets are processed separately the problems related to resampling are avoided.
3. *Avoiding the contrast differences in fused images*: The contrast of high resolution Pan image is mostly different and higher than the contrast in the lower resolution MS image, consequently direct combination of images makes the contrast modification unavoidable. This extra process will cause information distortion. As the DLDF will fuse data after classification performance, therefore the contrast modification problem is avoided.
4. *No spectral, radiometric and temporal limitations*: In the decision level as the data sources analyzed independently therefore on the contrary to pixel level fusion techniques, the spectral, spatial and radiometric resolutions of images do not have high and strict influences over the fusion process.
5. *No limitation of sharpening factor*: In DLDF any dataset with any spatial resolution can be fused and the problem of SF has no crucial role in fusion process.

6.2.2 Data fusion limitations

Despite the fast developments in methodologies, techniques, and algorithms for all levels of fusion, but the final results almost eventually loss some useful information. It should be considered that no rule of thumb exists for the right number of parameters that can be considered as limitations in data fusion. Based on the results of the presented research and extensive literature search some important restrictions are categorized on both levels of fusion.

6.2.2.1 Pixel level

1. *Sharpening Factor (SF)*: Due to the different spatial resolutions of data sources the SF (ratio of low spatial resolution pixel size to high spatial resolution pixel size) plays an important role in pixel level data fusion. Based on Darvishi Bolorani *et al.* [2005¹] an SF less than 7 offers more precise results.
2. *Image registration*: Generally data registration is one of the major elements in data fusion; specifically the pixel level techniques are very sensitive to miss-registration phenomenon.
3. *Spectral Overlap (SO)*: As a practical matter the spectral overlap of data must be considered in pixel level. In decision level spectral overlap is not necessity [Ranchin and Wald, 2000].
4. *Technique limitations*: Some techniques like Brovey are based on a simple ratio of input images that will change the spectral properties of the data sources if the number of bands gets higher. But for some others like wavelet these limitations are minimal.
5. *Temporal limitation*: The used data must be recorded simultaneously as much as possible. Experimentally the higher temporal and seasonal shifts the lower the accuracy Darvishi Bolorani *et al.* [2008²].
6. *Artifacts because of low correlation between datasets*: In the techniques which work using all panchromatic band frequencies when correlation between the replacing component (e.g. I from IHS and PC1 from PCT) with Pan is low consequently the results of these procedures are generally weak.
7. *Limited numbers of bands for fusion*: The IHS just can handle only three input images while the PCT and wavelet procedures can be applied to any number of bands.
8. *Over-influence of Pan in fusion process*: In some techniques, like PCT and GST, all the details of Pan are introduced into the fused dataset. For that reason the fused images are nicely spatially enhanced while the spectral distortion is high. The Ehler's procedure [Ling *et al.* 2006] is one of the alternative procedures that alleviate this problem.

9. *Spectral and spatial losses due to transformations:* In some techniques prior to the fusion process data transformation is performed. If the transformations are non-lossy such as PCT the only source of distortion is the fusion process. But in some techniques like fanbeam which is a lossy transformation in addition to the distortions from the fusion process the transformation itself also introduces some distortions.
10. *Resampling artifacts:* Almost all PLDF techniques have at least one resampling process that is from the lower resolution to the higher resolution and consequently these procedures will cause spectral distortions.
11. *Blocky appearance:* This is an important phenomenon in pixel level data fusion. The blocky appearance of fused data caused by the amount of SF can be treated by smoothing filter.
12. *Filter size:* Some techniques that work based on a moving filter like HPF are very sensitive to the filter size over which the high frequency details are computed. Thus due to the data properties and the relationship between object areas and pixel sizes a good filter size must be adapted.

6.2.2.2 Decision level

Due to the fact that this level of fusion was investigated over some few techniques therefore just the next limitation are clarified and extensive discussions can be found in [Benediktsson *et al.* 1992; Benediktsson *et al.* 2003].

Limited exploitation of data properties: Because data are primary classified thus synergetic combination of data properties (in comparison with PLDF) is not explored. In some applications the usability of dataset will be appeared when the individual images are fused. For example in Darvishi Bolorani *et al.* [2006²] the positive synergism of multi-temporal SAR datasets helped to discriminate the rice fields in central Sulawesi, Indonesia.

6.3 Recommendations and future works

Finally, some recommendations and topics for future research projects that could not be performed because of time limitations are:

1. Using the Iran dataset, the DLDF algorithms i.e. WBDF and CBDF show their ability for data fusion. But the ability of the innovated techniques must be evaluated with several other datasets and specifically with diverse dataset for different purposes.
2. More sophisticated and flexible fusion algorithms needed to be implemented in the commercial RS and GIS software. For example Ehler's methodology in ERDAS Imagine 9.1 and Dempster-Shafer theory in IDRISI-Andes are good examples for two levels of fusion.
3. Fusing datasets with different characteristics like SAR, optical imagery, GIS information and field-collected information is a very crucial aspect of DF. For example GIS information and object models in combination with satellite imagery are very emerging tasks of data fusion. These kinds of fusions have been used for several years but still there is more room to performance.
4. In addition to visual, spectral, and spatial evaluations that were carried out, other techniques for assessing the quality of fused images are needed. For example the comparison of land surface maps obtained by classification procedures or the results from target detection and object recognition could be very informative for a PLDF procedure.
5. In the decision levels of fusion, the low results of WBDF and CBDF techniques in compare with MCDF could be related to the use of just one classifier. Therefore adapting the mentioned methodologies to multi-classifier will probably increase the accuracy of results.
6. A conceptual framework allowing the fusion of datasets in all levels is required.
7. Regarding the fact that the real world objects are 3-Dimensional, therefore data fusers which enable us to model and build fused data in 3-D are required for

future. With 3-D-based fusion abilities the real world phenomena can be better modeled and understood.

8. The usage of data fusion in telecommunication services like mobile is also important. In mobile phone technology and other similar devices the information must be optimally compatible. Therefore DF is a proper basis to make such data compatibility.
9. Based on the definitions of precision farming, forestry, mining, etc that the needed information must be very complete and precise DF can play a very important role. For example for a precision farming system several layers of information like soil types, amount of humidity, type of fertilizer, etc must be simultaneously analyzed. As DLDF has good abilities to fuse multivariate dataset therefore decision fusion is an ideal basis to combine all of these datasets.
10. Extreme weather conditions such as hurricanes and floods and man-made disasters such as war and the consequences such as a huge refugee population, shortage of water and food supply etc are very necessary research areas for implementing state-of-art and real-time data fusion systems.

REFERENCES

- Abdi, H. (1994). A neural network primer. *Journal of Biological Systems* , 2, 247–281.
- Abdi, H., Valentin, D., & Edelman, B. (1999). *Neural networks*. Thousand Oaks: Sage.
- Agrwal, S., Mereddy, P., Shah, D., Dutta, A., Rao, V., & Baumgart, C. W. Adaptive sensor data fusion architecture for landmine detection and discrimination. *SPIE, the International Society for Optical Engineering, CODEN PSISDG*.
- Aiazzi, B., Alparone, L., Barducci, A., & Pippi, I. (1999). Multispectral fusion of multisensor image data by the generalized Laplacian pyramid. *IEEE International Geoscience And Remote Sensing Symposium*, (pp. 1183-1185).
- Aiazzi, B., Alparone, L., Baronti, S., & Pippi, I. (2001). Quality assessment of decision-driven pyramid-based fusion of high resolution multispectral with panchromatic image data. *Proceedings of the IEEE/ISPRS Joint Workshop on Remote Sensing and Data Fusion over Urban Areas*, (pp. 337–341). Rome, Italy.
- Albertz, J. (1998). *The geometric restitution of line scanner imagery: Three decades of technical development*. Wissenschaftliche Arbeiten der Fachrichtung Vermessungswesen der Universität Hannover.
- Amolins, K., Zhang, Y., & Dare, P. (2007). Wavelet based image fusion techniques — An introduction, review and comparison. *International Society for Photogrammetry and Remote Sensing, Inc. (ISPRS) Published by Elsevier* , 249–263.
- Anyas, H., Bannari, A., He, D. C., & Morin, D. (1994). Texture analysis for the mapping of urban areas using airborne MEIS-II images. *First International Airborne Remote Sensing Conference and Exhibition*, 3, pp. 231-245. Strasbourg, France.

- Apan, A., Held, A., Phinn, S., & Marklev, J. (2004). Detecting sugarcane orange rust disease using EO-1 Hyperion hyperspectral imagery. *International Journal of Remote Sensing*.
- Autrusseau, F., & Guedon, J. P. (2002). Image watermarking for copyright protection and data hiding via the mojette transform. *SPIE*, 4675, pp. 378 – 386.
- Bannari, A., Morin, D., Bonn, F., & Huete, A. R. (1995). A review of vegetation indices. *Remote Sensing Reviews*, 13, 95-120.
- Barillot, C., Lemoine, D., Le Briquer, L., Lachmann, F., & Gibaud, B. (1993). Data fusion in medical imaging: merging multimodal and multipatient images, identification of structures and 3D display aspects. *European Journal of Radiology*.
- Barry, P. (2001). *EO-1/ Hyperion science data user's guide, level 1_B*. Redondo Beach, CA: TRW.
- Bayes, T. (2007). introductory tutorial to Bayesian probability in 1763.
- Bernardo, J. M., & Smith, A. F. (1994). *Bayesian theory*. Chichester: Wiley Series in Probability and Mathematical Statistics, John Wiley & Sons.
- Borstad, G., & Vosburgh, J. (1993). Combined active and passive optical bathymetric mapping: using the LARSEN lidar and the CASI imaging spectrometer. *16th Canadian Symposium on Remote Sensing, June 7-10*, (pp. 153-157). Sherbrooke, Quebec.
- Bouzidi, S., Berroir, J.-P., & Herlin, I. (1998). A remote sensing data fusion approach to monitor agricultural areas. *Digital Object Identifier*, 2, pp. 1387 - 1389.
- Box, G. E., & Tiao, G. C. (1992). *Bayesian inference in statistical analysis*. New York: John Wiley and Sons, Inc.
- Bradley, A. P. (2003). Shift-invariance in the discrete wavelet transform. *Digital Image Computing: Techniques and Applications (DICTA'03)*. Sydney, Australia.
- Breuer, M., & Albertz, J. (2000). Geometric correction of airborne whiskbroom scanner imagery using hybrid auxiliary data. *Int. Archive of Photogrammetry and Remote Sensing, XXXIII, Part B3, Commission III*, pp. 19–23. Amsterdam.

- Bruno, A., Luciano, A., Stefano, B., & Andrea, G. (2002). Context-driven fusion of high spatial and spectral resolution images based on oversampled multiresolution analysis. *IEEE Transactions on Geoscience and Remote Sensing* , 40 (10), 2300-2312.
- Byeungwoo, J., & Landgrebe, D. A. (1999). Decision fusion approach for multitemporal classification. *IEEE Transactions on Geoscience and Remote Sensing* , 37 (3), 1227–1233.
- Cakir, H. I., & Khoram, S. (2003). Fusion of high spatial resolution imagery with high spectral resolution imagery using multiresolution approach. *ASPRS Annual Conference Proceedings*. Anchorage, Alaska.
- Carper, W. J., Lilesand, T. W., & Kieffer, R. W. (1990). The use of intensity–hue–saturation transformation for merging SPOT panchromatic and multispectral image data. *Photogrammetric Engineering and Remote Sensing* , 56 (4), 459–467.
- Chander, G., & Markham, B. (2003). Revised Landsat–5 TM radiometric calibration procedures and postcalibration dynamic ranges. *IEEE Transactions on Geoscience and Remote Sensing* , 41 (11), 2674–2677.
- Chander, G., Meyer, D. J., & Helder, D. L. (2004). Cross calibration of the Landsat–7 ETM+ and EO–1 ALI sensor. *IEEE Transactions on Geoscience and Remote Sensing* , 42 (12), 821 – 2831.
- Chang, C.-I. (2006). *Recent advances in hyperspectral signal and image processing*. Research Signpost, Transworld Research Network.
- Chavez, P. S. (1987). Digital merging of Landsat TM and digitized NHAP data for 1 : 24 000 scale image mapping. *Photogrammetric Engineering and Remote Sensing* , 52, 1637- 1646.
- Chavez, P. S. (1996). Image–based atmospheric corrections. *Photogrammetric engineering and remote sensing* , 62 (9), 1025–1036.
- Chavez, P. S., & Kwarteng, A. Y. (1989). Extracting spectral contrast in Landsat Thematic Mapper image data using selective principle component analysis. *Photogrammetric Engineering and Remote Sensing* , 55 (3), 339–348.

- Chavez, P. S., & MacKinnon, D. J. (1994). Automatic detection of vegetation changes in the Southwestern United States using remotely sensed images. *Photogrammetric Engineering and Remote Sensing* , 60 (5), 571-583.
- Chavez, P. S., Sides, S. C., & Anderson, J. A. (1991). Comparison of three different methods to merge multiresolution and multispectral data: TM & SPOT pan. *Photogrammetric Engineering and Remote Sensing* , 57 (3), 295-303.
- Chen, C., Hepner, G., & Forster, R. (2003). Fusion of hyperspectral and radar data using the IHS transformation to enhance urban surface features. *ISPRS Journal of Photogrammetry and Remote Sensing* , 58 (1), 19–30.
- Chen, Y., Fung, T., Lin, W., & Wang, J. (2005). An image fusion method based on object-oriented image classification. *IEEE Transactions on Geoscience and Remote Sensing Symposium IGARSS 05*, 6, pp. 3924–3927.
- Cheng, P., Toutin, T., & Stohr, C. (1999). Automated DEM extraction from aerial photos or optical satellite images. *13th International Conference Applied Geologic Remote Sensing*, 1, pp. 56-63. Vancouver, BC.
- Civco, D. L. (1989). Topographic normalization of Landsat thematic mapper digital imagery. *Photogrammetric Engineering and Remote Sensing* , 1303–1309.
- Cliché, G., Bonn, F., & Teillet, P. (1985). Integration of the SPOT panchromatic channel into its multispectral mode for image sharpness enhancement. *Photogrammetric Engineering and Remote Sensing* , 51 (3), 311-316.
- Colin, A., & Boire, J.-Y. (1999). MRI–SPECT fusion for the synthesis of high resolution 3D functional brain images: a preliminary study. *Computer Methods and Programs in Biomedicine* , 60, 107–116.
- Collado, A. D., Chuvieco, E., & Camarasa, A. (2002). Satellite remote sensing analysis to monitor desertification processes in the crop-rangeland boundary of Argentina. *Journal of Arid Environments* , 52, 121-133.
- Congalton, R. G., & Green, K. (1999). *Assessing the accuracy of remotely sensed data: Principles and practices*. Boca Raton, Florida: Lewis Publishers.

- Couloigner, I., Ranchin, T., Valtonen, V. P., & Wald, L. (1998). Benefit of the future SPOT 5 and of data fusion to urban mapping. *International Journal of Remote Sensing* , 1519–1532.
- Curran, P. J. (1988). The semivariogram in remote sensing: an introduction. *Remote Sensing of Environment* , 24, 493-507.
- Dai, X., & Khorram, S. (1999). Data fusion using artificial neural networks: a case study on multitemporal change analysis. *Computers Environment and Urban Systems* , 23 (1), 19–31.
- Daily, M. (2000). Hue–saturation–intensity split–spectrum processing of seasat radar imagery. *Photogrammetric Engineering and Remote Sensing* , 49 (3), 349–355.
- Dasarathy, B. V. (1993). *Decision fusion*. IEEE Computer Society Press, Los Alamitos, CA, USA.
- Datt, B., McVicar, T. R., Van Niel, T. G., Jupp, D. L., & Pealman, J. S. (2003). Pre–processing EO–1 Hyperion hyperspectral data to support the application of agricultural indices. *IEEE Transactions on Geoscience and Remote Sensing* , 41 (6), 1246–1259.
- De Bethune, S., Muller, F., & Donnay, J. P. (1998). Fusion of multi-spectral and panchromatic images by local mean and variance matching filtering techniques. *Fusion of Earth Data*.
- Dempster, A. P. (1968). A generalization of Bayesian inference. *Journal of the Royal Statistical Society , Series B*, 205–247.
- Devender, S. (1996). *Data analysis: A Bayesian tutorial*. Oxford: Clarendon Press.
- Diagenis, C. J., Hearn, D. R., Lencioni, D. E., & Mendenhall, J. A. (2002). *Project report, EO–1–9, EO–1 Advanced Land Imager technology validation report lincoln laboratory*. Massachusetts Institute of Technology.
- Dial, J., & Gene, G. (2003). Block adjustment of high–resolution satellite images described by rational polynomials. *Photogrammetric Engineering and Remote Sensing* , 69 (1), 59–68.

- Dulilleux, P. (1987). An implementation of the algorithme a trous to compute the wavelet transform. *In Compte-rendus du congres ondelenes et methodes temps-frequence el espace des phases* (pp. 298-304). Marseille: Springer-Verlag ed.
- Eastmen, J. R. (2006). IDRISI Andes version 15, Gouid to GIS and image processing. Clark Labs, Clark University.
- Ebanks, B. R. (1983). On measures of fuzziness and their representations. *Journal of Mathematical Analysis and Applications* , 92 (2), 24–37.
- Ehlers, M. (1991). Multisensor image fusion techniques in remote sensing. *ISPRS Journal of Photogrammetry and Remote Sensing* , 46 (1), 19–30.
- El Faouzi, N.-E. (2004). Data fusion in road traffic engineering: an overview. *SPIE*, 5434.
- Eskicioglu, A. M., & Fisher, P. S. (1995). Image quality measures and their performance. *IEEE Transactions on Communications* , 43, 2959–2965.
- Evans, D. (1988). Multisensor classification of sedimentary rocks. *Remote Sensing of Environment* , 25, 129-144.
- Fahimnejad, H., Soofbaf, S. R., Alimohammadi, A., & Zoej, M. J. (2007). Crop types classification by Hyperion data and unmixing algorithm. *Map World Forum Hyderabad, India*.
- Fatone, L., Maponi, P., & Zirilli, F. (2001). An image fusion approach to the numerical inversion of multifrequency electromagnetic scattering data. *Inverse Problems* , 17 , 1689-1701.
- Fisher, A. M., & Eskicioglu, P. S. (1995). Image quality measure and their performance. *IEEE Transactions on Communications* , 43 (12), 2959 – 2965.
- Ford, S. J., & Mckeown, D. M. (1992). Information fusion of multispectral imagery for cartographic feature extraction. *Commission VII:Interp of Photographic and R S Data XVII Congress ISPRS*. Washington DC.
- Forman, S. E. (2005). Advanced Land Imager: mechanical design, integration, and testing. *Lincoln Laboratory Journal* .
- Garguet-Duport, B., Girel, J., Chassery, J.-M., & Pautou, G. (1996). The use of multiresolution analysis and wavelet transform for merging SPOT panchromatic

- and multispectral image data. *Photogrammetric Engineering and Remote Sensing*, 62 (9), 1057-1066.
- Gens, R., Vekerdy, Z., & Pohl, C. (1998). Image and data fusion-concepts and implementation of a multimedia tutorial. *Second International Conference on Fusion of Earth Data*, (pp. 217-222). Sophia Antipolis, France.
- Gitelson, A. A., & Kaufman, Y. J. (1998). MODIS NDVI optimization to fit the AVHRR data series—spectral considerations. *Remote Sensing of Environment*, 66 (3), 343–350.
- Golub, G. H. (1996). *Matrix Computations* (3rd Edition ed.). Johns Hopkins.
- Gong, Y., Lim, T. J., & Farhang-Boroujeny, B. (2001). Adaptive least mean square CDMA detection with Gram–Schmidt pre-processing. *IEEE*, 148.
- Gonzalez, R. C., & Woods, R. E. (2002). *Digital Image Processing* (2nd edition ed.). Prentice Hall.
- Goodenough, D. G., Dyk, A., Niemann, O., Pearlman, J. S., Chen, H., Murdoch, M., *et al.* (2003). Processing Hyperion and ALI for forest classification. *IEEE Transactions on Geoscience and Remote Sensing*, 41, 1132–1331.
- Gross, H. N., & Schott, J. R. (1998). Application of spectral mixture analysis and image fusion techniques for image sharpening. *Remote Sensing of Environment*, 63, 85–94.
- Gu, D., & Gillespie, A. (1998). Topographic normalization of Landsat TM images of forest based on subpixel sun–canopy–sensor geometry. *Remote Sensing of Environment*, 64, 166–175.
- Guo, L., & Zhang, Q. (2005). Wireless data fusion system for agricultural vehicle positioning. *Biosystems Engineering*, 91 (3), 261-269.
- Haar, A. (1910). Zur Theorie der orthogonalen Funktionensysteme. *Mathematische Annalen*, 69, 331-371.
- Haefner, H., Holecz, F., Meier, E., Nuesch, D., & Piesbergen, J. (1993). Capabilities and limitations of ERS-1 SAR data for snowcover determination in mountainous regions. *Space at the service of our environment, proceedings of*

- the second ERS-1 symposium* (p. 971± 976). Hamburg, Germany 11± 14 October 1993: SP-361 (Paris: European Space Agency).
- Hagan, M. T., Demuth, H. B., & Beale, M. H. (1996). *Neural network design* (1st Edition ed.).
- Hall, D. L. (1992). *Mathematical techniques in multisensor data fusion*. Artech House.
- Hall, D. L., & Llinas, J. (1997). An introduction to multisensor data fusion., (pp. 6-23).
- Han, T., Goodenough, D. G., Dyk, A., & Love, J. (2002). Detection and correction of abnormal pixels in Hyperion images., 3, pp. 1327-1330. Toronto, Canada.
- Harris, J. R., & Murray, R. (1989). IHS transform for the integration of radar imagery with geophysical data. *12th Canadian Symposium on Remote Sensing*, (p. 923± 926). Vancouver, Canada (Vancouver: CSRS).
- Harsanyi, J. C., & Chang, C.-I. (1994). Hyperspectral image classification and dimensionality reduction: An orthogonal subspace projection approach. *IEEE Transactions on Geoscience and Remote Sensing* , 32 (4), 779–785.
- Hearn, D. R. (2005). Spatial Calibration and Imaging Performance Assessment of the Advanced Land Imager. *Lincoln Laboratory Journal* .
- Hill, J., & Sturm, B. (1991). Radiometric correction of multi-temporal Thematic Mapper data for use in agricultural land cover classification and vegetation monitoring. *International Journal of Remote Sensing* , 1471–1491.
- Houzelle, S., & Glraudon, G. (1991). Data Fusion SPOT and SAR images for bridge and urban area extraction. *IEEE IGARSS*.
- Huang, S. (2005). The potential of multi-sensor satellite data for applications in environmental monitoring with special emphasis on land cover mapping, desertification monitoring and fire detection Dissertation. *LMU München: Fakultät für Biologie* .
- Introductory tutorial to Bayesian probability*. (2007). Retrieved from Queen Mary University of London: <http://www.dcs.qmw.ac.uk/%7Enorman/BBNs/BBNs.htm>.

- Jensen, J. R. (1996). *Introductory digital image processing*. New Jersey: Prentice-Hall.
- Kalluri, S., Gilruth, P., & Bergman, R. (2003). The potential of remote sensing data for decision makers at the state, local and tribal level: experiences from NASA's Synergy program. *Environmental Science & Policy*, 6, 487-500.
- Karathanassi, V., Kolokousis, P., & Ioannidou, S. (2007). A comparison study on fusion methods using evaluation indicators. *International Journal of Remote Sensing*, 28 (10), 2309 – 2341.
- Kittler, J., & Pairman, D. (1985). Contextual pattern recognition applied to cloud detection and identification. *IEEE Transactions on Geoscience and Remote Sensing*, 23, 855-863.
- Klein, L. A. (1993). *Sensor and data fusion concepts and applications*. SPIE Optical Engineering Press.
- Koopmans, B. N., & Forero, R. G. (1993). Airborne SAR and Landsat MSS as complementary information source for geological hazard mapping. *ISPRS Journal of Photogrammetry and Remote Sensing*, 48, 28-37.
- Kruse, F. A., Lefkoff, A. B., & Dietz, J. B. (1993). Expert system-based mineral mapping in northern death valley. *Remote Sensing of Environment*, 44 (Special issue on AVIRIS), 309 - 336.
- Kurt, S. (2006). *Hyperion level 1G (L1GST) product output files data format control book (DFCB) Earth Observing-1 (EO-1)*.
- Kurz, F., & Hellwich, O. (2000). Empirical estimation of vegetation parameters using multisensor data fusion. 33 (Part B7), 733–737.
- L., V. G., & Pohl, C. (1994). Image fusion: Issues, techniques and applications. In J. L. Cappellini (Ed.), *Intelligent Image Fusion, Proceedings EARSeL Workshop*, (pp. 18-26). Strasbourg, France.
- Lau, W., King, B. A., & Li, Z. (2000). The influences of image classification by fusion of spatially oriented images. *International Archives of Photogrammetry and Remote Sensing*, 33 (Part B7), 752–759.

- Le Hegarat-Masclé, S., Bloch, I., & Vidal-Madjar, D. (1998). Introduction of neighborhood information in evidence theory and application to data fusion of radar and optical images with partial cloud cover. *Pattern Recognition* , 34, 1811–1823.
- Le Hegarat-Masclé, S., Quesney, A., Vidal-Madjar, D., Taconet, O., Normand, M., & Loumagne, C. (2000). Land cover discrimination from multitemporal ERS images and multispectral LANDSAT images: a study case in an agricultural area in France. *International Journal of Remote Sensing* , 21 (3), 435–456.
- Lemeschewsky, G. P. (1999). Multispectral multisensor image fusion using wavelet transforms. *SPIE*, 3716, pp. 214-222.
- Leung, Y., Mei, C.-L., & Zhang, W.-X. (2003). Statistical test for local patterns of spatial association. *Environment and Planning A* , 35, 725-744.
- Li, R. Y., Ulaby, F. T., & Eyton, J. R. (1980). Crop classification with a Landsat-radar sensor combination. *Machine Processing of Remote Sensing Data*. Purdue University.
- Li, S., Kwok, J. T., & Wang, Y. (2002). Using the discrete wavelet frame transform to merge Landsat TM and SPOT panchromatic images. *Information Fusion* , 3, 17-23.
- Liang, S., Fang, H., Thorp, L., Kaul, M., Van Niel, T. G., McVicar, T. R., *et al.* (2003). Estimation of land surface broadband albedos and leaf area index from EO-1 ALI data and validation. *IEEE Transactions on Geoscience and Remote Sensing* , 41 (6), 1260–1267.
- Lillesand, T. M., Kiefer, R. W., & Chipman, J. W. (2004). *Remote sensing and image interpretation* (5th edition ed.). John Wiley & Sons.
- Lisini, G., Dell'Acqua, F., Triani, G., & Gamba, P. (2005). Comparison and combination of multiband classifiers for Landsat urban land cover mapping. *IGARSS*, 4, pp. 2823–2826.
- Lnecioni, D. E., Hearn, D. R., Digenis, C. J., Mendenhall, J. A., & Bicknell, W. E. (2005). The EO-1 Advanced Land Imager: an overview. *Lincoln Laboratory Journal* .

- Loeve, M. (1955). *Probability theory*. D. van Nostrand Co., Princeton, Nj.
- Luo, R. C., & Kay, M. G. (1989). Multisensor integration and fusion in intelligent systems. *IEEE Transactions on SMC* , 19 (5), 905-912.
- Malandain, G., Bardinet, E., Nelissen, K., & Vanduffel, W. (2004). Fusion of autoradiographs with an MR volume using 2–D and 3–D linear transformations. *Neuroimage* , 23 (1), 111-127.
- Malila, W. A. (1985). Comparison of the information contents of Landsat TM and MSS data. *Photogrammetric Engineering and Remote Sensing* , 51, 1449–1457.
- Martens, J.-B., & Meetsters, L. (1998). Image dissimilarity. *Signal Processing* , 70, 155–176.
- Masek, J. G., Honzak, M., Goward, S. N., Liu, P., & Pak, E. (2001). Landsat-7 ETM+ as an observatory for land-cover: Initial radiometric and geometric comparisons with Landsat-5 Thematic Mapper. *Remote Sensing of the Environment* , 78, 118-130.
- Mather, P. M. (1999). *Computer processing of remotely sensed images: an introduction* (2nd Edition ed.). Chichester, West Sussex, England: John Wiley & Sons.
- Mesev, V. (2007). *Integration of GIS and remote sensing*. Wiley.
- NASA solar position calculator. (2007). Retrieved from http://www2.arnes.si/~gljsentvid10/nebes_pod/legasonca.html
- Nunez, J., Otazu, X., Fors, O., & Prades, A. (1997). Simultaneous image fusion and reconstruction using wavelets: Applications to SPOT + LANDSAT images. *Elsevier Science Ltd, Vistas in Astronomy* , 41 (3), 351–357.
- Nunez, J., Otazu, X., Fors, O., Prades, A., Pala, V., & Ariol, R. (1999). Multiresolution–based image fusion with additive wavelet decomposition. *IEEE Transactions on Geoscience and Remote Sensing* , 37 (3), 1204–1211.
- OConnell, M. J. (1974). Multivariate least squares fitting program using modified Gream–Schmidth transformations. *North–Holland Publishing Co.*, 8, pp. 56–69. Amsterdam.

- Oldfield, F., & Dearing, J. A. (2003). The role of human activities in past environmental change. 143-162. (K. D. In Alverson, Ed.) Berlin: Springer-Verlag.
- Ostermeier, R., Rogge, H. I., & Auernhammer, H. (2007). Multisensor data fusion implementation for a sensor based fertilizer application system. *Agricultural Engineering International: the CIGR Ejournal* , IX.
- Parrt, W., Sier, A. R., Battarbee, R. W., Mackay, A., & Burgess, J. (2003). Detecting environmental change: science and society perspectives on long-term research and monitoring in the 21st century. *The Science of the Total Environment* , 1-8.
- Patias, P. (2002). Medical imaging challenges photogrammetry. *ISPRS Journal of Photogrammetry & Remote Sensing* , 56, 295– 310.
- Pearl, J. (1990). Reasoning with Belief functions: An analysis of compatibility. *International Journal of Approximate Reasoning* , 4 (5/6), 363–389.
- Pearlman, J. S., Barry, P. S., Segal, C., Shepanski, J., Beiso, D., & Carman, S. (2003). Hyperion, a space-based imaging spectrometer. *IEEE Transactions on Geoscience and Remote Sensing* , 41, 1160–1173.
- Pellemans, A., Jordans, R., & Allewijn, R. (1993). Merging multispectral and panchromatic SPOT images with respect to the radiometric properties of the sensor. *Photogrammetric Engineering and Remote Sensing* , 59 (1), 81-87.
- Pohl, C., & Van Genderen, J. L. (1998). Multisensor image fusion in remote sensing: concepts, methods and applications. *International Journal of Remote Sensing* , 19 (5), 823–854.
- Price, J. C. (1987). Combining panchromatic and multispectral imagery from dual resolution satellite instruments. *Remote Sensing of Environment* , 21 (9), 119–128.
- Pujadas, M., Plaza, J., Reres, J., Artnano, B., & Millan, M. (2000). Passive remote sensing of nitrogen dioxide as a tool for tracking air pollution in urban areas: the Madrid urban plume, a case of study. *Atmospheric Environment* , 34, 3041-3056.

- Ranchin, T., & Wald, L. (2000). Fusion of high spatial and spectral resolution images: The ARSIS concept and its implementation. *Photogrammetric Engineering and Remote Sensing* , 66 (1), 49–61.
- Rebillard, P., & Nguyen, P. T. (1982). An exploration of co-registered SIR-A, SEASAT and Landsat images. *RS of Environment, RS for Exploration Geology, Proceedings International Symposium, Second Thematic Conference*, (pp. 109-118). Forth Worth, U.S.A.
- Robinson, G. D., Gross, H. N., & Schott, J. R. (2000). Evaluation of two application of spectral mixing models to image fusion. *Remote Sensing of Environment* , 71 (3), 272-281.
- Rodriguez, E., Morris, C. S., Belz, J. E., Chapin, E. C., Martin, J. M., Daffer, W., *et al.* (2005). *An assessment of the SRTM topographic products*. Pasadena, CA, USA.
- Rohwer, N.-K. (2006). Object oriented image analysis of high resolution satellite imagery: a land cover change analysis in the Palolo Valley, Central Sulawesi, Indonesia, based on Quickbird and IKONOS satellite data. *Msc. thesis* . Goettingen University.
- Ruck, D. W., Rogers, S. K., Kabrisky, M., Oxley, M. E., & Suter, B. W. (1990). The multilayer perceptron as an approximation to a Bayes optimal discrimination function. *IEEE Transactions on Neural Networks* , 1, 296–298.
- Sabins, F. F. (1999). Remote sensing for mineral exploration. *Ore Geology Reviews* , 14, 157–183.
- Saghri, J. A., Cheatham, P. S., & Habibi, A. (1989). Image quality measure based on a human visual system model. *Optical Engineering* , 28 (7), 813–818.
- Schaefer, K., Harbusch, A., Emeis, M., Peicu, G., Hoffmann, H., Sarigiannis, D., *et al.* (2004). Fusion of air pollution data in the region of Munich, Germany, by the ICAROS NET platform. *SPIE*, 5571, pp. 322-333. Bellingham, WA, USA.
- Schowengerdt, R. A. (1992). Enhanced thermal mapping with landsat and HCMM digital data. *Techn papers:ACSM-ASP Convention 48th Annual Meeting ASP*. Denver Colorado.

- Schroeder, T. A., Cohen, W. B., Song, C., canty, M. J., & Yang, Z. (2006). Radiometric correction of multi-temporal Landsat data for characterization of early successional forest patterns in western Oregon. *Remote Sensing of Environment*, 103, 16–26.
- Schowengerdt, R. A. (1980). Reconstruction of multispatial, multispectral image data using spatial frequency content. *Photogrammetric Engineering and Remote Sensing*, 46 (10), 1325-1334.
- Schowengerdt, R. A. (1997). *Remote sensing models and methods for image processing* (2nd ed.). Academic Press.
- Scramuzza, P., Micijevic, E., & Chander, G. (2004). *SLC gap-filled products: Phase one methodology*.
- Sellers, P. J. (1989). Vegetation-canopy spectral reflectance and biophysical processes. In G. Asrar, *Theory and applications of optical remote sensing* (pp. 297-335). New York: Wiley.
- Shafer, G. (1976). *A mathematical theory of evidence*. Princeton University Press.
- Shafer, G. (2002). *Dempster–Shafer theory*.
- Sharpe, B., Kerr, A., & Dettwiler, M. (1991). Multichannel fusion technique for resolution enhancement during ground processing. *IEEE IGARSS*.
- Shaw, G. A., & Burkem, H.-h. K. (2003). Spectral imaging for remote sensing. *Lincoln Laboratory Journal*.
- Shen, S. S. (1990). Summary of types of data fusion methods utilized in workshop papers. *Multisource Data Integration in Remote Sensing*, (pp. 145–149). Maryland, U.S.A.
- Shensa, M. J. (1992). Discrete wavelet transforms: wedding the à trous and Mallat algorithms. *IEEE Transactions on Signal Processing*, 40 (2), 464–2,482.
- Shettigara, K. (1992). A generalized component substitution technique for spatial enhancement of multispectral images using a higher resolution dataset. *Photogrammetric Engineering and Remote Sensing*, 58 (5), 561–567.
- Shettigara, K. V. (1989). A linear transformation technique for spatial enhancement of multispectral images using a higher resolution dataset. *IEEE IGARSS*.

- Shi, W. Z., Ehlers, M., & Molenaar, M. (2005). Uncertainties in integrated remote sensing and GIS. *International Journal of Remote Sensing* , 26 (14), 2911–2915.
- Shi, W., Zhu, C., Zhu, C., & Yang, X. (2003). Multi-band wavelet for fusing SPOT panchromatic and multispectral images. *Photogrammetric Engineering and Remote Sensing* , 69 (5), 513-520.
- Simone, G., Farina, A., Morabito, F. C., Serpico, S. B., & Bruzzone, L. (2002). Image fusion techniques for remote sensing applications. *Information Fusion* , 3, 3–15.
- Singh, R. P., Cervone, G., Kafatos, M., Prasad, A. K., Sahoo, A. K., Sun, D., *et al.* (2007). Multi-sensor studies of the Sumatra earthquake and tsunami of 26 December 2004. *International Journal of Remote Sensing* , 28 (13 & 14), 2885 – 2896.
- Smith, S. W. (1999). *The scientist and engineer's guide to digital signal processing* (Second ed.). California Technical Publishing.
- Special issue on data fusion. (1997). *Proceedings of the IEEE* , 85 , 1-208.
- Sroka, R. (2004). Data fusion methods based on fuzzy measures in vehicle classification process. *Proceedings of the 21st IEEE Instrumentation and Measurement Technology Conference*, 3, pp. 2234 - 2239.
- Star, J. L. (1991). *The integration of remote sensing and geographic information systems*. American Society for Photogrammetry and Remote Sensing.
- Subramani, P., Sahu, R., & Verma, S. (2006). Feature selection using Haar wavelet power spectrum. *BMC Bioinformatics* , 7 .
- Sun, W., Heidt, V., Gong, P., & Xu, G. (2003). Signal and image processing–information fusion for rural land–use classification with high–resolution satellite imagery. *IEEE Transactions on Geoscience and Remote Sensing* , 41 (4), 883–890.
- Sunar, F., & Musaoglu, N. (1998). Merging multi-resolution SPOT Pan and Landsat TM data: the effects and advantages. *International Journal of Remote Sensing* , 19 (2), 219-224.

- Taranik, J. V. (1988). First results of international investigations of the applications of SPOT-1 data to geologic problems, mineral and energy exploration. *CNES/SPOT Image, International Conference on SPOT-1 image utilization, assessment, results*, (pp. 701 - 708). Paris, France.
- Temimi, M., Leconte, R., Brssette, F., & Chaouch, N. (2005). Flood monitoring over the Mackenzie River Basin using passive microwave data. *Remote Sensing of Environment*, 98 (2 and 3), 344-355.
- Toft, P. (1996). The Radon transform: theory and implementation. Denmark: Technical University.
- Tom, V. T. (1986). A synergistic approach for multispectral image restoration using reference imagery. *IGARSS'86 Symposium* (pp. 559–564). Zurich: ESA publications division Noordwijk, Netherlands.
- Toutin, T. (2001). DEM generation from new VIR sensors: IKONOS, ASTER and Landsat-7. *IEEE IGARSS*, (pp. 9-13). Sydney, Australia.
- Toutin, T. (2001). Elevation modelling from satellite VIR data: A review. *International Journal of Remote Sensing*, 22 (6), 1097-1125.
- Toyra, J., Pietroniro, A., Martz, L. W., & Prowse, T. D. (2002). A multi-sensor approach to wetland flood monitoring. *Published online in Wiley InterScience*, 16, 1569–1581.
- Tu, M.-T., Su, S.-C., Shyu, H.-C., & Huang, P. S. (2001). A new look at IHS like image fusion methods. *Information Fusion*, 2 (3), 177–186.
- Tucker, C. J., Dregne, H. W., & Newcomb, W. W. (1994). AVHRR datasets for determination of desert spatial extent. *International Journal of Remote Sensing*, 15, 3547- 565.
- Tucker, C. J., Grant, D. M., & Dykstra, J. D. (2003). NASA's global orthorectified landsat dataset. *Photogrammetric Engineering and Remote Sensing*, 70 (3), 313–322.
- Tupin, F., Bloch, I., & Maitre, H. (1999). A first step toward automatic interpretation of SAR images using evidential fusion of several structure detectors. *IEEE Transactions on Geoscience and Remote Sensing*, 37 (3), 1327–1343.

- Ulaby, F. T. (1982). Crop classification using airborne radar and Landsat data. *IEEE Transactions on Geoscience and Remote Sensing*, 20, 42-51.
- Van Der Meer, F. D., & Dejong, S. M. (2001). *Imaging spectrometry basic principles and prospective applications*. Kluwer Academic Publishers.
- Van Der Meer, F. (1997). What does multisensor image fusion add in terms of information content for visual interpretation? *International Journal of Remote Sensing*, 18 (2), 445–452.
- Van Genderen, J., & Pohl, C. (1994). Image fusion: issues, techniques and applications. In J. Van Genderen, & V. Cappellini (Ed.), *EARSeL Workshop on Intelligent Image Fusion*.
- Varshney, P. K., & Arora, M. K. (2004). *Advanced image processing techniques for remotely sensed hyperspectral data*. Berlin: Springer-Verlag.
- Verbyla, D. (1995). *Satellite remote sensing of natural resources*. Boca Raton: Lewis Publishers.
- Vijayaraj, V., Younan, N. H., & O'Hara, C. G. (2004). Quality metrics for multispectral image processing. *Annual ASPRS Conference*.
- Vincent, B., & Boire, J.-Y. (2001). A general framework for the fusion of anatomical and functional medical images. *NeuroImage*, 13, 410–424.
- Voegtle, T., & Steinle, E. (2005). Fusion of 3D building models derived from first and last pulse laserscanning data. *Information Fusion*, 6 (4), 275-281.
- Vrabel, J. (1996). Multispectral imagery band sharpening study. *Photogrammetric Engineering and Remote Sensing*, 62 (9), 1075–1083.
- Vrabel¹, J., Doraiswamy, P., & Stern, A. (2002). Application of hyperspectral imagery resolution improvement for site-specific farming. *ASPRS*.
- Vrabel², J., Doraiswamy, P., McMurtrey, J., & Stern, A. (2002). Demonstration of the accuracy of improved resolution hyperspectral imagery. *SPIE Symposium*.
- Wald, L. (1997). An overview of concepts in fusion of Earth data. *Future Trends in Remote Sensing*, (pp. 385–390). Lyngby, Denmark.
- Wald, L. (2002). *Data fusion definitions and architectures fusion of images of different spatial resolutions*. Paris: Les Presses de l'École des Mines Paris.

- Wald, L. (1998). Data fusion: a conceptual approach for an efficient exploitation of remote sensing images. In T. Ranchin, & W. L. (Ed.), *EARSeL Conference on Fusion of Earth Data*, (pp. 17-23).
- Wald, L. (1999). Some terms of reference in data fusion. *IEEE Transactions on Geoscience and Remote Sensing* , 37 (3), 1190–1193.
- Wald, L. (2000). The present achievements of the EARSeL - SIG Data Fusion. *EARSeL Symposium*. Dresden, Germany.
- Wald, L., Ranchin, T., & Mangolini, M. (1997). Fusion of satellite images of different spatial resolutions: assessing the quality of resulting images. *Photogrammetric Engineering and Remote Sensing* , 63 (6), 691–699.
- Walth, R. A., & Ehlers, M. (1988). Cartographic feature extraction with SIR-B and Landsat TM images. *International Journal of Remote Sensing* , 9, 873-889.
- Waltz, E., & Llinas, J. (1990). *Multisensor data fusion*. Artech House.
- Wang, Z., & Bovik, A. C. (2002). A universal image quality index. *IEEE Signal Processing Letters* , 9 (3), 81–84.
- Wang, Z., Bovik, A. C., Sheikh, H. R., & Simoncelli, E. P. (2004). Image quality assessment: from error visibility to structural similarity. *IEEE Transactions on Image Processing* , 13 (4), 600–612.
- Wang, Z., Ziou, D., Armenakis, C., Li, D., & Li, Q. (2005). A comparative analysis of image fusion methods. *IEEE Transactions on Geoscience and Remote Sensing* , 43 (6), 1391 – 1402.
- Welch, R., & Ehlers, M. (1987). Merging multiresolution SPOT HRV and Landsat TM data. *Photogrammetric Engineering and Remote Sensing* , 53 (3), 301-303.
- Williams, D. (2007). *Landsat-7 science user data hand book*. Retrieved from responsible NASA official: <http://landsathandbook.gsfc.nasa.gov/handbook.html>.
- Williams, J. (1995). *Geographic information from space : processing and applications of geocoded satellite images*. Chichester, Wiley.
- Winkler, S. (2005). *Digital video quality*. Chichester: John Wiley & Sons, Ltd.

- Woodcock, C., & Strahler, A. (1987). The factor of scale in remote sensing. *Remote Sensing of Environment* , 21, 311-332.
- Yesou, H. (1993). Merging SEASTA and SPOT imagery for the study of geologic structure in a temperate agricultural region. *Remote Sensing and Environment* , 43, 265-280.
- Yesou, H., Besnus, Y., & Rolet, J. (1993). Extraction of spectral information from Landsat TM data and merger with SPOT panchromatic imagery—a contribution to the study of geological structures. *ISPRS Journal of Photogrammetry and Remote Sensing* , 48 (5), 23–36.
- Yocky, D. A. (1996). Artifacts in wavelet image merging. *Optical Engineering* , 37 (7), 2094-2101.
- Yocky, D. A. (1995). Image merging and data fusion by means of the discrete two-dimensional wavelet transform. *Optical Society of America* , 12 (9).
- Yocky, D. A. (1996). Multiresolution wavelet decomposition image merger of Landsat Thematic Mapper and SPOT panchromatic data. *Photogrammetric Engineering and Remote Sensing* , 62 (9), 1067-1074.
- Zhang, Y. (1999). A new merging method and its spectral and spatial effects. *International Journal of Remote Sensing* , 20 (10), 2003–2014.
- Zhang, Y. (2002). Automatic image fusion: a new sharpening technique for Ikonos multispectral images. *GIM International* , 16 (5), 54–57.
- Zhang, Y. (2002). Problems in the fusion of commercial highresolution satellite images as well as Landsat 7 images and initial solutions. *International Archives of Photogrammetry and Remote Sensing* , 34 (Part 4) .
- Zhang, Y., & Hong, G. (2005). An IHS and wavelet integrated approach to improve pan-sharpening visual quality of natural colour Ikonos and QuickBird images. *Information Fusion* , 6 (3), 225–234.
- Zhou, G. (2001). *Architecture of future intelligent earth observing satellites (FIEOS) in 2010 and beyond, 1st technical report.*

- Zhou, G. K. (2001). Orthorectifying 1960's declassified intelligence satellite photography (DISP) of greenland. *IEEE Transactions on Geoscience and Remote Sensing* .
- Zhou, J., Civco, D. L., & Silander, J. A. (1998). A wavelet transform method to merge Landsat TM and SPOT panchromatic data. *International Journal of Remote Sensing* , 19 (4), 743–757.
- Zhu, H., Beling, P., & Overstreet, G. (2002). A Bayesian framework for the combination of classifier outputs. *Journal of the Operational Research Society* , 53, 719–727.
- Zhu, Y.-M., & Cochoff, A. M. (2006). An object-oriented framework for medical image registration, fusion, and visualization. *computer methods and programs in biomedicine* , 82, 258–267.
- Zhukov, B., Oertel, D., & Lanzl, F. (1995). A multi-sensor multi-resolution technique for satellite remote sensing. *IGARSS'95 Symposium*, (pp. 51– 53). Firenze, Italy.

Appendix I

Data fusion organizations, journals and useful websites

1. Data fusion server which includes four main subsections: International Conferences of earth data fusion; fundamentals in data fusion including data fusion methods, tools, properties; general information about the portal; and the EARSeL special interest group (SIG). This online website offering very useful information almost about all aspects of remote sensing data fusion. <http://www.data-fusion.org/topics.php>.
2. The Special Interest Group (SIG) as a part of data fusion server was created in 1996 under the umbrella of the European Association of Remote Sensing Laboratories (EARSeL), the Data Fusion group contributes to a better understanding and use of data fusion in the field of Earth observation by organizing regular meetings of its members and tackling fundamentals of Data Fusion in remote sensing. <http://www.data-fusion.org/search.php?query=&topic=32>.
3. IEEE-GRSS Data Fusion Technical Committee. The DFC committee serves as a global, multidisciplinary, network for geospatial data fusion, connecting people and resources. It aims at educating students and professionals and at promoting best practice in data fusion applications. http://150.145.84.68/index.php/Main_Pag.
4. International Journal on Multi-Sensor, Multi-Source Information Fusion. This journal is intended to present within a single forum all of the developments in the field of multi-sensor, multi-source information fusion and thereby promote the synergism among the many disciplines that are contributing to its growth. The journal is the premier vehicle for disseminating information on all aspects of research and development in the field of information fusion. http://www.elsevier.com/wps/find/journaldescription.cws_home/620862/description#description.

<http://asrt.cad.gatech.edu/Mission-control/simon/paper1/intro.html>

<http://cma.cma.fr/Personnel/Monget/cours/page34.htm>

<http://cmp.felk.cvut.cz/~kraus/Mirrors/iris.usc.eduNision-Notes/bibliography/kwic/fus.html>

http://cns-web.bu.edu/pub/dorman/sensor_fusion

<http://ic-www.arc.nasa.gov/ic/projects/condition-based-maintenance/bibliography.html>

<http://imagets10.univ.trieste.it/ipl/research.html>

<http://roger.ucsd.edu/search/dMultisensor+data+fusion+%2D%2D+Congresses/-5,-1/browse>

<http://sabre.afit.af.mil/MARION?S=MULTISENSOR+DATA+FUSION>

<http://systemg.gmu.edu/InSERT/credits/PACHO~1.HTM>

Appendix II

Author's publication in data fusion

1. Darvishi Boloorani, Ali; Erasmi, Stefan; and Kappas, Martin, Multi-Source Remotely Sensed Data Combination: Projection Transformation Gap-Fill Procedure, *Journal of SENSORS*, 8, 4429-4440; DOI: 10.3390/s8074429, 2008¹.
2. Darvishi Boloorani, Ali; Erasmi, Stefan; and Kappas, Martin, Multi-source image reconstruction: exploitation of EO-1/ALI in Landsat-7/ETM+ SLC-off gap filling, *Proceeding of IS&SPIE's 20th Annual Symposium, Electronic Imaging Science and technology, California, USA, 2008*².
3. Darvishi Boloorani, Ali; Erasmi, Stefan; and Kappas, Martin, Urban Land Cover Mapping Using Object/Pixel-Based Data Fusion and Ikonos Images, *Remote Sensing: From Pixels to Processes (ISPRS), Enschede, Netherlands, 2006*¹.
4. Darvishi Boloorani, Ali; Erasmi, Stefan; and Kappas, Martin, Rice Field Discrimination and classification with Multitemporal SAR Imagery, *Second Goettingen GIS & Remote Sensing Days Conference (GGRS2006), Environmental Studies, Goettingen, Germany, 2006*².
5. Riyahi B., Hamid Reza; Darvishi Boloorani, Ali; and Abasi, Mozghan, Comparing Spectral and Object Based Hyperspectral Image Analysis for Palm Cover Mapping Using EO-1/Hyperion Imager, *Map and Spatial Information For Disaster Management Conference (Geomatic 85), Tehran ,Iran, 2006*³.

6. Darvishi Bolorani, Ali; Kappas, Martin; and Erasmi, Stefan, Hyper-Spectral/High- Resolution Data fusion: Assessing the Quality of EO1-Hyperion/Spot-Pan & Quickbird-MS Fusion in Spectral Domain Models. *High-Resolution Earth Imaging For Geospatial Information (ISPRS), Hannover, Germany, 2005¹.*

7. Darvishi Bolorani, Ali; Hamid Reza Riyahi B.; and Mehran Shaygan, Multi Spectral/Panchromatic-Based Data Fusion: Analysis of Techniques to Road Network Extraction, In Urban Area, Using ETM+ Images, *Geospatial Information for Knowledge Based Development conference (Geomatics 84), Tehran, Iran, 2005².*

Lebenslauf (Curriculum Vitae)

PERSÖNLICHE DATEN

Name Ali Darvishi Boloorani
Adresse Goldschmidtstr. 5 - 37077 Goettingen,
Deutschland.
Telefon +49(0)551/39-14364
Nationalität Iranisch
Geburtsdatum 11.Juli 1975
Geburtsort Kuhdasht, Iran
E-Mail adarvis@uni-goettingen.de,

AUSBILDUNG

Remote Sensing and GIS Department, Tarbiat Modares
University (TMU), Tehran, Iran

M.A. Fernerkundung und GIS 2001

Thesis: "Model-Based Image Analysis: Semi-Automatic
Urban Roads Extraction Using High Resolution Images"

Cartography Department, University of Tehran (UT),
Tehran, Iran

B.A. Kartographie 1998

Bsc. Projekt: "Providing Land Use and Land Cover Maps
Using Satellite Imagery, (study area Kouhdasht, Lorestan, Iran)".

Emam Jafare Sadegh Gymnasium 1994
Gymnasium

STIPENDIUM

PhD Scholarship, Ministry of Science, Research
and Technology of Iran (MSRTI) in
Fernerkundung und GIS.

2004 – 2008

Göttingen, den 25. August 2008

Unterschrift